AN ABSTRACT OF THE THESIS OF

José Bañuelos for the degree of Master of Science in Civil Engineering presented on June 12, 2014

Title: The Use of Blended Synthetic Fibers to Reduce Cracking Risk in High Performance Concrete (HPC)

Abstract approved:

_____

Jason H. Ideker

High Performance Concrete (HPC) is used in our crucial pieces of infrastructure, such as bridge decks, due to its enhanced durability and engineering properties. However, HPC is highly susceptible to early-age cracking. Cracking within the first months of a bridge deck's lifespan can severely hinder its long-term performance and durability. Fiber reinforced concrete (FRC) is concrete with the incorporation of dispersed fibers. The main role of dispersed fibers is to control the crack opening and propagation; however, mixed results in literature suggest that FRC can reduce the total shrinkage of concrete. Therefore, the incorporation of blended sizes of synthetic fibers could provide resistance to shrinkage-related cracking. Cracking risk was evaluated using the restrained shrinkage ring test (ASTM C1581). The purpose of this study was to investigate the effect fibers on the fresh properties, mechanical properties, drying shrinkage, cracking risk, and durability (freeze-thaw and chloride ion penetrability) in HPC. In addition, recommendations on fiber dosages for use in the field were suggested. Moreover, there

was an investigation on the effect of total cementitious material content, supplementary cementitious materials (SCM's), and aggregate type on the drying shrinkage of HPC.

It was found that the inclusion of blended synthetic fibers reduced the cracking risk of HPC. The fibers did not reduce drying shrinkage; however, the time-to-cracking in the ring test was increased and crack widths were notably reduced. Fibers improved the freeze-thaw and chloride ion penetrability of HPC. A dosage rate between 5lb/yd^3 and 7.5lb/yd^3 is recommended. Additionally, using slag instead of fly ash in HPC also reduced the cracking risk. The use of limestone as a coarse aggregate showed the most significant reduction in in drying shrinkage and cracking risk.

The Use of Blended Synthetic Fibers to Reduce Cracking Risk in High Performance Concrete (HPC)

by

José Bañuelos

A THESIS

submitted to

Oregon State University

in partial fulfillment of
the requirements for the
degree of

Masters of Science

Presented June 12, 2014

Commencement June 2015

Masters of Science thesis of José Bañuelos presented on June 12, 2014.

APPROVED:

Major Professor, representing Civil Engineering

Head of the School of Civil & Construction Engineering

Dean of the Graduate School

I understand that my thesis will become part of the permanent collection of Oregon State University libraries. My signature below authorizes release of my thesis to any reader upon request.

José Bañuelos, Author

ACKNOWLEDGEMENTS

First of all, I want to thank my advisor Jason H. Ideker for his support and patience throughout the course of this project. I consider you a great mentor and an excellent teacher. You are truly an inspiration to me.

I want to thank my fellow co-workers Tengfei Fu, Tyler Deebodt, David Rodriguez, Chang Li, Matt Adams, and Monica Morales for their support on this project. Tengfei, Tyler and David a special thanks for your advice with laboratory procedures. Also, I want to thank undergraduate research assistants Silas Shields, Nick Briesach, and Andrew Wilson for their laboratory and experimental support.

Thank you as well, to my graduate committee: Dr. Chris Bell, Dr. Arijit Sinha, and Dr. Chinweike Eseonu.

Finally, I want to thank my parents who have always given me love and support when I have needed it most. And to my loving and amazing wife, I want to thank you for your patience and encouragement over the course of my educational career.

CONTRIBUTION OF AUTHORS

Dr. Jason H. Ideker advised on the writing, interpretation and analysis of this thesis. Tyler Deebodt, OSU PhD student assisted in the writing of sections 2.3 and 2.9. Tengfei Fu, OSU PhD graduate assisted in the writing of sections 2.5.2 and 2.9.

TABLE OF CONTENTS

Page

Page

LIST OF FIGURES

Figure Page

Figure | Page

LIST OF TABLES

Table Page

1.0 INTRODUCTION

Concrete is the most used building material and its consumption is increasing in all countries around the globe. The materials to make concrete are readily available and are relatively inexpensive when compared to other building materials such as wood and steel. Concrete production is relatively simple, and its application covers a large variety of civil infrastructure. High performance concrete (HPC), which was developed about 35 years ago, is defined as 'a concrete in which certain characteristics are developed for a particular application' (Brandt 2008). These characteristics include enhanced strength and durability properties. The only disadvantage to concrete is its brittleness, which is characterized through its low tensile strength and poor resistance to crack opening and propagation (Brandt 2008). Thus, the development of HPC reinforced with dispersed fibers plays an important role.

1.1 FIBER REINFORCED CONCRETE (FRC)

Fiber reinforced concrete (FRC) is concrete with the incorporation of dispersed fibers. There are a wide variety of fiber material types (e.g. steel, synthetic, glass and carbon etc.). The main role of FRC is to control the crack opening and propagation. Moreover, it has been established that synthetic fibers of uniform size (nominally 1" or greater) can increase fracture toughness and ductility of concrete, reduce the potential for cracking and if cracking occurs, reduce crack widths and lengths (Folliard et al., 2006). Smaller fibrillated (micro-fibers) have also shown benefits for reducing plastic shrinkage cracking when concrete is still in the fresh state. However, blending fibers of different sizes, both length and thickness, and composition, to improve performance have not been thoroughly investigated and are thus not well understood. The potential for reduction in cracking exists, however, as evidenced by a recently constructed concrete bridge deck - Willamette River Bridge on I-5 in Eugene, OR. This bridge deck experienced significant cracking without fibers for spans 1, 2 and 4-9. These deck sections required crack sealing after construction resulting in increased construction costs and delays in opening the bridge to the public. Span 3, however, was constructed with a fiber blend (mixed fiber size and type), and to date no cracking has been observed and thus no crack sealing was

needed. Fiber incorporation into concrete has been shown to provide increased durability, but investigations into mixed fiber sizes have not been conducted.

1.2 RESEARCH SCOPE

The goal of this thesis is to investigate the potential for mixed fiber blends to reduce shrinkage and ultimately cracking risk in HPC. DOTs need additional tools to reduce (if not eliminate) cracking risk of bridge decks (Brown et al., 2006). Recommendations for dosage rates of mixed fiber blends will be provided to aid in specification development. This thesis was organized into 5 chapters. The following outline provides a brief description of the chapter contents:

Chapter 2: Literature Review – The literature review highlights current knowledge behind cracking mechanisms of HPC. Shrinkage mitigation techniques and the test methods used are explained. The effect of Synthetic (polypropylene) fibers on toughness, mechanical properties, volume stability, and durability is discussed. Also, a brief overview of past DOT research on FRC was carried out.

Chapter 3: Materials and Methods- This chapter presents the materials used, which include ASTM C150 Type I/II cement (Lafarge) , class F fly ash from Centralia WA plant (Lafarge), Ground Granulated Blast-Furnace Slag (GGBS) (Lafarge), Silica Fume (BASF), and admixtures (GRACE) . Methods used as per ASTM are further described.

Chapter 4: Results and Discussion- Mechanical properties, drying shrinkage, cracking risk and durability results are discussed. The mixture design is based on a standard HPC ODOT bridge deck mixture (w/cm = 0.37, 30% fly ash, 4% silica fume). In addition to the blended synthetic fiber investigation, the effect of supplementary cementitious material (SCM) content, total cement content, and aggregate type on drying shrinkage and cracking risk was also assessed. Durability results for freeze thaw resistance and chloride ion penetrability were reported.

Chapter 5: Conclusions and Recommendations: Conclusions on effect of synthetic fiber blends on the cracking risk of HPC are given. Recommendations for use in the field and future work were suggested.

1.3 NOMENCLATURE

In chapter 2 fiber dosages are usually specified as a percentage by volume. Fiber dosages in chapter 3, 4 and 5 are in units of lb/yd^3 and used 85% macro and 15% micro synthetic fibers. Micro fibers are often referred to as "Type 1", "fine", "fibrillated" and "monofilament". Macro fibers are often referred to as "Type 2", "coarse", "collated" and "structural". Listed below are acronyms and abbreviations used throughout this thesis:

OPC- Ordinary portland cement
CC- Conventional concrete
HPC- High Performance Concrete
SCM- Supplementary cementitious material
FA- Fly Ash
SF- Silica Fume
GGBS- Ground granulated blast-furnace slag
SRA- Shrinkage Reducing Admixture
w/cm- water to cement ratio

2.0 LITERATURE REVIEW

2.1 HIGH PERFORMANCE CONCRETE (HPC)

Typically, HPC differs from conventional concrete (CC) through the variety of cement types, supplementary cementitious materials (SCM's), aggregates, chemical admixtures as well as the inclusion of fibers. These mixtures typically have a high cementitious material content (>600lb/yd^3), low water-to-cement ratio (<0.40), and use a wide variety of chemical admixtures to provide good workability and protection against a variety of durability concerns. According to Kosmatka and Wilson the following are some of the characteristics that may be required in HPC:

- Enhanced Durability
    - High Abrasion Resistance
    - Low permeability and diffusion
    - Resistance to chemical attack
    - High resistance to freeze-thaw, and deicer scaling damage
    - Resistance to alkali silica reaction (ASR)
- Enhanced Engineering Properties
    - High Strength
    - High early strength
    - High modulus of elasticity (MOE)
    - Toughness and impact resistance
    - Volume Stability (Shrinkage Control)
- Other Enhanced Properties
    - Ease of placement
    - Temperature control
    - Compaction without segregation
    - Inhibition of bacterial and mold growth (2011)

For bridge decks, a normal strength concrete with high durability and low permeability is considered HPC (Lane 2010). Recently HPC has become widely utilized in applications where severe environment leads to premature deterioration (Radlinski and Olek 2010). In addition, HPC almost always implies the use of fly ash or slag and silica fume. For example, fly ash is known to reduce early strength (Juenger et al. 2008) and early age resistance to chloride –ion penetration, as well as resistance to salt scaling (Radlinski and Olek 2010). Furthermore, fly ash has reported to be sensitive to curing conditions when compared to CC (Bentz 2002, Bouzoubaâ et al. 2004, Radlinski and Olek 2010). Slag has been known to delay setting time when replacement levels exceeded 40% (Brooks et al. 2000). ACI Committee 233 (2004) report states that delays in setting time can be expected when more than a 25% slag replacement for portland cement is used in concrete mixtures (Juenger et al. 2008). Although, Juenger et al. later concluded that slag had little to no effect on the setting time and early strength of HPC (Juenger et al. 2008). On the other hand silica fume may increase susceptibility to shrinkage cracking in hot weather (Al-Amoudi et al. 2007), and potentially reduced resistance to freezing and thawing (Palecki and Setzer 2006, Radlinski and Olek 2010).

2.2 CRACKING IN HPC

Shrinkage is one of the most common cracking mechanisms in HPC. Cracking occurs when the tensile stress exceeds the tensile strength of the concrete. This is a time dependent phenomenon since both the stress and the strength change at early ages (Delatte 2006). Cracking can severely hinder the durability of bridge decks. In freeze-thaw climates, they provide direct access for water, which may expand during freezing cycles and increase the potential damage to the concrete (Darwin et al. 2010). In the presence of deicing chemicals, they severely compromise the corrosion protection provided by the concrete to the reinforcing steel (Lindquist et al. 2006). According to Darwin et al. “Recent research demonstrates that even epoxy-coated bars are affected, with bars located at cracks exhibiting significantly more disbondment between the epoxy coating and the reinforcement than bars located in uncracked concrete” (2010).

2.3 CHEMICAL AND AUTOGENEOUS SHRINKAGE

Chemical shrinkage occurs due to a reduction in absolute volume of solids and liquids in the hydrating paste. The absolute volume of cement and water is greater than the eventual hydration products due to chemical reactions forming new products of higher density than the original reactants. This reduction in volume is commonly referred to chemical shrinkage. According to Jensen and Hansen autogenous deformation is defined as "the bulk deformation of a closed, isothermal, cementitious material system not subjected to external forces" (Jensen and Hansen 2001). Autogenous shrinkage occurs "when the internal relative humidity is reduced below a given threshold (extra water is not available), self-desiccation of the paste occurs, resulting in a uniform reduction of volume" (Kosmatka et al. 2011). Therefore, autogenous shrinkage can be mitigated by keeping the surface of concrete continually wet (wet curing). In ordinary portland cement concretes with high w/cm (> 0.42), autogenous shrinkage is negligible when compared to drying shrinkage (Holt 2001). In HPC, as the internal RH decreases due to increasing water demand, the resulting capillary pressure arising from water leaving small capillaries can be high enough to cause these pores to collapse, as a result in this collapse macroscopic shrinkage may occur – termed autogenous shrinkage (Mehta and Monteiro 2006). While in HPC with low w/cm with the addition of silica fume, autogenous shrinkage can be significant enough to induce micro- or macro-cracking and may reduce the concrete quality (Lura 2003).

2.4 PLASTIC SHRINKAGE

Plastic shrinkage cracks are formed while the concrete is in the plastic stage (has not set). Plastic shrinkage cracking occurs when the rate of evaporation of moisture from the surface exceeds the rate at which moisture is being supplied from bleed water. Rapid drying of the surface (i.e. evaporation from the sun) of the plastic concrete causes it to shrink and crack. Wang et al. describe plastic shrinkage in the 4 phases (2001). The first phase is plastic settlement, which takes effect when the concrete is placed. During plastic settlement the solid particles start to settle and water rises or bleeds, forming a layer of water on the surface. In phase 2 the concrete surface water evaporates in hot or windy weather. This happens when the rate of evaporation exceeds the rate of bleeding, causing the concrete to shrink. Shrinkage can occur before and/or during concrete setting, and is presumably attributed to the pressure that develops in the capillary

pores of concrete during evaporation. Additionally, according to Wittmann the capillary pressure is generated within the concrete which reduces the distance between the concrete solid particles, causing the concrete to become compacted or shrunken (1976). Phase 3 is autogenous shrinkage which is the result of cement hydration. According to Wang et al. "Hydration products form around the cement particles and fill up the water-filled spaces between solid particles in concrete and as hydration proceeds, the hydration products develop into a network that bonds all loose aggregate particles together" (2001). Autogeneous shrinkage can contribute a few hundred microstrains. The last phase, phase 4, is secondary plastic shrinkage. At this stage the concrete begins to harden and cement hydration slows. Plastic shrinkage tends to cease as concrete strength develops.

Furthermore, the use of SCM's and low water-to-cement ratios has increased the potential for plastic shrinkage cracking (Wang 2001). To prevent plastic shrinkage cracking, one of the most widely accepted methods is the use of randomly distributed fibers, particularly fine synthetic fibers with a volume fraction below 0.5% (Naaman 2005).

2.4.1 Plastic Shrinkage Cracking in the Field

Plastic shrinkage cracking generally occurs within the first 24 hours after the cement begins to hydrate. Shown in Figure 2.1 is an example of plastic shrinkage cracking behavior. The cracks are generally found parallel to one another. Plastic shrinkage cracking often occurs in high-quality concrete when curing is not promptly or adequately applied, and appropriate measures to avoid excessive evaporation have not been taken. According to Walker and co-workers the intrinsic quality of the concrete is not necessarily adversely affected by plastic shrinkage cracking (Walker et al. 2006). However, plastic shrinkage remains a major concern since cracking at early ages can accelerate deterioration, promote steel corrosion, and cause significant durability concerns in the long run (Banthia and Gupta 2006).

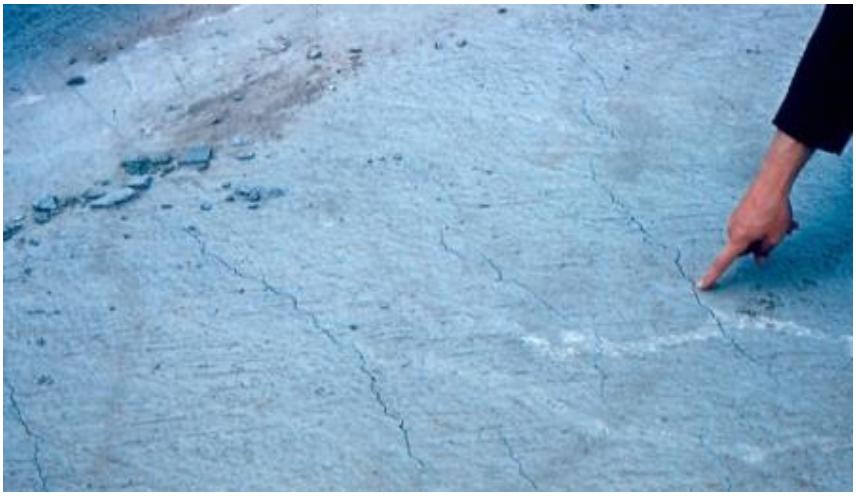

Figure 2.1: Plastic Shrinkage Crack Example (ACI 2014)

Plastic settlement is caused by uneven settlement of fresh concrete over obstructions such as reinforcing steel (Saadeghvaziri and Hadidi 2002). Figure 2.2 shows an example of plastic shrinkage cracking due to uneven settlement.

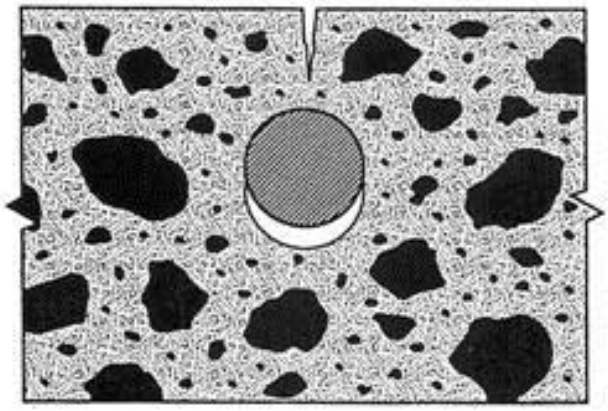

Figure 2.2: Plastic shrinkage cracking due to uneven settlement (Saadeghvaziri and Hadidi 2002)

According to Walker and co-workers, "This cracking is directly related to shrinkage and settlement of the concrete over the steel as the bleed water leaves the concrete and the volume of the paste is diminished, and may be accompanied by segregation of the coarse aggregate from the paste" (Walker et al. 2006).

2.4.2 Test Methods

ASTM C 1579-13 is the standard test method for evaluating plastic shrinkage cracking of restrained fiber reinforced concrete (using a steel form insert). "The test method is intended to

evaluate the effects of evaporation, settlement, and early autogenous shrinkage on the plastic shrinkage cracking performance of fiber reinforced concrete up to and for some hours beyond the time of final setting" (ASTM 2013). Both setting time and penetration tests should be performed in accordance to ASTM C403/C403M during the testing procedure. This test requires an environmental chamber where temperature and relative humidity can be controlled, although commercially available heaters, humidifiers, and de-humidifiers can be used to achieve the desired environmental conditions. A fan is used to simulate wind and an evaporating pan is used to monitor the rate of evaporation. After the concrete is placed the temperature and humidity must be recorded every 30 minutes, and the initial time of cracking may be recorded. Environmental conditions should be recorded until the mixture has set. Shown below in Figure 2.3 is the testing apparatus for ASTM C1579-13.

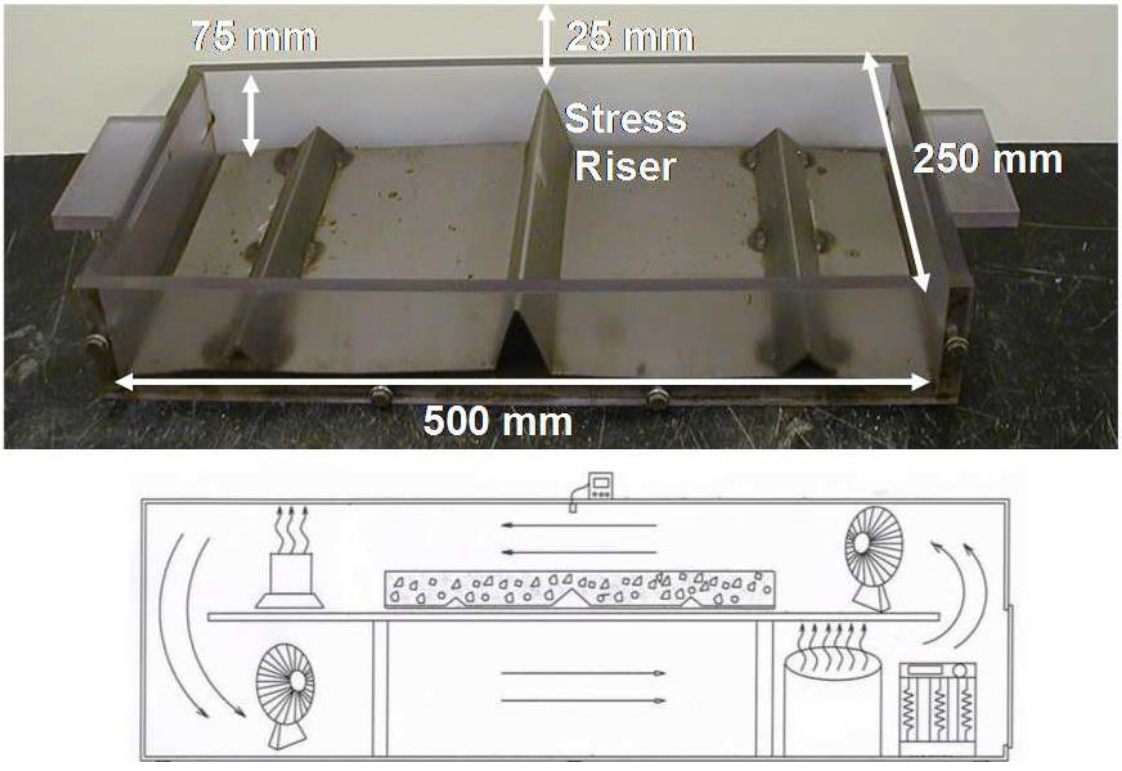

Figure 2.3: ASTM C1579-13 Testing Apparatus (Luna 2011)

After 24±2 hours the amount of cracks and crack widths can be measured to the nearest 0.1mm along the crack path over the stress riser in progressive order from one side of the panel to the other (ASTM 2013). Imaging analysis may be used for crack width

measurement. The average crack width can be calculated and should be reported to the nearest 0.002in (0.05mm).

2.5 DRYING AND RESTRAINED SHRINKAGE

The mechanism for drying shrinkage is best described by Radlinska and co-workers (Radlinska et al. 2008). According to them, drying shrinkage is caused by capillary tension. Internal or external drying causes the formation of "liquid-vapor interfaces (menisci)" inside the pores of the cement paste, which cause the generation of negative pressure inside the pore fluid. This negative pressure is known as capillary tension. Drying shrinkage is caused by external drying, in this case the liquid-vapor menisci form at the surface of concrete and self-desiccation occurs internally. The capillary tension pulls the pore walls together, which may cause the pore to collapse (Radlinska et al. 2008). When the pore collapses it causes the volume change observed as drying shrinkage.

The drying of concrete accounts for a major part of the total shrinkage. Drying shrinkage is caused by the evaporation of internal water in hardened concrete (Jianyoung and Yan 2001). Additionally, "Drying shrinkage is the result of evaporation from surfaces of a specimen when exposed to drying conditions and continuing hydration of cement, which is self-desiccation" (Ru et al. 2010). It is widely accepted that drying shrinkage is the consequence of a decrease in the internal relative humidity of the concrete (Hasen 1987). For a wet cured concrete specimen, the initial relative humidity can be considered equal to 100% (Andrade et al 1999). Ru et al. further explains the role of internal relative humidity on drying shrinkage in concrete:

> "When exposed to a drying environment with a lower constant relative humidity (and temperature), the evaporation of moisture from the surfaces of the specimen occurs, causing a decrease in the relative humidity of the surface layer. Hence, a difference in the relative humidity between the surface layer and the interior is created. With the onset of evaporation, a relative humidity gradient over the section of the concrete specimen is created and it is this gradient which drives the moisture diffusion within the paste." (Ru et al. 2011).

Drying shrinkage will continue to occur until the internal relative humidity of the cement paste reaches equilibrium with the atmospheric relative humidity (Radlinska et al. 2008). There are

many factors that affect the drying shrinkage of concrete. These factors include cement fineness, aggregate type, w/cm ratio, relative humidity, admixtures, curing, and specimen size (Hou and Wong 2000).

If concrete is restrained from shrinking freely, tensile stresses develop and often results in cracking, especially at early ages (Weiss et al. 1998). Restraint to shrinkage caused by the subgrade, reinforcement, or another part of the structure causes tensile stresses to develop in hardened concrete.

2.5.1 Drying and Restrained Shrinkage Cracking in the Field

The time at which drying shrinkage occurs depends on the rate of drying, but it is usually several months to 3-4 years after casting (PCA 2014). Typically contractions joints are placed in concrete to pre determine the location of drying shrinkage cracks (PCA 2014). In many cases drying shrinkage cracks are inevitable. Shown below in Figure 2.4 is an example of a drying shrinkage crack in a concrete bridge deck.

Figure 2.4: Drying Shrinkage Crack (Di Bella et al. 2012)

Where more restraint is provided by the reinforcement or surrounding structures drying shrinkage cracks will travel and propagate in different directions (see Figure 2.5).

Figure 2.5**:** Drying Shrinkage Crack (Restrained) (Luna 2011)

Cracking can be minimized by good workmanship, proper use of curing methods, proper proportioning of the mixture and sufficient jointing performed soon after hardening (Walker 2006). In jointed concrete, uncontrolled cracks may form if the joints were not formed early enough, are not working properly, or the shrinkage in the hardened state is excessive (Walker 2006).

2.5.2 Test Methods

ASTM C 157

Drying shrinkage is typically measured as total shrinkage resulting from a length change after a prescribed period of time. ASTM C 157 is one of the most accepted testing methods to measure the length change of hardened concrete. These specimens are exposed to controlled temperature and relative humidity. The length change is caused by forces other than externally applied forces or temperature changes. Measuring the change in length allows for the assessment of expansion or contraction of different concrete or mortar mixtures. This test method may be useful for testing samples that require nonstandard mixing or curing conditions.

ASTM C 1581

The restrained shrinkage ring test has been frequently used as a testing technique to identify potential cracking risk of concrete and mortar mixtures. There are two standard testing

procedures based on similar principles. The major difference is the concrete thickness, where ASTM C1581 uses 1.5 in (38mm) and AASHTO T334 specifies 3 in (76mm) ASTM C1581, 2009 and AASHTO T334-08, 2008). Figure 2.6 shows the dimensions and components of both the ASTM and AASHTO ring apparatus.

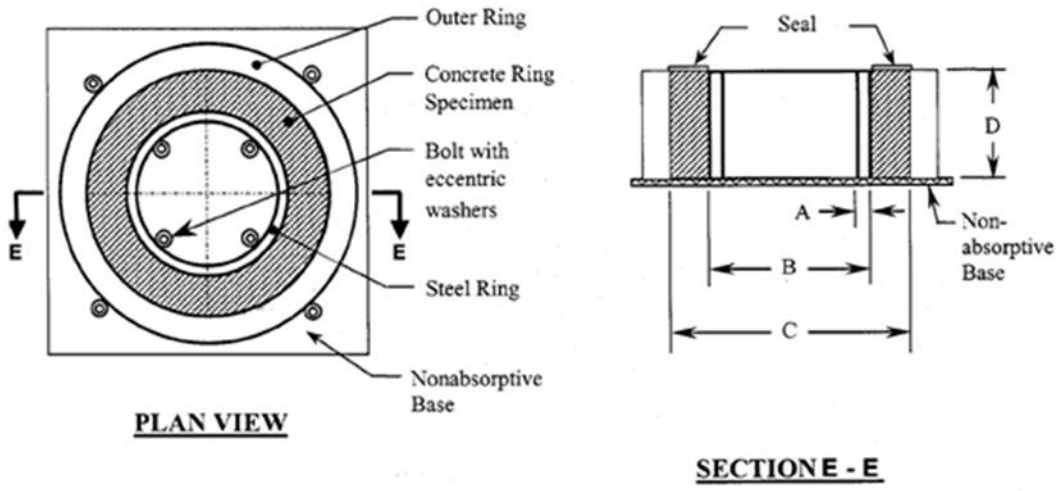

Figure Dimensions	ASTM	AASHTO
A	12.5 ± 0.13 mm	13 ± 0.4 mm
B	330 ± 3 mm	324 ± 5 mm
C	406 ± 3 mm	476 ± 5 mm
D	150 ± 6 mm	152 ± 5 mm

Figure 2.6: Dimension of rings test setup (ASTM, 2009)

Figure 2.7 shows a typical strain gauge reading from the time the concrete was initially cast, through the peak heat of hydration, during wet curing and then exposure to the drying environment followed by cracking.

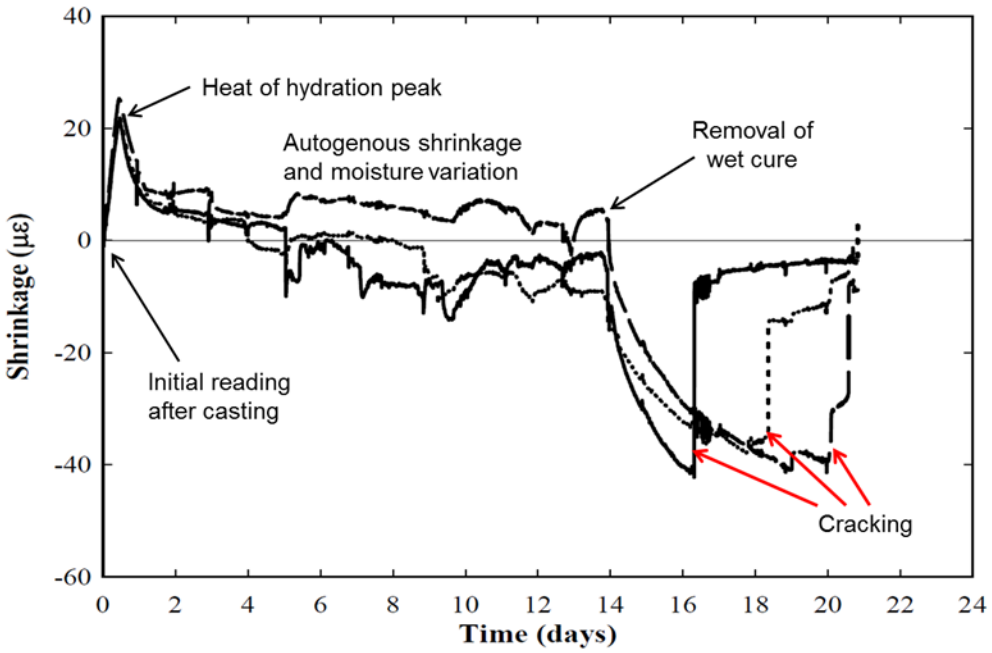

Figure 2.7: A typical averaged strain gauge reading in ring tests (3 replicates) (Fu, 2013)

The strain gauge reading was recorded almost immediately (~30 min.) after the specimens were cast and moved into the environmental chamber. It can be seen in Figure 2.7 that the steel ring first registered expansive strain due to the heat released from hydration of the concrete reaching a peak at about 24 hours after casting. After the removal of the outer mold (24hrs from casting), the concrete ring specimens were cured using wet burlap until the end of the desired curing duration. The concrete then cools over the next 24-hour period to the environmental chamber conditions of 23 C +/- 1.5 C. From this point until removal of the wet burlap the concrete most likely experiences some minor autogenous shrinkage. Some fluctuation in the strain gauge reading was also recorded during this period, which may be a result of moisture variation within the sample, or localized stress concentrations due aggregate/mortar arrangement against the steel ring. Once the burlap was removed the compressive strain due to drying and subsequent shrinkage of the concrete was observed. During the drying phase, a sharp jump in the strain gauge reading toward zero indicated cracking in the concrete. The time between exposure to drying and cracking is called time-to-cracking (days), which is an important parameter to evaluate the cracking resistance of the tested concrete. According to the strain gauge reading, an

averaged stress rate (psi/day) in the concrete can be calculated and used as another parameter in cracking risk evaluation. The cracking potential can be evaluated based on Table 2.1.

Table 2.1: Potential for cracking classification (ASTM 2009)

Net Time-to-Cracking t_{cr} (days)	Average Stress Rate, S (MPa/day)	Average Stress Rate, S (psi/day)	Potential for Cracking
$0 < t_{cr} \leq 7$	$S \geq 0.34$	$S \geq 50$	High
$7 < t_{cr} \leq 14$	$0.17 \leq S < 0.34$	$25 \leq S < 50$	Moderate-High
$14 < t_{cr} \leq 28$	$0.10 \leq S < 0.17$	$15 \leq S < 25$	Moderate-Low
$t_{cr} > 28$	$S < 0.10$	$S < 15$	Low

Table 2.1 also shows the qualitative cracking risk potential per ASTM, where concrete must remain crack free in the rings at least 14 days to be considered "moderately low" in cracking potential. Time-to-cracking is the time elapsed between initiation of drying and the cracking in the rings. Upon cracking, a sudden change will show in two or more strain gauges, which can also be confirmed by visual inspection. Stress rate at time-to-cracking was calculated according to ASTM C1581. Based on time-to-cracking or stress rate, a cracking potential can be assigned to each mixture (See et al, 2004). When determining the cracking potential classification, high priority should be given to stress rate at cracking. Stress rate better quantifies the stress of the concrete, which is directly related to cracking potential. On the other hand, time-to-cracking is involved in stress rate calculation. In other words, stress rate indicates a more comprehensive evaluation. Shown below is the stress rate equation in accordance with ASTM C1581.

$$\delta_{day} = \frac{G * \alpha}{2 * \sqrt{t}}$$

where:
G = 10.47×10^6 psi
α = slope of strain/sqrt of time graph (10^{-6})
t = average time of cracking

The constant "G" is based on the ring dimensions used in this test method. According to ASTM the stress rate should be calculated at the time-to-cracking or when the test is terminated. However, at the time-to-cracking the stress rate is high due to the sharp jump in the strain, and

when the test is terminated the stress rate is low since the rings have already cracked. Therefore, the stress rate was calculated prior to cracking where there was enough strain data to consistently achieve a coefficient of determination (R2) value above 98%.

2.6 THERMAL CRACKING

Concrete temperature rises after placement due to hydration. Thermal cracking occurs due to excessive temperature differentials within a concrete structure or its surroundings. The temperature differences causes the cooler portion to contract more than the warmer portion, which restrains the contraction and causes cracking when the retraining tensile stresses exceed the in-place concrete tensile strength (NRMCA 2009). According to Walker et al. "Thermal effects on concrete volume can cause cracking with a disposition similar to that caused by drying shrinkage and, in fact, thermal and drying effects will often occur in concert" (2006). Material compatibility may also influence the performance HPC against thermal effects. Since common aggregate materials differ considerably in their CTE, they consequently exert considerable influence on the concrete CTE (Scanlon and McDonald 1994, Lane 1994). Thermal cracking is most significant in mass concrete structures such as dams. Thermal cracking can still occur in structures that are not mass concrete structures. In most cases the upper surface of pavements or slabs is exposed while the bottom surface is relatively protected. A significant temperature differential between the bottom and top surface can cause cracking.

2.6.1 Thermal Cracking in the Field

Transverse cracks, such as those shown in Figure 2.8, are the result of thermal expansion and contraction combined with other shrinkage mechanisms.

Figure 2.8: Thermal Crack Example (Saadeghvaziri and Hadidi 2002)

According to the National Ready Mixed Concrete Association (NRMCA), cracks usually occur perpendicular to the longest axis of concrete (transversely) and may become apparent any time after placement. These cracks usually occur within the first year or summer-winter cycle (NRMCA 2009).

2.7 FREEZE-THAW CRACKING

It is imperative to provide concrete that will endure freezing and thawing cycles. The effect of freeze/thaw cycles on concrete is well documented. The accumulative effect of freeze/thaw cycles on non-air entrained concrete will eventually cause cracking, scaling and crumbling of concrete. The most effective way to provide freeze/thaw protection is through the addition of air entraining admixtures. Air entraining admixtures add a uniform distribution of air voids to the cement paste during the mixing action (Kosmatka 2011). Concrete that lacks either sufficient strength (maturity) or an adequate air-void system will develop laminar cracking if critically saturated and exposed to freezing and thawing cycles (Walker et al. 2006). Deterioration is usually in the form of scaling or aggregate pop-outs but severe deterioration can lead to cracking.

In bridge decks freeze-thaw attack is of high concern due to exposure conditions of most decks and impacts the service-life of the structure.

2.7.1 Freeze Thaw Testing Methods

ASTM C666 is used to determine the resistance of concrete to freezing and thawing cycles. This test method follows one of two procedures. In Procedure A, the concrete is subjected to rapid freezing and thawing in water. In Procedure B, the concrete is subjected to rapid freezing in air and rapid thawing in water. These two procedures both determine the effects of variations in proportions, curing and soundness of the aggregates. The low temperature of the freeze cycle is -17.8 ºC (0 ºF) and the target thaw temperature is 4.4 ºC (40 ºF).

2.8 REINFORCEMENT CORROSION CRACKING

Normally, the high pH in concrete protects the reinforcing steel from corrosion. It is well known that a passive film is created around the surface of the steel reinforcement at highly acidic levels pH levels exceeding 12) (PCA 2014). However, deicing chemicals (chloride ions) or carbonation may break or negate the passive layer and the corrosion is lost. Corrosion and the resulting expansion of the reinforcement will cause lateral cracking in the plane in which the reinforcement is situated (Walker et al. 2006). HPC inherently has low permeability due to the low water-to-cement ratio, and the use of SCM's such as silica fume. Therefore, it is of paramount importance that randomly distributed fibers do not decrease the permeability of HPC.

2.8.1 Test Methods

The rapid chloride permeability test (RCPT), ASTM C1202, is used to determine the concrete's ability to resist chloride ion penetration. This rapid test method determines the electrical conductance of concrete to determine the ability of concrete to resist the penetration of chlorides. A constant potential difference of 60 V is applied to the ends of the specimen. One end is immersed in a 3% sodium chloride solution, while the other end is immersed in a 0.3 N sodium hydroxide solution. The total charge passed through a 2 in (50 mm) thick, 4 in (100 mm) diameter piece of concrete during a 6-hour period provides an indication of the permeability. The

sample age may have a significant effect on the results. Samples should be cured for a minimum of 28 days, unless specified otherwise. Typically, in most concrete, the permeability is reduced if the sample is properly cured.

However, issues have arisen with using ASTM C1202 for determining the chloride permeability. During testing, the conductivity of the specimen may change due to the migration of chloride and hydroxyl ions (Beaudoin et al., 2000). Furthermore, with the addition of some SCMs (e.g. silica fume) a false estimate of the chloride permeability may result (Feldman et al. 1999). In mixtures that have low porosity, overheating of the specimens may occur, causing the test to be ended prematurely (Adam, 2009). Although there is dispute to the accuracy of this test method, it is the acceptable test method for chloride permeability according to ODOT (ODOT 2008).

2.9 SHRINKAGE MITIGATION

There are various conventional techniques to reduce shrinkage and cracking in HPC. These techniques apply during the mixture design and structural design, as well as the curing methods used thereafter. Currently there are various innovative shrinkage mitigation techniques. These include the use of admixtures such as shrinkage reducing admixture (SRA), shrinkage compensating cements (SCC), and internal curing methods such as using light weight fine aggregate (LWFA) and super absorbents polymers (SAP) (Kovler and Jensen 2005). However, there are also many traditional methods to reduce shrinkage. These methods include water cement ratio, the use of SCM's at various replacement levels, aggregate type, and reinforcement.

2.9.1 Water-to-Cement Ratio

According to Kosmatka and co-workers the most important controllable factor affecting drying shrinkage is the water to cement ratio (Kosmatka et al. 2002). A denser cement paste matrix resulting from a lower w/cm, contributes to decreased permeability. Therefore, less drying shrinkage is expected due to less evaporation after curing. It is estimated that the drying shrinkage is reduced by up to 30 microstrains per 9.9 lb/yd^3 (5.9 kg/m^3) of water removed from the mix design (Babaei and Fouladgar 1997).

2.9.2 SCM's

Increasing the amount of fly ash in HPC has been observed to reduce the amount of drying shrinkage. The drying shrinkage decreases with the addition of fly ash due to the overall reduction of OPC, thereby lowering the reaction rate which may lead to a slower development of very fine pores that could lead to early-age autogeneous shrinkage (Fu, 2011). Figure 2.9 below shows that drying shrinkage was reduced as fly ash replacement levels are increased.

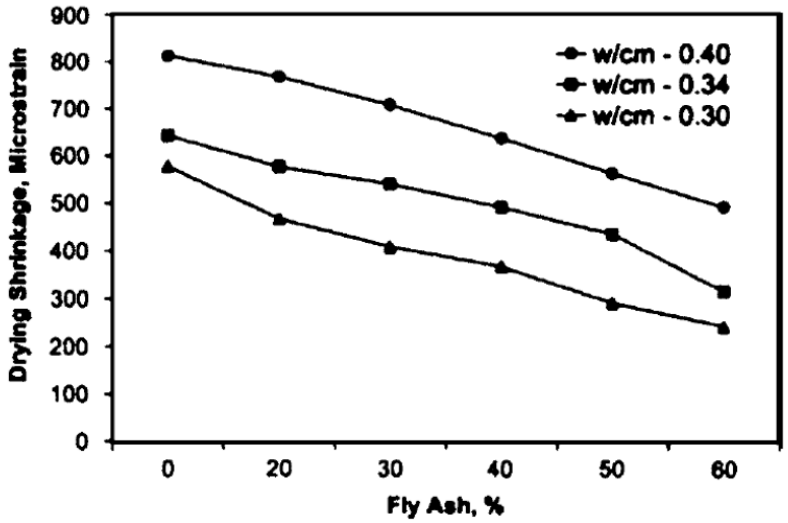

Figure 2.9: Drying shrinkage variation with different fly ash replacements (Kumar et al. 2007)

In addition, a reduction of drying shrinkage was reported at different water to cement ratios, and roughly the same amount of shrinkage reduction (about 300 microstrains) was noticed from 0% to 60% replacement levels.

Similarly, ground granulated blast-furnace slag (GGBS) has also shown shrinkage reduction. Jianyong and Yan investigated the effect of GGBS on both creep and drying shrinkage (Jianyong and Yan 2001). Shown in Figure 2.10 are drying shrinkage results from three HPC mixtures. The HPC mixture used a crushed lime stone for the coarse aggregate and quartz for the fine aggregate to achieve a low shrinkage mixture (<400 microstrains). Concrete A was the control, Concrete B used a 30% GGBS cementitious material replacement, and Concrete used a GGBS 30% and 10% silica fume cementitious material replacement. The water to cement ratio was 0.26.

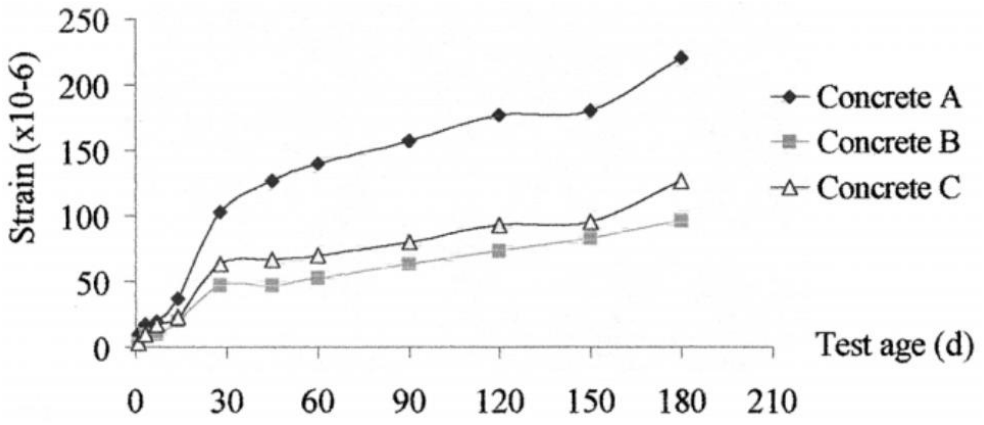

Figure 2.10: Drying shrinkage of HPC concrete with GGFS (Jianyong and Yan 2001)

Ultimately, drying shrinkage was reduced by over 50% at 180 days of drying when adding GGBS alone. The drying shrinkage was reduced further when using both GGBS and silica fume. This could be attributed to the well-known synergistic effect when OPC, GGBS or fly ash, and silica fume are used.

Conversely, silica fume as a cementitious material replacement alone has shown negative results in shrinkage reduction. Zhang and co-workers investigated the effect of silica fume on both autogeneous and drying shrinkage (Zhang et al. 2003). Two replacement levels (5% and 10%) and three water to cement ratios (0.26, 0.30 and 0.35) were used. Also, the prisms were wet cured for 7 days prior to exposure to drying and monitored regularly for 98days. Their research concluded that autogenous shrinkage increased with decreasing water to cement ratio and increasing silica fume content. The drying shrinkage results also showed no significant reduction. The drying shrinkage decreased with when the lower 0.26 and 0.30 water to cement ratios were used. Furthermore, the drying shrinkage was similar at the lower water to cement ratios. The 0.35 water to cement ratio had the highest influence at all dosage rates, increasing the total shrinkage by roughly 100 microstrains on the control mixture and approximately 50 microstrains at both 5% and 10% silica fume replacement levels. Ultimately, Zhang and co-workers showed the water to cement ratio had more impact on drying shrinkage than the silica fume replacement levels.

2.9.3 Aggregates

Intrinsically, shrinkage occurs in the cement paste, however; it is mechanically restrained by the aggregates (specifically the coarse aggregate) within the concrete (Ru et al. 2011). The mechanical properties of aggregates, such as the elastic modulus, also affect shrinkage in concrete (Goto and Fujiwara 1976). According to Saje and co-workers, the shrinkage of a concrete made with a higher-strength rock is less than aggregate made with a lower strength rock (Saje et al. 2011). Hikotsugo et al. found that the elastic modulus and drying shrinkage of the coarse aggregate were directly proportional (Hikotsugo et al. 2007). Neville explained that the restraint of aggregate on shrinkage depends on the ratio of modulus of elasticity of the aggregate to the paste (Neville 1995). Given that coarse aggregate restrains shrinkage, an increase in course aggregate content should reduce drying shrinkage. Zhang et al. investigated the effect of w/cm ratio and coarse aggregate content on drying shrinkage of concrete. Drying shrinkage decreased as the coarse aggregate content was increased (Zhang et al. 2014).

According to Ru and co-workers, "The moisture diffusing from the interior to the surface may be impeded by the aggregate and any extra moisture released from the aggregate can disturb the equilibrium of the diffusion process" (Ru et al. 2011). If the moisture cannot diffuse through the aggregates than the diffusion path will increase. In addition, moisture may also diffuse through the interfacial transition zone (ITZ). Generally, the ITZ is more porous than the main body of the paste; therefore, moisture diffuses easier through the ITZ. Also, water may be absorbed by the aggregates during the initial 'wet' condition but released when drying occurs; this will also disturb the moisture diffusion in the paste (Ru et al. 2011). Thus, the coarse aggregate has a significant effect on the drying shrinkage of concrete.

2.9.4 Curing

Curing is one of the most effective methods to reduce drying shrinkage. In addition, it plays an important role on strength development and durability of concrete (Zemajtis, 2014). There are various methods to provide external curing for concrete. Fogging, spraying or wet burlap will prevent shrinkage until the concrete has hardened. Curing compounds, which are applied

immediately after finishing, are also commonly used. In a study by Nasiff and co-workers it was found that dry curing had the highest shrinkage, followed by the curing compound, and then moist curing (Nasiff et al. 2003). After hardening and the external curing source has been removed, the concrete will shrink when exposed to a relative humidity of less than 100 % and have the potential for cracking caused by stress generation during shrinkage (Kosmatka et al. 2002). Therefore, the external curing should be prolonged long enough to eliminate drying shrinkage during the curing process (Nilson et al. 2004). However, because the permeability of HPC drops quickly in the first few days, external curing might not be sufficient to eliminate drying shrinkage.

2.9.5 Reinforcement

Reinforcement in concrete restricts drying shrinkage, but does not prevent it. Shrinkage in reinforced concrete may be less than the shrinkage in unreinforced concrete. However, the restraint provided by reinforcement might increase stress due to shrinkage and result in cracking. The amount of shrinkage depends on the quantity of steel placed in the concrete (Kosmatka et al. 2002). It also depends on the bond. If the concrete does crack; reinforcement is beneficial for reducing the size of the cracks. By placing smaller bars in the concrete to achieve the needed requirement of steel will perform better at controlling crack width than utilizing larger bars (Babaei and Fouladgar 1997). According to Babei and Purvis, "Large bars increase the possibility of the formation of a plane of weakness over the bars thereby increasing the risk of cracking" (Babei and Purvis 1994). Ramey and co-workers recommend that No. 5 bars or smaller be used (Ramey et al. 1997).

2.9.6 Shrinkage Compensating Cement (SCC)

SCC involves the use of expansive cement, which when mixed with water forms a paste and after setting, increases in volume (Chen and Chung 1996). The expansive cement is used to compensate for the volume decrease due to shrinkage. The use of SCC remains limited partly due to the need to allow for the concrete to expand prior to the drying shrinkage (Chen and Chung 1996). This limits the amount of application and adds to the inconvenience of usage.

Moreover, SCC requires more water than OPC due to the fact that the expansion is associated with the formation of ettringite or high sulfate calcium sulfoaluminate (Chen and Chung 1996). Type K cement is one type of SCC. As Type K cement hydrates, it forms ettringite which expands during the first several days of curing. After the maximum amount of expansion has occurred, the Type K cement concrete will shrink at a rate similar to that of OPC. However, due to the additional time spent in a state will typically gain additional beneficial strength to resist shrinkage forces. If the specimen is reinforced, the expansion of Type K cement may cause compressive stresses in the concrete due to the restraint of the reinforcement. Then the concrete shrinks internal compressive stresses decrease. Since the concrete is already in an expanded state the shrinkage may not be enough to induce tensile stresses that are greater than the tensile capacity of the concrete.

2.9.7 Admixtures

Shrinkage reducing admixtures (SRA) have been shown to be successful in reducing autogeneous and drying shrinkage, as well as the potential for cracking. Work by Bentz showed that SRA's are successful in reducing plastic shrinkage and autogeneous deformation due to the reduction in capillary tension (Bentz 2006). SRA's reduce the capillary tension by as much as 50% and the corresponding tensile forces that occur in hardening concrete (Bentz 2006). In addition, Bentz showed that SRA reduced drying shrinkage in cement paste when there is a potential for drying shrinkage. Some chemical admixtures do not have much effect on shrinkage. Air entrainment typically has little to no effect on drying shrinkage (Kosmatka et al. 2002). Conversely, using an accelerator can increase shrinkage. This is caused by a rapid increase in the heat of hydration and can promote drying shrinkage. Some research suggests that superplasticizer can increase drying shrinkage. Work by Atis showed that concrete with super plasticizer increased shrinkage by up to 50% (Atis 2003).

2.9.8 LWA and SAP

Research since the early 1990s has shown that saturated light weight aggregate (LWA) could provide internal curing to mitigate autogenous shrinkage in concretes incorporating silica fume,

thereby reducing shrinkage related stresses and the potential for early-age cracking (Hammer 1992). Momentum in the area of internal curing using saturated LWA's has increased since the year 2000 with increasing evidence of application of internal curing in field concretes (Roberts 2004). Internal water curing using saturated LWFA or SAP, which has become increasingly popular options in the last 10 years (Roberts 2004), is capable of providing internal sources of water that could replace the water consumed by the hydration process. Several field applications have shown that autogenous shrinkage in HPC can be significantly mitigated using this type of internal curing approach (Cusson et al. 2008 and Villarreal 2008). Recent research investigating free and restrained shrinkage of high performance concrete prism test samples incorporating internal curing showed that the reduction in autogenous shrinkage corresponded to a reduction in the generation of tensile stresses (Cusson and Hoogeveen 2008).

Super absorbent polymers (SAP) have also been analyzed as internal curing agents. One concern with SAP is that it generates voids in concrete and thus reduces strength. Since it generates voids SAP's can also be used to replace air entrainment admixtures and to improve the frost resistance of concrete. However, the internal curing provided by the SAP may enhance the degree of hydration and thereby increase strength (Jensen 2013). Like with LWA shrinkage is mitigated by slowing down or preventing the loss of water. Work by Jensen showed that autogenous shrinkage in an ultra-high-performance cementitious binder can be controlled by very small (0.2%-0.4% by volume) amounts of SAP (Jensen and Hansen 2002).

2.10 FIBER-REINFORCED CONCRETE

Fiber-reinforced concrete (FRC) is concrete containing fibers to increase its structural integrity. The main role of dispersed fibers is to control the crack opening and propagation (Brandt 2008). Fiber types may include steel, synthetic, glass and natural fibers. Plain portland cement concrete is an inherently brittle material, with low tensile strength and strain capacity (Sharma 2013, Folliard et al. 2006). While the traditional means of overcoming these inherent flaws has been to add steel reinforcing bars at specified locations in the matrix, during the past century there have been developments to use randomly oriented, discrete fibers to remedy these weaknesses. This is known as fiber-reinforced concrete (Folliard et al. 2006). The use of randomly distributed fibers may improve or control the initiation, propagation or coalescence of cracks (Sharma 2013).

2.10.1 Theory

In theory, the addition of fibers should increase ultimate strength and fracture toughness. According to Cha et al., fibers intersect micro cracks in concrete and bridge the gap between two surfaces of the crack, as shown in Figure 2.11. Under loading conditions when a crack starts to propagate, the fibers apply a restraining force, opposing to the crack propagation.

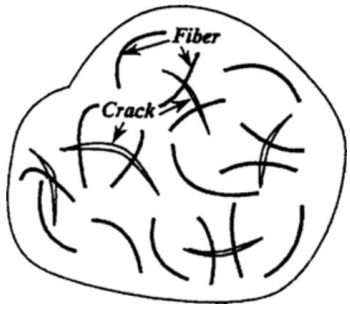

Figure 2.11: Fibers bridging gap between 2 surfaces of cracks (Cha et al. 1998)

It is logical to assume that the restraining force applied by the fibers is coming from the friction and cohesive force between the fiber and the matrix material (Cha et al., 1998). However, cohesive and frictional forces can vary depending on the fiber geometry, volume fraction and texture. Fine fibers control opening and propagation of microcracks as they are densely dispersed in the cement matrix, and longer fibers control larger cracks (Brandt 2008).

2.10.2 Synthetic Fibers

Synthetic fibers have become attractive in recent years as reinforcements for cementitious materials. Fiber types that have been incorporated into cement matrices include polyethylene (PE), polypropylene (PP), acrylics (PAN), polyvinyl alcohol) (PVA), polyamides (PA), aramid, polyester (PES) and carbon. The physical properties of synthetic fibers are highly variable. The most commonly used synthetic fibers are made from polypropylene (Folliard et al. 2006).

Polypropylene is a thermoplastic polymer used in a wide variety of applications including packaging, textiles and rope among others. Like most polymer based materials polypropylene is resistant to chemicals and fatigue. Manufacturers make two types of fiber, which include macro-

synthetic and micro synthetic, often referred as type 1 and type 2 synthetic fibers respectively. Macro-synthetic fibers are also often referred to as structural fibers since they are used to carry load. These fibers range from 1-2in length and have a young's modulus between 725-1450 ksi (5-10 GPa). Micro-synthetic fibers are mainly used for early age cracking (plastic shrinkage cracking), range from 0.25-1 in length and have a young's modulus of 435-725 ksi (3-5 GPa). According to manufacturers, the use of polypropylene fibers will reduce plastic shrinkage cracking; improve shatter, impact and abrasion resistance; and reduce damage from freeze/thaw attack. Manufacturer dosage rates vary, but most suggest a minimum 3lb/yd^3 of concrete. Researchers present dosage rates as a percentage of concrete volume, usually between 0 and 0.75%

Effect on Toughness

In addition to the benefits claimed by manufacturers, one of the material properties with most significant improvement is toughness. Toughness is the ability for a material to absorb energy and plastically deform without fracturing. Shown below in Figure 2.12 is a Load-deflection diagram that highlights the increase in toughness using FRC.

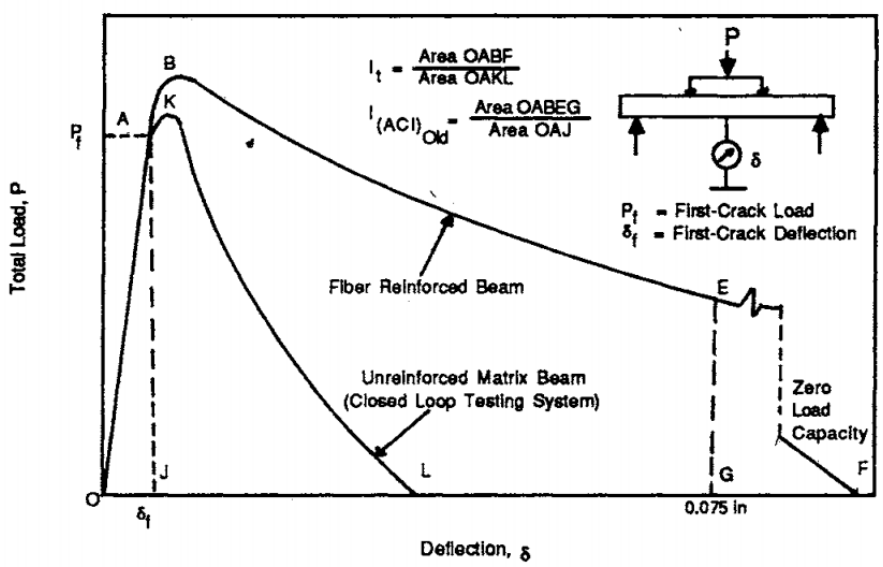

Figure 2.12: Flexural Performance, ASTM C 1018 (Now ASTM C 1609) (Gopalaratnam et al., 1991).

Plain concrete is a brittle material, and when loaded to fracture does not continue to carry load or deflect. FRC is able to continue to carry load and deflect after it has reached its fracture strength. Although toughness is a desirable property for any structural material it is not related to any parameters used in structural design However, the performance of concrete structures (bridge-decks, slabs, pavements etc.) is critical therefore; the use of FRC is easily justified.

Figure 2.13 below shows load-deflection curves for polypropylene FRC using various dosage rates.

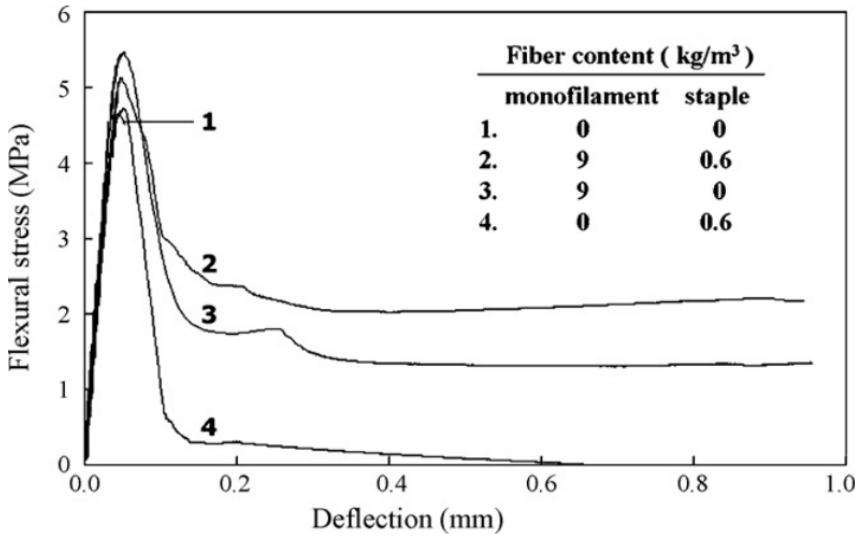

Figure 2.13: Load-deflection curves of polypropylene concretes (Hsie et al. 2008)

Monofilament refers to macro-synthetic and staple refers to micro-synthetic fiber. As shown above, the use of FRC increases toughness since mixtures 2-4 where able to continue carrying load after their ultimate stress was reached. In addition, the use of a blended system had superior performance when compared to the control mixture (1) and when used independently (3 and 4).

Effect on Shrinkage and Cracking

Polypropylene fibers have been used in concrete mainly for plastic shrinkage control; however, field results have shown improved cracking resistance. This has recently sparked further interest for the use of fibers in HPC where cracking affects the durability of concrete structures. Kovler et al. stated that the inclusion of polypropylene fibers was highly effective in reducing plastic shrinkage (Kovler 1992). Fiber reinforcement made of steel or other artificial fibers has been

documented to affected ductility, crack widths and even the fresh properties of cement-based materials (Saje et al., 2011). In addition, the geometry of the fibers affects the bond between the fibers and the concrete matrix (Swamy 1994). Saje and co-workers also found that the drying shrinkage of HPC reinforced by pre-moistened polypropylene fibers was approximately twice as large as that of dry polypropylene fiber reinforced HPC (Saje et al. 2011). According to Banthia and Gupta, the use of polypropylene fibers generally results in the decrease of crack width and number of cracks and thinner smaller fibers are more effective than longer and thicker fibers (Banthia and Gupta 2006).

The mitigation of drying shrinkage related cracking may be expected; however, researchers have reported mixed results about the effect polypropylene fibers have on shrinkage reduction. Saje et al. found that HPC with polypropylene fibers reduced the overall autogenous and drying shrinkage when compared to plain HPC (Saje et al. 2011). With regards to total shrinkage Kovler et al. stated that there was no significant reduction up to a volumetric content of 0.2% (1992). Aly and co-workers concluded that the use of polypropylene fibers in normal strength concrete at a 0.50% by volume dosage rate increased shrinkage by as much as 22% when compared to concrete containing no fiber (Aly et al. 2008). Myers and co-workers mentioned that polypropylene fibers exert a very small influence on shrinkage (Myers et al. 2008). Although many researchers are in disagreement, all agree that polypropylene fibers provide crack resistance, which is observed mainly in the number and width of the cracks. Much of the research was done with micro-synthetic fiber, which may be due to the findings from Banthia and Gupta in their fiber geometry study (Banthia and Gupta 2006).

In 1990 Grzybowski and Shah studied the effect of polypropylene on drying and restrained shrinkage (Grzybowski and Shah 1990). Fibers (collated and fibrillated) were tested at a dosage of 0.10, 0.25, 0.50 and 1.00 percent by volume. The mix proportions by weight for the matrix were: 1:2:2:0.5 (cement: sand: coarse aggregate: water). It was concluded that the addition of fibers did not substantially alter the drying shrinkage. The restrained shrinkage test specimen dimensions were slightly smaller than those specified by ASTM C1581. Specimens were wet cured for 4 days then immediately exposed to a 20ºC, 40 percent relative humidity environment.

A special microscope was used to measure the crack width. The crack widths (largest cracks were plotted) are shown in Figure 2.14.

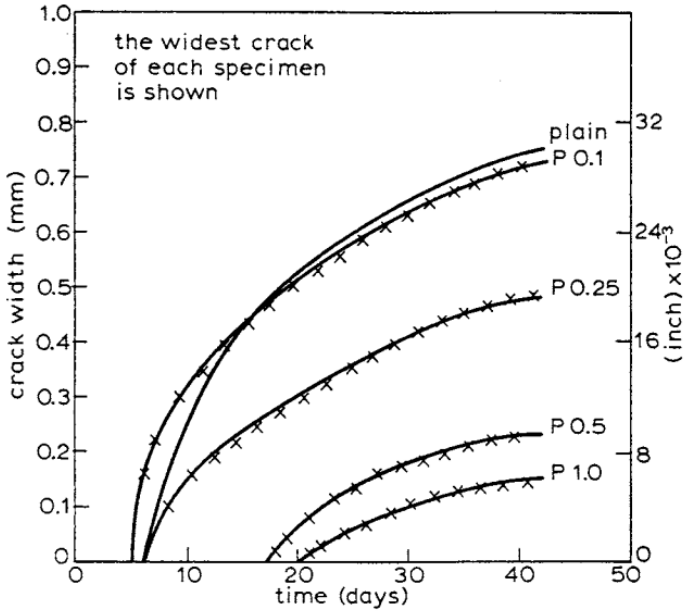

Figure 2.14: Crack widths for various synthetic fiber dosages (Grzybowski and Shah 1990).

Although this is not an HPC mixture there are still positive results in terms of crack width and propagation. According to Grzybowski and Shah, the average crack width for plain concrete was 1mm (0.04in), whereas for a specimen reinforced with 0.25% polypropylene fiber, it was less than 0.5mm (0.015 in), or one-half the value of plain concrete. Time-to-cracking was not reported, but Figure 2.14 indicates that when using 0.1% and 0.25% fiber there is no increase in time-to-cracking. However, at 0.5% and 1% fiber the time to cracking was increased by 11 and 15 days respectively.

In a more recent study, Saje and co-workers researched the shrinkage of polypropylene FRC in HPC (Saje et al. 2011). The HPC mixture was a 0.36 water to cement ratio using a washed crushed limestone and fine silica sand (10% replacement). Polypropylene fiber dosage rates were 0.25, 0.50 and 0.75 percent. The fibers were tested for both autogeneous and drying shrinkage in a moist and dry state. Test specimens were demolded after 24 hrs (1-day cure) and placed in a 22±3°C and 70±3% RH chamber. The humidity level is much higher than the ASTM standard

(European standards were used). Shown in Figure 2.15 are total shrinkage results for the various fiber dosages in a dry state.

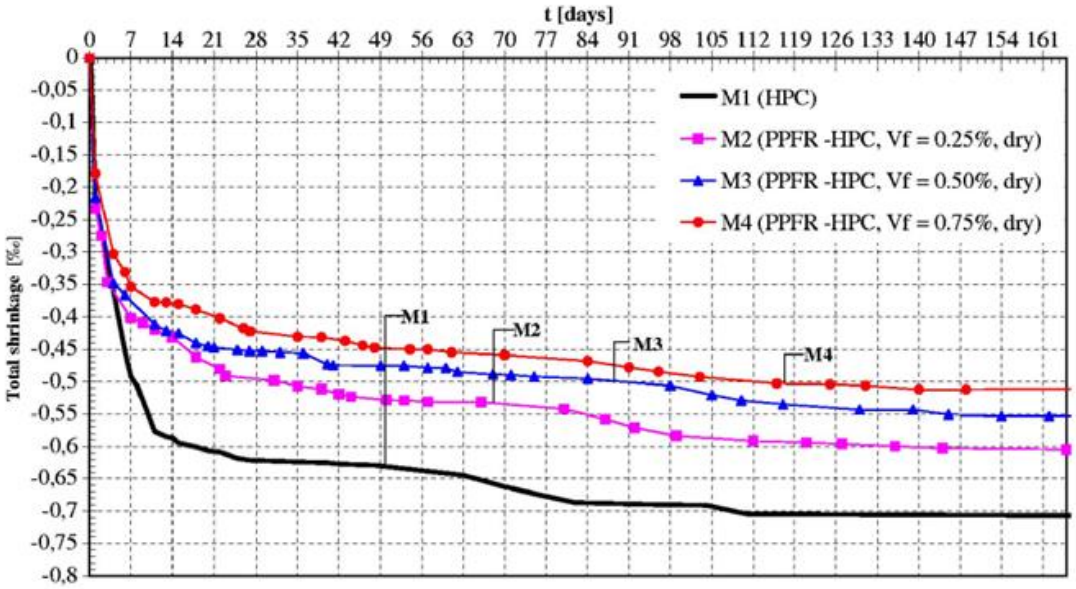

Figure 2.15: Total shrinkage results for various fiber dosages in a dry state (Saje et al. 2011)

All fiber dosages showed lower shrinkage, and shrinkage decreased as higher dosages were used. A marginal decrease in shrinkage was observed when the polypropylene fibers were moistened at the 0.25% and 0.50% dosage rate, and only the M4 mixture showed a notable 50 microstrain (0.05%) decrease in shrinkage. Saje et al. concluded that a dosage between 0.25%-0.50% is recommended considering both the workability and shrinkage simultaneously in HPC (Saje et al. 2011).

Effect on Slump and Workability

The negative effect on slump with increasing fiber additions in FRC is well documented (Hsie et al. 2008, Song et al. 2005, Zhang et al. 2011, and Folliard et al. 2006). Ozyildirim also noticed a considerable decrease in his HPC air entrained bridge deck mixture trials (2005). According to Folliard and Simpson, “The typical method of determining slump, ASTM C143, is a valid method of determining the slump of a given mix only if low dosages of fiber reinforcement are implemented” (Folliard and Simpson 1998). Therefore slumps with mixtures of high volume fractions may be misleading. This can be attributed to the improved plastic stability and cohesion

provided by the fiber reinforcement (Folliard et al. 2006). With regards to workability provided by air entraining admixtures, synthetic fibers have also been found to have no impact on the air content of the concrete matrix (Folliard and Simpson 1998, Bayasi 1993).

Effect on Mechanical Properties

Polypropylene fibers are well known for their ductility, but many researchers have reported positive effects on mechanical properties. Researchers have reported increases in compressive, spit tensile strength, and modulus of rupture when using polypropylene fibers (Hsie et al. 2008, Song et al. 2005). Hsie et al. reported that the compressive strength of polypropylene hybrid fiber-reinforced concrete increased by 14.60–17.31%; the splitting tensile strength did by 8.88–13.35%; modulus of rupture did by 8.99–24.60% when compared to plain concrete (Hsie et al. 2008). However, Hsie et al. and Song et al. only used FRC mixtures with type I portland cement. Zhang et al. further investigated the use of polypropylene fiber using a 15% replacement of fly ash and 6% replacement of silica fume (2011). The fiber volume fractions are shown in Figure 1.12 (0, 0.04, 0.06, 0.08, 0.10 and 0.12 percent). Zhang et al. concluded that "The addition of polypropylene fiber decreases the compressive strength of the concrete with 15% fly ash and 6% silica fume, the splitting tensile strength is improved and compressive modulus of elasticity is decreased effectively, which can decrease the rigidity and increase the ductility of the concrete containing fly ash and silica fume to protect the concrete from damages for large deformation" (2011). Additionally, compressive strength decreased with increased fiber dosages, as shown in Figure 2.16 below.

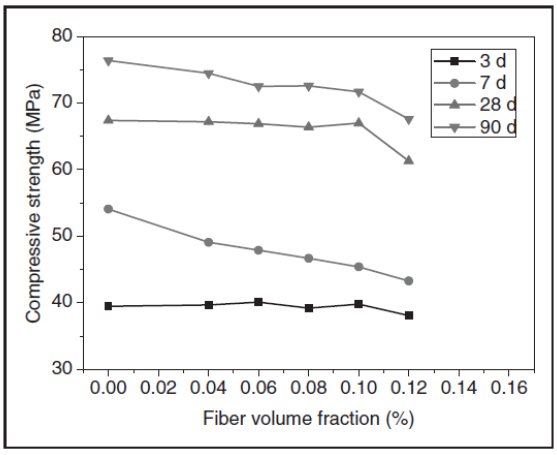

Figure 2.16: Effect of volume fraction on strength (Zhang et al. 2011)

Although reports from Hsie et al. and Song et al. reported increased strength, a decrease in strength in bridge decks is expected in HPC based on the findings from Zhang et al. (Zhang et al. 2011).Folliard and co-workers also noticed no significant strength change in his low cement (564lb/yd ^{3} cement content) mixtures with 20% and 25% fly ash replacement (Folliard et al. 2006).

Effect on Durability

According to Richardson, "many workers have documented improvement in the freeze/thaw resistance of polypropylene fiber concrete over that achieved by concrete without fiber" (Richardson 2012). When comparing plain concrete to air entrained and fiber concrete Richardson's analysis showed that air entrained concrete was 76 times more effective and fiber concrete was up to 88 times more effective than conventional concrete based on the durability factor as per ASTM C 666 (Richardson 2012). Richardson's study also showed that "the inclusion of fibers can increase the air void system when compared to plain concrete, thus providing an alternative to air entrainment as a method of freeze/thaw protection" (Richardson 2012). According to Rouhi et al., concrete with polypropylene fibers had a lower permeability when compared to concrete with no fibers due to the fibers crack resisting properties (Rouhi et al. 2012). Najafi et al., who also achieved similar results, explains that "ion penetration has considerably decreased probably due to reduction in inner conductivity of pores and less capillary porosity, which can make the bars of concrete to be more secured from corrosion" (Najafi et al. 2013).

Test Methods

There are various test methods to evaluate the flexural performance of FRC. Listed below are three commonly used test methods.

- ASTM C 1550- Flexural Toughness of Fiber Reinforced Concrete (Using Centrally Loaded Round Panel)

- ASTM C 1609- Standard Test Method for Flexural Performance of Fiber-Reinforced Concrete (Using Beam With Third-Point Loading)
- ASTM C1399- Standard Test Method for Obtaining Average Residual-Strength of Fiber-Reinforced Concrete

All tests use a testing machine that is capable of servo-controlled operation where the net deflection of the center of the beam is measured and used to control the rate of increase of deflection. Devices such as electronic transducers or electronic deflection gages shall be located in a manner that ensures accurate determination of the net deflection at the mid-span exclusive of the effects of seating or twisting of the specimen on its supports (ASTM 2012). A data acquisition system is used to obtain the relationship between load and deflection. Shown below in Figure 2.17 is an example of a testing setup in accordance with ASTM C 1609.

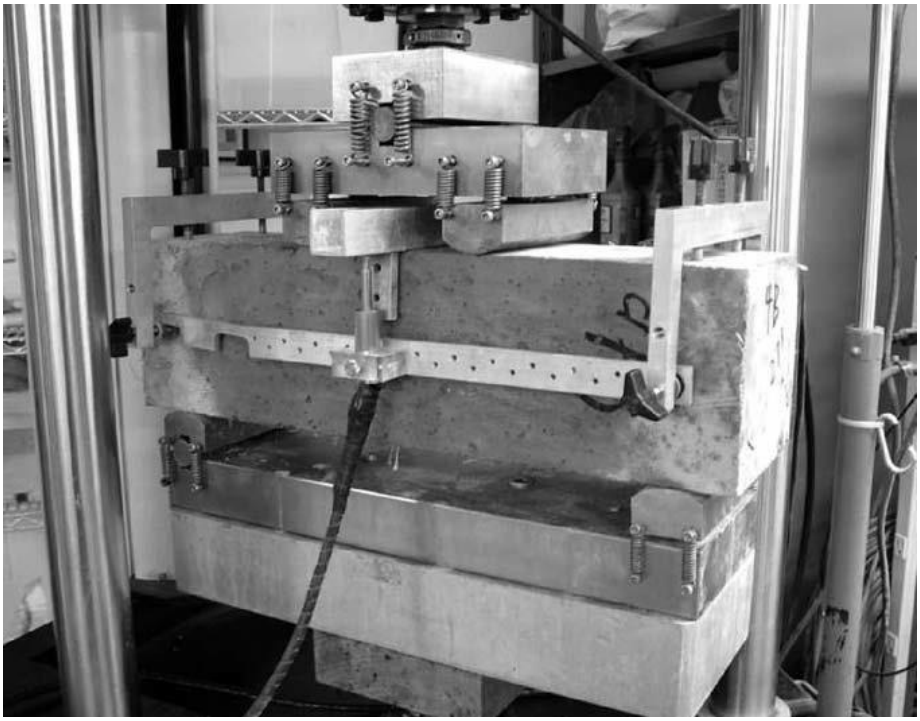

Figure 2.17: ASTM C 1609 test setup (2010)

The flexural performance of FRC beams can measure the cracking resistance and toughness of the concrete specimen. As discussed previously, these properties are enhanced in FRC.

2.11 RECENT DOT REASEARCH USING SYNTHETIC FIBERS IN HPC

2.11.1 Florida Department of Transportation (FDOT)

The Florida DOT investigated four types of fiber that included polypropylene, PVA (polyvinyl alcohol), steel and cellulose in Florida environmental conditions. The project was titled, "Durability of fiber reinforced concrete in Florida environments" (Roque et al. 2009). The exposure conditions were salt water (immersed and wet/dry) and swamp (acid) for 27 months. All beams were moist cured for 14 days prior to exposure. Beams were cast to determine residual strength testing according to ASTM C1399 and flexural performance testing according to ASTM C1609. The intent was to identify the cracking resistance under the exposure conditions. Although the testing methods differed, the observations and results from the Florida study informed the current research with respect to cracking resistance of fiber concrete, especially concrete with polypropylene fibers.

The steel fiber had the strongest resistance to crack propagation in limewater immersion due to the excellent bonding with the matrix (Roque et al., 2009). However, the steel fibers corroded in immersed saltwater and during cyclic wetting and drying cycles. The PVA fibers were the weakest due to their poor resistance to saltwater, which caused them to degrade over time. The polypropylene fibers exhibited good performance in all environments due to their inherent resistance to chemicals and shrinkage effects. Cellulose fiber results were not included as problems with fiber dispersion affected the outcomes. Work performed at Oregon State University on a separate project has addressed the fiber dispersion issue. Also, according to Roque et al.:

> "Effect of fibers on cracking resistance could not be assessed based on the test results from either average residual strength (ASTM C1399) or flexural performance (ASTM C1609). It was determined that the conventional beam approach resulted in non-uniform degradation and stress/strain distributions through the cross-section. Also, beam tests generally resulted in multiple cracks initiating at the bottom of the specimen and instability subsequent to matrix cracking. These critical factors significantly affected

pull-out mechanism of fibers and disturbed the evaluation of failure during post-cracking" (2009).

Due to the difficulties with their test set ups Florida DOT was not able to clearly identify the cracking resistance of each fiber type. However, they do make interesting observations about polypropylene fibers that achieved higher performance in the most aggressive exposure conditions.

2.11.2 Oregon Department of Transportation (ODOT)

In 1997 ODOT overlaid the Link River Bridge with microsilica (silica fume) concrete, reinforced with polypropylene fibers. Two years later, an inspection was made by Eric W. Brooks, who reported the findings in 2000 (Brooks 2000). According to the fiber manufacturer, plastic shrinkage and settlement cracking would be reduced during the early life of the concrete as well as the formation of intrinsic cracking. Only the Northbound lane contained fiber, yet the result was similar for both lanes. According to Brooks, cracking resistance was found to be no better in the northbound lane with fibers, compared to the southbound lane without fibers.

2.11.3 Texas Department of Transportation (TXDOT)

Folliard et al. studied the use of fiber in continuously reinforced concrete pavements (CRCP) (Folliard et al. 2006). One of the major concerns in this study was concrete spalling due to the poor performance of siliceous river gravel. According to Folliard et al., pavements constructed in the winter experienced the most severe cases of spalling, which were caused by induced cracks in the upper portion of the slab due to the low temperature gradient (Folliard et al. 2006). As the temperature increased, the cracks propagated further into the slab, and the way the cracks propagated was dependent on the aggregate type. Folliard explained that in river gravel the cracks tend to travel around the aggregate due to a weaker bond to the cement paste. In addition, according to Dossey and McCollough, field performance in Texas has shown that pavements constructed with limestone aggregates generally perform better with respect to spalling than those constructed with siliceous river gravel (Dossey and McCollough 1999). This is due to a stronger bond between the limestone and the paste, which encourages the cracks to propagate directly through the aggregate (Folliard et al., 2006).

To mitigate spalling the inclusion of fibers was evaluated both in the laboratory and in the field. Two steel fiber (corrugated and hooked end) and two micro-synthetic fibers (monofilament and fibrillated) were used. Flexural toughness was the only hardened property that was significantly affected by the addition of fibers. This was specifically important to this project due to the spalling concerns with existing CRCP in Texas. According to Folliard et al., "Steel fibers typically provide greater improvements in toughness and residual strength than synthetic fibers, and both parameters are proportional to dosage rate for any fiber used", in addition "toughness and residual strength should be good indicators of improved spalling performance of CRCP, but field evaluations of CRCP containing fibers will be critical for verifying this hypothesized correlation" (Folliard et al. 2006). During the time allotted to this research project there was no significant cracking and unfortunately the field performance of fibers was not fully evaluated. No significant improvement in cracking resistance was observed due to the age of the concrete during field monitoring.

2.11.4 Virginia Department of Transportation (VDOT)

Dr. Celik Ozyildirim studied high performance fiber-reinforced concrete for the bridge deck application (Ozyildirim 2005). This project covered both field monitoring and laboratory testing. A bridge deck was placed on steel beams over 4 piers on Route 11 over the Maury River in Lexington, Virginia. Control sections were cast on the same deck and were monitored over a 5-year period. Synthetic fibers were used at a dosage rate of 8.75 lb/yd3 and the HPC was air entrained to achieve 6.5% air. In the laboratory dosage rates of fiber of 5-15lb/yd3 were used and air contents of 2.6-10% were recorded. It was immediately noticed that only 2 batches were on target (5.1% and 6.4%). The batch with 10% air did not meet 28-day strength requirements (4000 psi). Permeability was also tested; however, there was no mention of the standard used, and all batches met the minimum charge passed (2500 coulombs) requirement. Testing according to ASTM C 1399 showed that increasing the fiber dosage also significantly increased the residual strength.

Although there were differences between the batches used in the laboratory and those produced in the field, the addition of fibers showed similar results. Synthetic fibers provided higher

residual strength and controlled cracking. According to Ozyildirim, the following conclusions where observed:

- The fibers provided residual strength, which was directly proportional to the fiber content, and controlled cracking. Fewer and smaller cracks were observed in the FRC even though the FRC had higher shrinkage than the control. T
- During the residual strength test, the deflection had to be controlled through the actuator, which affected the residual strength. The residual strength was higher when the rate was controlled through the actuator (possible limitations to this test).
- The incorporation of fibers reduced workability.
- "Pumping in a vertically downward direction reduced the air content and slump of freshly mixed concrete. However, concretes with reduced air content can provide satisfactory resistance to freezing and thawing if a satisfactory air void system is maintained. Differences in slump and air content were observed before and after pumping depending on the location of the sample."
- The permeability of FRC was similar to that of conventional concrete. (Ozyildirim, 2005).

Like other researchers Ozyildirim found that cracking control was one of the most significant improvements. Also, similar to the problems observed at FDOT, the residual strength test according to ASTM C 1399 was not ideal.

2.12 LITETURE REVIEW SUMMARY

It is well known that FRC reduces plastic shrinkage and both the propagation and width of cracks in concrete. Mixed drying shrinkage results have been shown and little to no research has been done on the cracking risk of FRC. Shrinkage reduction is still being debated, and some researchers have found that polypropylene fibers either increased or reduced total shrinkage. There has not been a major study where blended synthetic fibers are used. Generally only macro or micro synthetic fibers are used, but regardless of fiber type fewer cracks were observed in both laboratory and field. The main test being used to assess cracking risk was the residual strength test, but there were noted concerns with this method due to instability and deflection.

Otherwise, precise measurements of crack widths were regularly monitored to show that synthetic fibers control cracking. The inclusion of synthetic fibers results in lower concrete workability, and fiber dosages of less than 0.50% have shown good workability. Much of the work done did not include low water to cement ratios, SCM's or air entrainment. In extreme durability conditions polypropylene were superior to all other fibers (steel, PVA, and cellulose) due to their inherent anticorrosive and chemical resistant properties.

3.0 CHAPTER 2: MATERIALS AND METHODS

3.1 CEMENTITIOUS MATERIALS

The cementitious materials used in this research project included an ASTM C150 Type I/II ordinary portland cement (OPC), ASTM C618 Class F fly ash, ASTM C 989 Ground Granulated Blast-Furnace Slag. These materials were manufactured by Lafarge North America. An ASTM C 1240 silica fume, Rheomac 100 manufactured by BASF was also used. The oxide analysis for the cementitious materials is shown in Table 3.1.

Table 3.1: Oxide Analysis (wt. %)

Oxide	OPC	Class F Fly Ash	Slag	Silica Fume
CaO	63.57	10.20	30-50	-
SiO_2	19.95	55.24	-	60-100
Al_2O_3	4.71	15.77	-	-
Fe_2O_3	3.50	3.64	-	-
MgO	0.85	3.64	0-20	-
Na_2O	0.25	2.08	-	-
K_2O	0.27	2.08	-	-
TiO_2	0.24	0.94	-	-
MnO_2	0.09	0.12	-	-
P_2O_5	0.09	0.23	-	-
SrO	0.16	0.32	-	-
BaO	0.06	0.62	-	-
SO_3	3.19	0.70	-	-
Total Alkalis as Na_2O	0.43	-	-	-
Loss on Ignition	3.19	0.23	-	-

**Oxide analysis of slag and silica fume was taken from the manufacture

The specific gravity of the Type I/II OPC, fly ash, slag, and silica fume were 3.15, 2.62, 2-3(proprietary) and 2.20 respectively.

3.2 ADMIXTURES

An ASTM C494 Type F polycarboxolate-based high-range water reducer (ADVA Flex®) supplied by Grace Construction Products was used to achieve consistent workability (target 3-5 in slump). An air-entraining admixture (DARAVAIR® 1000) supplied by Grace Construction Products was also added to achieve a target air content of 6 ± 1.5% to ensure proper freeze/thaw resistance. Fresh concrete temperature was measured at the end of each mixture using an infrared thermometer.

3.3 AGGREGATES

The coarse and fine aggregate used in this study were from one local source. The local aggregate was siliceous river gravel and river sand. The crushed aggregate used in this study to investigate the effect of aggregate angularity was from the same source and had similar aggregate properties with the only difference being crushed rather than predominantly rounded surface texture. The crushed limestone aggregate was used to investigate the effect of mineralogy. Shown below in Table 3.2 are the aggregate properties for all aggregates used.

Table 3.2: Aggregate Properties

Aggregate Property	Siliceous Fine	Siliceous Coarse	Siliceous Crushed Coarse	Limestone Crushed Coarse
Oven Dry Bulk Specific Gravity	2.52	2.58	2.75	2.71
Absorption Capacity (%)	3.08	2.44	2.42	0.44

3.4 FIBERS

Propex Novamesh 950® synthetic blended fibers were used. Shown below in

Table 3.3: Synthetic fiber material properties are the physical and chemical components of each fiber type. As mentioned previously, micro-synthetic are the smaller fibrillated fibers and macro-synthetic are the coarser longer fibers.

Table 3.3: Synthetic fiber material properties

	Micro-Synthetic	**Macro-Synthetic**
Material	Polypropylene	Coarse Macro-Monofilament Polypropylene
Absorption	None	None
Specific Gravity	0.91	0.91
Fiber Length (in)	0.5	1.8
Fiber Diameter	-	0.33 Nominal
Electrical Conductivity	Low	Low
Melting Point (°F)	324	328

The application rate suggested by the manufacturer is a minimum of 5 lb/yd^3 of concrete where 85% of fibers by weight are macro-synthetic and 15% are micro-synthetic (pre-mixed by the manufacturer). No modifications to the weight percentages were made. In addition, fibers were added directly into each concrete mixture without mixture design modifications as specified by the manufacturer. Only super plasticizer dosages were modified to insure good workability (3-5 in slump).

3.5 MIXTURE DESIGN

All concrete mixtures in this project were based on a specific ODOT HPC mixture design for bridge decks. The target compressive strength was 5000 psi and the minimum strength was 4000 psi. A w/cm of 0.37 was used in all mixtures. The total cementitious materials content was 633 lb/yd^3, containing 30% class F fly ash or slag and 4% silica fume as mass replacement. The coarse and fine aggregate content were 1074 lb/yd^3 and 659 lb/yd^3 respectively for local materials. High range water reducer and air entraining admixture were adjusted to achieve similar workability and air content for all mixtures. This mixture design was used as the control. Modifications were made to this mixture design to include blended fibers at varying dosage levels. Other modifications included SCM replacement or the use of different coarse aggregates. Table 3.4 shows the detailed mixture proportions for each mixture.

Table 3.4 Concrete mixture proportioning

Mixture	Cement ((lb/yd^3)	Fly ash (lb/yd^3)	Slag (lb/yd^3)	Silica fume (lb/yd^3)	Water (lb/yd^3)	Coarse aggregate (lb/yd^3)	Sand (lb/yd^3)	Fiber Dosage (lb/yd^3)
HPC1	419	189	-	25	234	1810	1110	0
HPC2	419	-	189	25	234	1810	1110	0
FHPC D5	419	189	-	25	234	1810	1110	5
FHPC D7.5	419	189	-	25	234	1810	1110	7.5
FHPC D10	419	189	-	25	234	1810	1110	10
LCM1	363	165	-	22	204	1810	1110	0
LCM2	347	158	-	21	194	1695	1387	0
OPC1	633	-	-	-	234	1810	1110	0
OPC + FA	248	128	-	-	234	1810	1110	0
OPC + SF	361	0	-	25	234	1810	1110	0
CHPC	419	189	-	25	234	1810	1110	0
LS2	419	189	-	25	234	1810	1110	0
F/T D7.5	419	189	-	25	234	1810	1110	7.5
F/T D10	419	189	-	25	234	1810	1110	10

A mixture identification system is described next. HPC represents a high performance concrete mixture. “HPC1” uses Class F fly ash and “HPC2” uses slag. The prefix “F” added to HPC represents fiber addition, and the suffix “D” represents the dosage followed by the rate in pounds per cubic yard (lb/yd^3). CHPC is an HPC mixture using crushed local siliceous river aggregate. LS2 is an HPC mixture using limestone for the coarse aggregate, siliceous river sand was used as the fine aggregate. Two low cement mixtures (LCM1 and LCM2) are distinguished by their cement content shown in Table 3.4. In addition to the low cement investigation, mixtures based on ordinary portland cement (OPC), OPC plus fly ash (OPC + FA), and OPC plus silica fume (OPC + SF) were investigated to determine their shrinkage potential. “F/T” are fiber mixtures used for freeze thaw testing and are followed by the fiber dosage rate used. Table 3.5 provides mixtures that were tested as per ASTM C1581.

Table 3.5 Mixtures for ASTM C 1581 restrained ring tests

Mixture ID	Coarse aggregate type	Fine aggregate type	w/cm	Curing duration (days)	Other descriptions
HPC1	Local	Local	0.37	14	Control with Fly Ash ¾" MSA
HPC2	Local	Local	0.37	14	Control with Slag ¾" MSA
FHPC1 D5	Local	Local	0.37	14	¾" MSA
FHPC D7.5	Local	Local	0.37	14	¾" MSA
FHPC D10	Local	Local	0.37	14	¾" MSA
CHPC	Local	Local	0.37	14	Crushed Local ¾" MSA
LS2	Limestone	Local	0.37	14	Crushed ¾" MSA
LCM 2	Local	Local	0.37	14	Low Cement Content ¾" MSA
OPC1	Local	Local	0.37	14	¾" MSA

3.6 MECHANICAL PROPERTIES AND CURING CONDITIONS

Mechanical properties were tested for each mixture at 7, 14 and 28 days age, including compressive strength (ASTM C39), splitting tensile strength (ASTM C496), and modulus of elasticity (ASTM C469). For each mixture, ϕ4 × 8 in cylindrical samples were cured in two conditions: standard 28-day wet cure and 28-day matched cure. For standard curing, samples were demolded 24 hours after casting and stored in an ASTM C 511 standard moisture room (23°C and 100% RH) until testing. For matched curing, samples were demolded 24 hours after casting and stored in the standard moisture room until the end of desired wet curing periods. Then these samples were moved to a drying environment (23°C and 50% RH) and stored near the specimens used for restrained cracking (ASTM C 1581). This was to ensure the measured mechanical properties were representative of ring specimens.

3.7 FREE SHRINKAGE

Free drying shrinkage was monitored using the ASTM C157 test, which is a common method to determine length change of hardened concrete prisms (3 × 3 × 11.25 in). The specimens were de-molded 24 hours after concrete mixing and placing. The specimens were then stored in an ASTM C 511 moist room (23 ± 2°C and >95% RH) until desired curing duration (i.e. 3, 14 and 28 days in this study). Upon the end of curing duration, the specimens were moved into a drying environment (23 ± 2°C and 50 ± 4 % RH). During drying, the length was monitored by a comparator. The mass change was also recorded during the testing period.

This test utilizes test concrete specimens measuring 100×100×285 mm (4 x 4 x 11.25 in) in size are used if the aggregate passes a 50mm (2 in) sieve. However, if all the aggregate passes a 25 mm sieve (1 in), a specimen of 75×75×285 mm (3 x 3 x 11.25 in) may be used. After mixing and placing concrete in the molds, the specimens are placed in a moist room in accordance to ASTM C 511. The specimens are removed from the molds at an age of 23½ ± ½ hours after mixing. Upon demolding, the specimens are placed in a lime-saturated solution maintained at 23±0.5 °C for a minimum of 30 minutes. The specimens are removed from the solution at 24±½ hour after water-cement contact and an initial comparator reading is taken. After taking the initial reading, specimens are placed in a lime-saturated solution 46 and cured for 28 days at 23±1 °C. When this

curing period has commenced, the specimens are placed in a drying room that is maintained at 23±1 °C (73 +/- 1 °F) and at a relative humidity of 50±4%. It is important to provide adequate spacing between prisms to allow for even drying. The spacing requirement recommended by the ASTM standard is a minimum of 25 mm (1in) on all sides of the specimen. Comparator readings should take place at 4, 7, 14, and 28 days, and after 8, 16, 32, and 64 weeks. Length change can be calculated by using the following equation:

$$\Delta L_x = \frac{\text{CRD} - \text{Initial CRD}}{\text{G}} x\ 100 \qquad \text{Equation 1}$$

Where:

ΔL_x = Length change of specimen at any age (%)
CRD = Difference between the comparator reading of the specimen and reference bar at any age
G = gage length (250 mm [10 in])

This test is effective for evaluating drying shrinkage of concretes with a high w/cm, but problems may arise when testing concrete with a w/cm of < 0.42 (Aitcin 1988). The problems can be attributed to the self-desiccation of the cement paste. In return, the self-desiccation leads to autogenous shrinkage that develops in the first 24 hours before the specimen has been demolded. (Sant et al. 2006) Since autogenous deformation is a cement paste phenomena, different studies need to be performed to quantify the amount of deformation that occurs in early-ages in HPC. The amount of autogenous shrinkage needs to be accounted for when using the ASTM C 157 on HPCs. This may be done on companion sealed specimens that are stored under the same conditions. In essence the difference in shrinkage between the two methods is the drying component of shrinkage. Knowing the main mechanisms responsible for shrinkage can help to make a determination of the best approach for mitigation methods to reduce the risk of drying shrinkage.

3.8 RESTRAINED SHRINKAGE

Compared to the standard testing procedure, several modifications were applied in this project: 1) to achieve more accurate cracking evaluation, three rings instead of two were tested for each mixture; 2) a specific curing duration (14 days) was used to simulate field curing conditions; 3) mechanical properties at 28-day age were tested on match cured cylinders. A sample of freshly mixed concrete was compacted into three circular molds formed by concentric steel rings. The compressive strain developed in the inner steel ring caused by initial hydration, curing and restrained shrinkage of the specimen under drying was measured from the time of casting. The specimens were moist cured using wet burlap covered with a polyethylene film for at least 24 h at 23.0 ±2.0 °C. The outer rings were removed at 24 h, and wet curing using saturated burlap was done until the end of the desired curing duration. During the curing process, the burlap was re-wetted as necessary to maintain 100% RH environment for the concrete. At the end of the curing process, the burlap was removed and the top surfaces of the specimens were sealed with silicone sealant to allow for drying only in the horizontal direction. The strain gauge readings were recorded every 5 minutes until all 3 concrete rings showed visible cracking along the height of the ring.

The strain gauge reading was recorded right after the specimens were cast and moved into the environmental chamber. The time between exposure to drying and cracking is called time-to-cracking (days), which is an important parameter to evaluate the cracking resistance of the tested concrete. According to the strain gauge reading, an averaged stress rate (psi/day) in the concrete can be calculated and used as another parameter in cracking risk evaluation. The cracking potential was evaluated based on Table 2.1.

3.9 FREEZE-THAW TESTING

ASTM C666 was used to determine the resistance of concrete to freezing and thawing cycles. This test method can be performed in two different ways. In Procedure A, the concrete is subjected to rapid freezing and thawing in water. In Procedure B, the concrete is subjected to rapid freezing in air and rapid thawing in water. These two procedures both determine the effects

of variations in proportions, curing and soundness of the aggregates. The low temperature of the freeze cycle is -17.8 ^{o}C (0 ^{o}F) and the target thaw temperature is 4.4 ^{o}C (40 ^{o}F). Procedure A was used to assess the freeze/thaw performance of concrete with synthetic blended fibers.

Test specimens were cast according to ASTM C192, and demolded at an age of 24 +/- ½ hours after initial contact. Specimen dimensions were 3"x4"x16" rectangular beams. The specimens were then allowed to cure for 28 days. Upon completion of curing, the specimens were cooled to a temperature within ±2 ^{o}F of the target thaw temperature. The specimens were protected from moisture loss during the cooling until the freeze-thaw testing began. Prior to the initial cycle, the mass and initial fundamental transverse frequency was measured. ASTM C215 outlines the procedures for determining the fundamental transverse frequency. Once freeze-thaw cycles began, the specimens were tested for fundamental transverse frequency and the mass recorded during the thawed condition. The fundamental transverse frequency was recorded every 36 cycles. The specimens were placed back in the chamber either randomly or in a predetermined rotation to ensure that the specimens were subjected to all conditions throughout the chamber. The test was continued until the specimens were subjected to either 300 cycles or their relative dynamic modulus had reached 60% of the initial modulus. The relative dynamic modulus was then calculated by the following equation:

$$P_c = (n_1^2/n^2) \times 100$$

Where:

P_c = relative dynamic modulus, after *c* cycles of freezing and thawing, percent,

n = fundamental transverse frequency at 0 cycles of freezing and thawing,

n_1 = fundamental transverse frequency after *c* cycles of freezing and thawing.

3.10 RAPID CHLORIDE PERMEABILITY TEST

For consistency all samples were wet cured for 56 days. At the desired duration of curing, 2 in (50 mm) thick slices of concrete were cut using a water-cooled diamond saw, and the specimens were conditioned for testing. The specimens were allowed to air dry for at least 1 hour before applying a rapid setting (approx. 1-3 hrs.) sealant on the sides of each specimen. After the sealant

set, the specimens were placed in a vacuum desiccator with all surfaces exposed. Once all specimens were in the desiccator, a vacuum pump was started, and a pressure of less than 0.039 in. (1mm) Hg was maintained for 3 hours. While the vacuum pump was still running, de-aerated water was introduced through a stopcock. Once the specimens were submerged, the stopcock was closed, and the vacuum was applied for 1 more hour. At the end of the 4 hour conditioning, air was allowed to re-enter the desiccator, and the specimens were soaked in this condition for 18 +/- 2 hours.

After completing the conditioning, the specimens were removed from the desiccator and excess water was removed. A circular vulcanized rubber gasket was placed on each half of the test cell and the halves were bolted together. The side filled with 3% NaCl solution and was connected to the negative side of the power supply. The other side (filled with 0.3N NaOH solution) was connected to the positive side of the power supply. The power supply was turned on, the voltage was set to 60.0 +/- 0.1 V, and the initial current was recorded. The current was recorded at least every 30 minutes for 6 hours. The test was terminated after 6 hours, unless the temperature of the solutions reached 190 ^{o}F (88 ^{o}C). If the solutions exceed this temperature, boiling of the solutions or damage to the cell may occur. To determine the total charge passed during the six hour period, the following equation was used:

$$Q = 900(I_0 + 2I_{30} + 2I_{60} + \ldots + 2I_{300} + 2I_{330} + I_{360})$$

Where:

Q = charge passed, coulombs,
I_0 = current immediately after voltage is applied, amperes,
I_t = current at t min after voltage is applied, amperes.

To increase the accuracy of this test the current was recorded every second during the 6-hour test duration using a data acquisition system (DAS). Upon completion of the test the current was plotted over time. To calculate the total charge passed in coulombs the current-time curve was integrated. Using the DAS data was the preferred method of analysis; however, manual recordings were still taken in the case of equipment malfunction.
Table 3.6 was used to evaluate the chloride ion penetrability in qualitative terms.

Table 3.6: Chloride ion penetrability based on charge passed (ASTM Standard C1202, 2010)

Charge Passed (coulombs)	Chloride Ion Penetrability
>4000	High
2000-4000	Moderate
1000-2000	Low
100-1000	Very Low
<100	Negligible

3.11 TESTING SUMMARY

The focus of this project was to optimize the fiber dosage to achieve the best results in free shrinkage, cracking risk, and durability properties. For each mixture, the following tests were performed:

- 6 Cylinders (ϕ100 × 200 mm) for compressive strength (3 replicates), splitting tensile (2 replicates), and static modulus of elasticity (2 replicates) for 28-day wet cured condition;
- 6 Cylinders (ϕ100 × 200 mm) for compressive strength (3 replicates), splitting tensile (2 replicates), and static modulus of elasticity (2 replicates) for 28-day match cured condition (several mixtures did not test match cured cylinders);
- 3 ASTM C157 prisms for each of 3, 14 and 28 day curing durations;
- 3 ring specimens (ASTM C1581 or AASHTO T344).

It should be noted that the free shrinkage prisms and concrete in the restrained ring testing went through the same curing conditions. Durability testing (Freeze/thaw and RCPT) was only conducted on the best candidates based on shrinkage reduction and time duration in the ring test.

4.0 RESULTS AND DISCUSSION

The main goal of this research was to test the potential for blended synthetic fibers to reduce the cracking risk of HPC. This section outlines the results attained and provides discussion of the implication of those results particularly in terms of the ability of blended fibers to reduce the risk of cracking in HPC.

4.1 FRESH PROPERTIES

Table 4.1 shows the summary of fresh properties for all mixtures. The target slump was 5in ±2.5in and the target air content was 6.5% +/- 1.5%.

Table 4.1: Fresh Properties

Mixture ID	Slump (in)	Air content (%)	Unit Weight (lb/ft^3)	Temperature (°C)
HPC1	5.0	6.0	144	21
HPC2	3.0	6.0	142	22
FHPC1 D5	2.5	6.2	143	22
FHPC1 D7.5	5.5	7.0	140	24
FHPC D10	3.0	6.0	143	20
CHPC	3.3	7.5	139	22
LS2	2.5	5.2	145	19
LCM 525	2.5	6.6	140	24
LCM 550	3.8	8.0	135	24
OPC1	2.5	3.0	142	22
F/T D7.5	2.5	6.0	140	24
F/T D10	2.0	6.0	140	26

Only mixtures within target air entrainment were tested for restrained and free shrinkage. Table 4.2 shows the summary of compressive strength, splitting tensile strength, and modulus of elasticity of all mixtures. Most mixtures were within the 4000psi minimum compressive strength,

as outlined by the 2008 ODOT structural specialty code for bridge decks (ODOT, 2008). In addition to the standard 28-day curing regime, samples were exposed to the environmental chamber drying conditions after 14 days of wet curing. This was done to match the curing regime of the drying shrinkage prisms that were wet cured for 14 days after casting before being placed into the 50% RH and 23C environmental chamber. At 28 days they were tested to determine the "match cured" strength.

Table 4.2 Concrete Mechanical Properties

Mixture ID	28-Day, Wet Cured			28-Day, Match Cured		
	Compressive Strength (psi)	Tensile Strength (psi)	Modulus of Elasticity (ksi)	Compressive Strength (psi)	Tensile Strength (psi)	Modulus of Elasticity (psi)
HPC1	5126 (241)	588 (59)	4679(192)	5787 (513)	638 (4)	4479 (171)
HPC2	4620 (144)	485 (26)	4190 (303)	-	-	-
FHPC1 D5	3930 (236)	462 (0.3)	3480 (72)	-	-	-
FHPC1 D7.5	4050 (102)	536 (13)	3908 (146)	5010 (467)	587 (10)	4107 (66)
FHPC1 D10	4090 (614)	520 (19)	3910 (56)	5180 (265)	511 (22)	4230 (16)
CHPC	3599 (29)	412 (16)	4103 (363)	3920 (81)	345 (5)	3793 (135)
LS2	5710 (126)	529 (42)	4411 (91)	6069 (548)	610 (37)	4745 (85)
LCM 525	3450 (285)	517 (22)	4100 (223)	-	-	-
LCM 550	2980 (59)	392 (23)	3590 (51)	3091 (255)	392 (32)	3470 (78)
OPC 1	6480 (131)	533 (29)	5260 (143)	6624 (579)	622 (51)	5400 (60)

Match cured mechanical properties were notably higher, roughly a 1000 psi increase in some cases, than the 28-day cured specimens. This was also noted in a previous study at OSU and was further investigated by Tengfei Fu, PhD and fellow graduate student David Rodriguez (Fu and Rodriguez 2014). Historically, it has been established that longer moist curing durations achieve higher strength. The main goal was to determine if a 14-day wet cure mixture could achieve a higher strength than a 28-day cure mixture at 90-days. Various HPC mixtures were tested using a 0.37 and 0.42 water to cement ratio, other mixtures included HPC with SRA, HPC using limestone coarse aggregate, and HPC using FLWA. All mixtures used the standard ODOT HPC mix design for bridge decks (as explained in section 3.5). In all mixtures the compressive

strength of the 14-day wet cure specimens at 90 days was similar if not slightly lower than the compressive strength of the 28-day wet cure specimens. Moreover, the mixture with coarse limestone showed roughly a 1000psi increase in strength when wet cured for 14days, rather than 28 days.

It was initially predicted that adding fibers to the mixtures would result in lower mechanical properties due to the inherent paste replacement. In general, the inclusion of fibers reduced mechanical properties. However, all fiber mixtures were relatively close or within the 4000 psi minimum. Additionally, the modulus of elasticity was lowered significantly, which indicated increased ductility. This may also provide a reduction in cracking risk of the HPC incorporating blended fibers.

CHPC strengths were lower than expected. The lower strength may have been due to the higher amount of air (7.5%), which was at the higher limit to ensure freeze/thaw protection. Also this mixture may have required further optimization for aggregate particle size and appropriate paste content. This was the first usage of a crushed aggregate from this source (same as the rounded river gravel); therefore, further work may be necessary to ensure that this mixture meets ODOT requirements. The HPC limestone mixture (LS2) showed higher compressive strength at 28 days. OPC1 showed significantly higher mechanical properties. This was likely due to the absence of SCM's, which can slow down the strength gain. As for mixtures with low cement content the mechanical properties notably decreased and did not meet ODOT strength requirements.

4.2 FREE SHRINKAGE

4.2.1 Blended Fiber Mixtures

Free drying shrinkage tests of HPC that was wet cured for 3, 14, and 28 days were done for all synthetic blended fiber and control mixtures. All prisms were regularly monitored for 90 days to achieve accurate, consistent and timely results. The 3-day cure drying shrinkage results are shown in Figure 4.1.

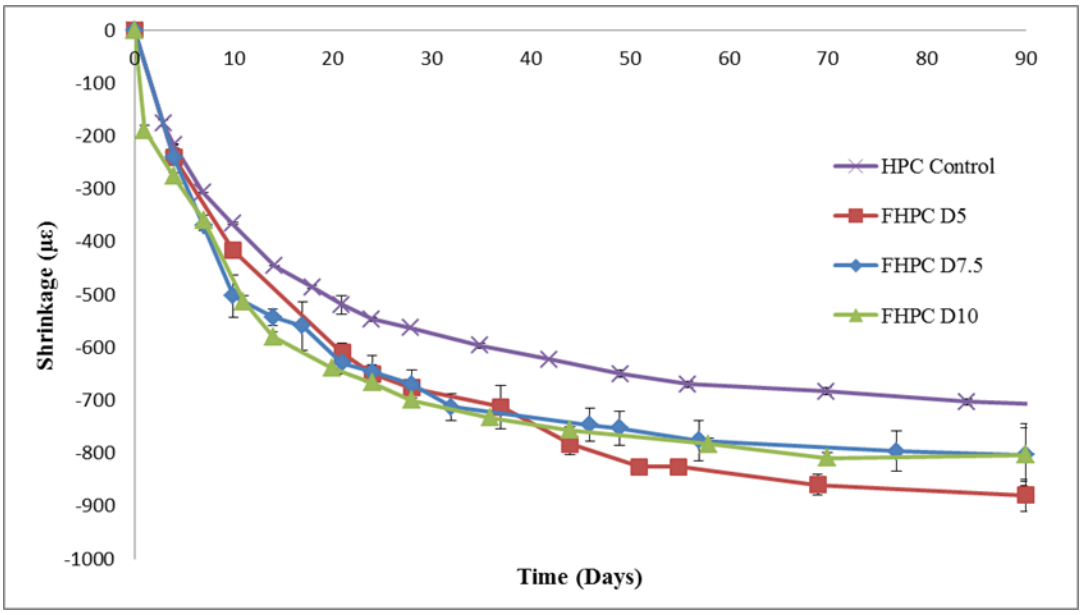

Figure 4.1: 3-day cure free drying shrinkage

The HPC control mixture clearly showed lower free shrinkage after the 3-day curing duration compared to the mixtures with fibers. The same correlation was found at the 14 and 28 day curing durations. However, the drying shrinkage in fiber mixtures progressively converged towards the control at the 14 and 28 day curing durations. This interaction is shown in Figures 4.2 and 4.3.

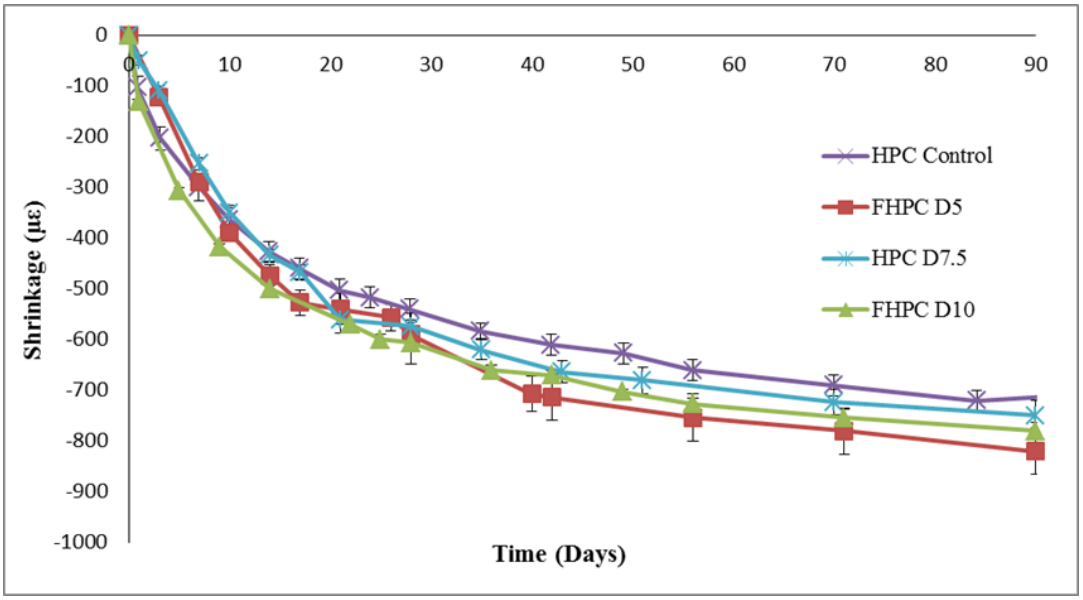

Figure 4.2: 14-day cure free drying shrinkage

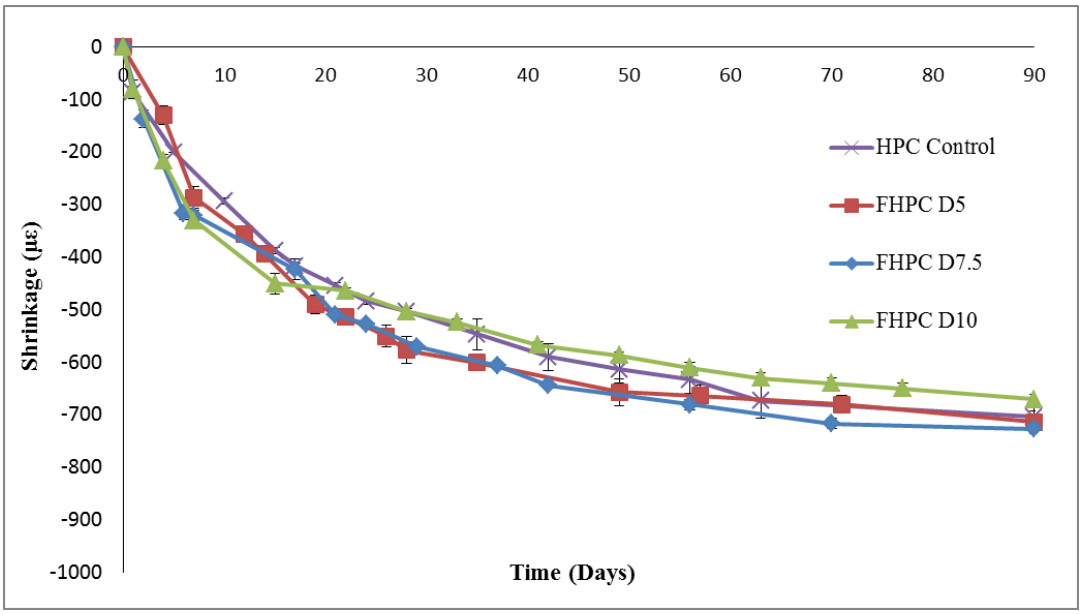

Figure 4.3: 28-day cure free drying shrinkage

The 14-day and 28-day curing durations showed similar drying shrinkage results. However, when the specimens were cured for 28 days all specimens had similar drying shrinkage (roughly 700 micro-strain at 90 days of drying) and FHPC D10 showed the lowest shrinkage. There was no significant increase or decrease in drying shrinkage when using blended synthetic fibers in HPC.

4.2.2 Investigation to Reduce Drying Shrinkage

Modifications to the standard HPC mixture were made to study the effect of drying shrinkage. According to Tarr and Farney, for unrestrained concrete specimens (prisms), a low ultimate shrinkage is considered to be less than 520 microstrains (at 50% RH and 73ºF), and typical concrete shrinkage has been measured at 520 to 780 microstrains (Tarr and Farney 2008). The effect of SCM's and cement content on drying shrinkage was only studied at the 14-day curing duration. Specimens were monitored for 56 days to determine if lower drying shrinkage was achieved. The first objective was to find out if SCM's were affecting the drying shrinkage of the ODOT mixture design. A mixture without any SCM's (OPC1) was cast to identify the effect of

the various SCMs when used as a percent replacement for the portland cement. Shown below in Figure 4.4 is the 14-day cure free drying shrinkage for mixtures with SCM modifications.

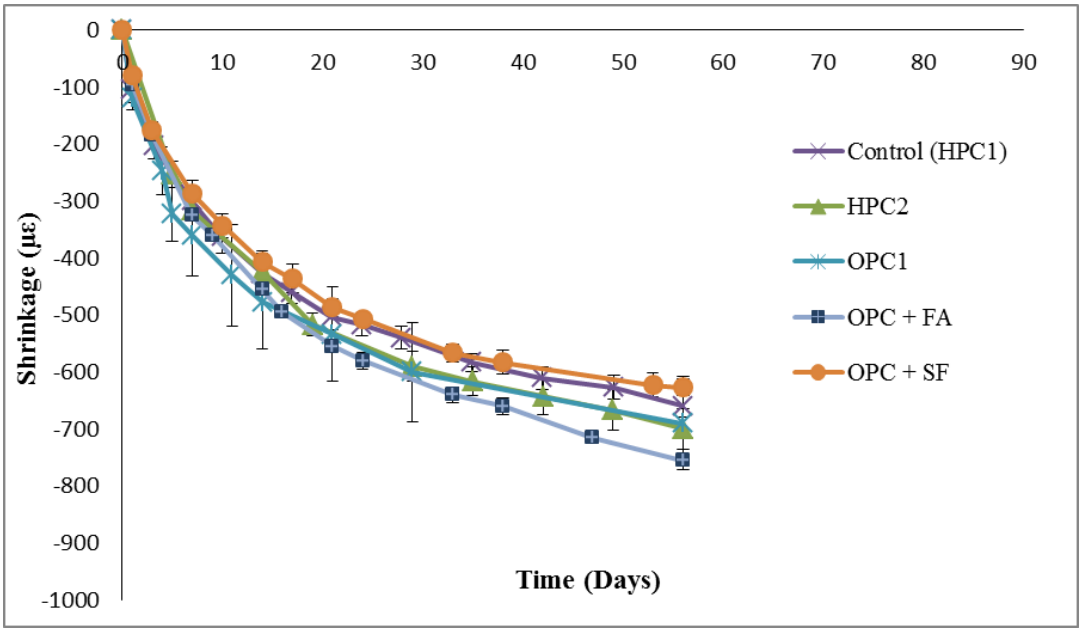

Figure 4.4:14-day cure drying shrinkage for mixtures with SCM modifications

As shown in Figure 4.4 none of the SCM modifications reduced the total shrinkage at 56 days of drying. In addition, mixtures with higher OPC content achieved approximately the same drying shrinkage as the control mixture. However, when using slag at the same replacement level in a high performance mixture, the drying shrinkage was slightly higher than the original control. There is a synergistic effect when using OPC in conjunction with fly ash and silica fume; however, there may be room for improvement since fly ash notably increases drying shrinkage. Subramaniam et al. showed that mixtures with ultra-fine (mean particle size equal to 3μm) Class F fly ash showed higher drying shrinkage when compared to mixtures with plain OPC and OPC with silica fume (Subramaniam et al. 2005).

Next, the effect of coarse aggregate type and cement content on drying shrinkage was investigated. Previous research at Oregon State University from Fu and Ideker showed that a mixture incorporating limestone (LS) as the coarse aggregate showed low drying shrinkage (457 microstrains at 90 of drying) (Fu and Ideker 2013). The LS mixture used the same ODOT mixture design, siliceous river sand, and angular limestone coarse aggregate. To further

investigate the effect of limestone and coarse aggregate angularity on drying shrinkage mixtures using a local crushed limestone and crushed siliceous river gravel (CHPC) were evaluated. Shown in below in Figure 4.5are the drying shrinkage results for the mixtures with cement and aggregate modifications.

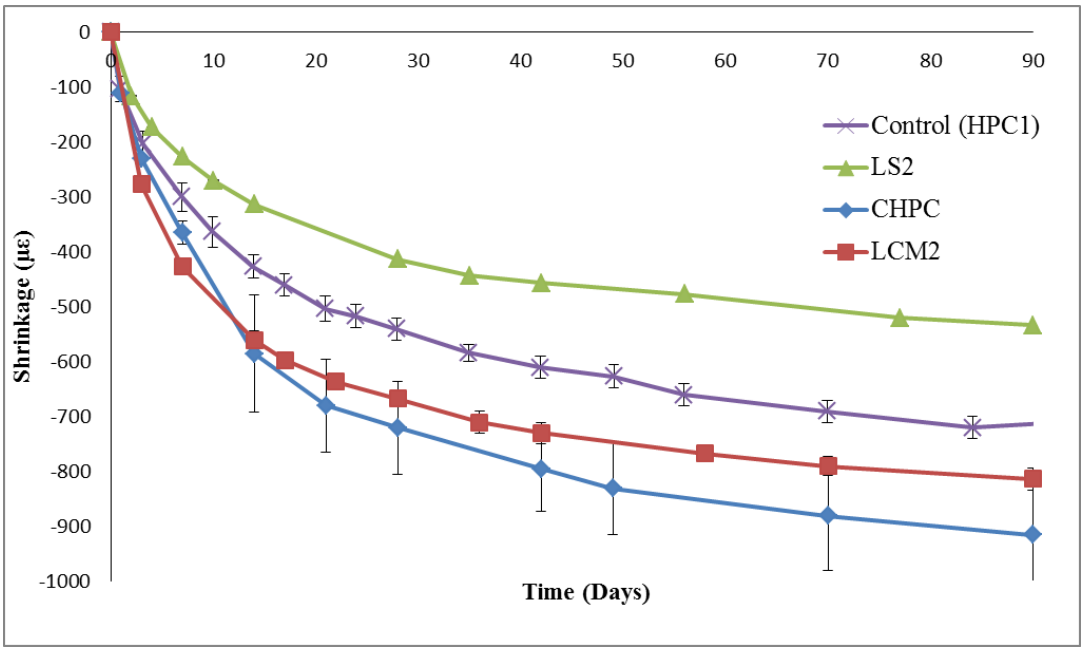

Figure 4.5: 14-day cure drying shrinkage for mixtures with cement and coarse aggregate modifications

The cement content in current HPC mixtures has been regarded as one of the most important factors for high shrinkage. Lowering the cement content to what is considered "low cement content" or (500-550lb/yd^3) should have provided a reduction in shrinkage. According to Darwin et al., a cement content of 540lb/yd^3 will limit the potential for shrinkage cracking and achieve moderate strength (Darwin 2010). In addition, cracking occurs up to 3 times as much in concrete with strength of 6500 psi when compared to concrete with 4500psi strength (Darwin, 2010). The compressive strength was far lower than both the 4500psi suggested by Darwin, and the 4000psi minimum for concrete bridge decks as prescribed by ODOT. However, as shown above lowering the cement content was not successful in reducing the drying shrinkage. 1-day cure drying shrinkage results for LCM1 can be found in the appendix (>1000 microstrain at 90 days).

Both SCM and cement content modifications had negative results on the drying shrinkage of the ODOT HPC mixture. The limestone mixture (LS2) had a total shrinkage of 533 microstrains at 90 days of drying. The crushed river gravel had adverse effects on drying shrinkage. This suggests that the angularity of the aggregate is not positively correlated with drying shrinkage. These results suggest that the mineralogy of the aggregate had the most significant effect on drying shrinkage, however further work to characterize the aggregate is warranted.

4.3 RESTRAINED SHRINKAGE

4.3.1 Time-to-cracking

Table 4.3 provides a summary of the ASTM C1581 ring results, including time-to-cracking and the corresponding stress rate. All individual strain gauge readings can be found in Appendix A.

Table 4.3 Summary of time-to-cracking and stress rate of ASTM ring tests

Mixture	Curing Duration (days)	Time-to-Cracking, (days)				Stress Rate, (psi/day)				Cracking Potential Classification*
		1	2	3	Ave.	1	2	3	Ave.	
HPC1	14	4.4	4.6	3.6	4.2	50	41	70	54	H
HPC2	14	6.2	6.2	8.2	6.9	47	48	40	45	MH
FHPC D5	14	5.9	5.9	4.9	5.6	64	45	56	55	H
FHPC D7.5	14	4.6	6.6	7.1	6.1	53	51	53	52	H
FHPC D10	14	7.3	7.9	8.0	7.7	49	54	56	53	MH
CHPC	14	9	5.7	9	7.9	37	31	37	35	MH
LS2	14	20.5	8.7	23.4	17.5	21	31	18	23	ML
LCM2	14	6.1	3.4	5.2	4.9	87	78	64	76	H
OPC1	14	2.7	5.7	5.4	4.6	40	56	46	47	MH

* H – High; MH – Moderate High; ML – Moderate Low; L – Low.

The first notable result was the difference between HPC1 and HPC2. The average time to cracking of HPC2 was about 3 days longer than HPC1. The main difference between these two mixtures was that HPC1 contained class F fly ash and HPC2 contained slag. The shrinkage investigation discussed in section 3.2.2 showed similar results, where the use of OPC and fly ash

had the highest free shrinkage. Another important observation is the time-to-cracking of ring A for the FHPC D7.5 mixture. The time-to-cracking was notably lower than ring B and C, which obtained similar results. This mixture should be repeated at least twice to definitively confirm the cracking potential. Although low cement content mixtures did not achieve mechanical property requirements one set of rings was cast to determine the cracking risk. The LCM2 mixture increased the time-to-cracking by roughly 1 day when compared to HPC1.

Time-to-cracking in fiber mixtures improved as higher amounts of fibers were added. The highest amount of fibers tested was at the 10lb/yd^3 dosage rate, which is double the manufacture's recommended dosage. Overall, there was a 29%, 37%, and 59% increase in time-to-cracking when applying synthetic blended fibers at a 5lb/yd^3, 7.5lb/yd^3, and 10lb/yd^3 dosage rate respectively (compared to HPC1). However, the use of slag at a 30% replacement had a similar reduction in time-to-cracking compared to concrete with fibers.

4.3.2 Strain Behavior

One of the most significant observations was the stability of the strain signal in each ring before and after cracking. Typically, it was observed that in concrete with no fibers the strain curves sharply decreased (high slope) and then a nearly vertical change in strain to near zero was observed at the time of cracking. In the control mixture (see Figure 4.6) there was some fluctuation before cracking, but not considerably. After the rings cracked there was also little to no fluctuation and generally smooth strain curves. The strain behavior was markedly different when fibers were added. Figure 4.7 shows an example of this interaction. First, instead of an abrupt decrease in strain there was a gradual decrease with a considerable amount of fluctuation. This was likely due to the synthetic fibers, which provided crack propagation resistance, as the compressive strain due to drying overcame the tensile strength of the concrete matrix. In addition, after the specimens cracked there was a more gradual reduction in stress rather than the sharp decrease observed in mixtures without fibers. This suggests that the fibers continued to provide cracking resistance (toughness) after the ring had cracked. Another observation was that in rings incorporating fibers; the crack width was further reduced compared to the control mixtures. This is further explained in section 4.3.3. Figure 4.6 and Figure 4.7 below show the

average strain data for each ring in the control mixture (HPC1) and the 5lb/yd^3 fiber dosage respectively.

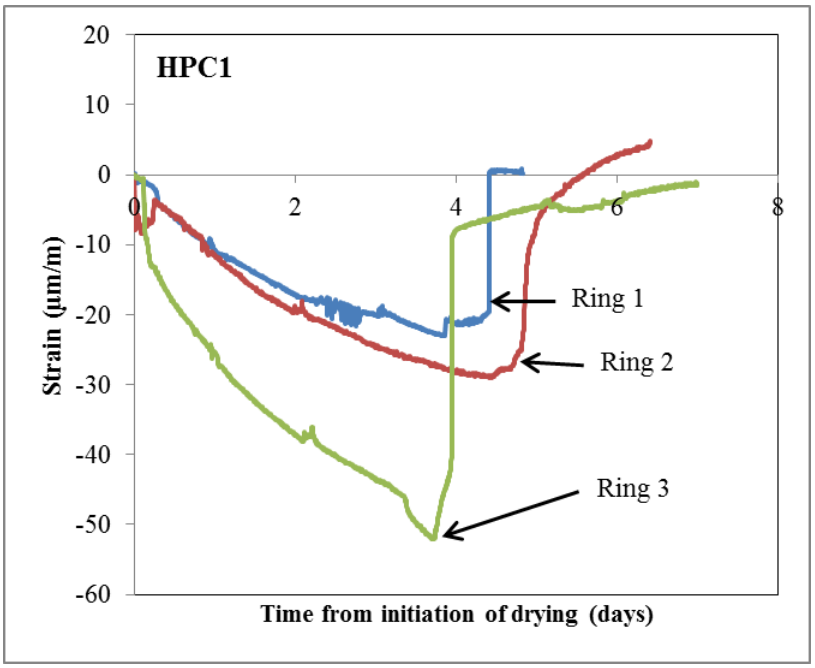

Figure 4.6: Restrained shrinkage strain data for control

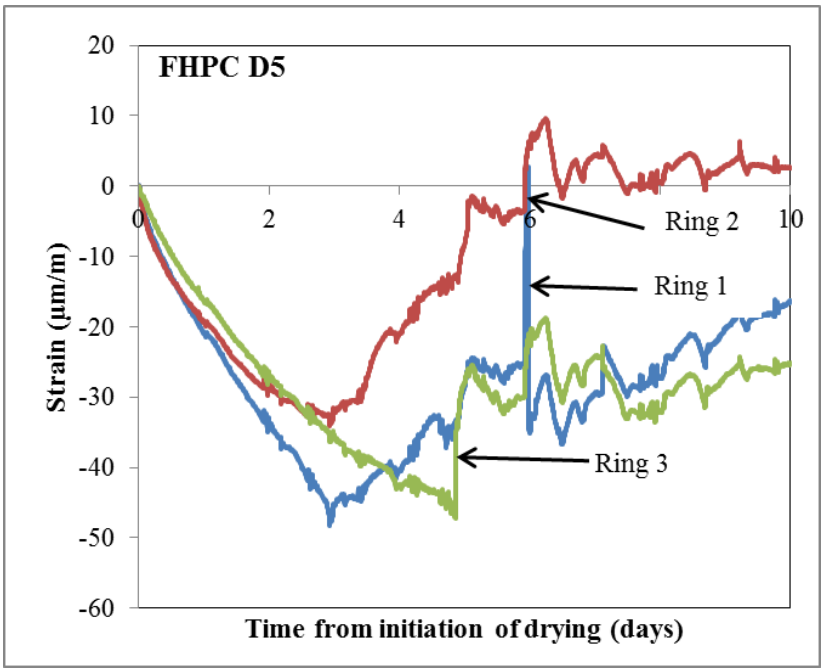

Figure 4.7: Restrained shrinkage strain data for 5lb/yd^3 fiber dosage (FHPC D5)

Similar results were shown in FHPC D7.5 where fluctuation is observed before and after cracking. Figure 4.8 below shows the restrained shrinkage results for FHPC D7.5.

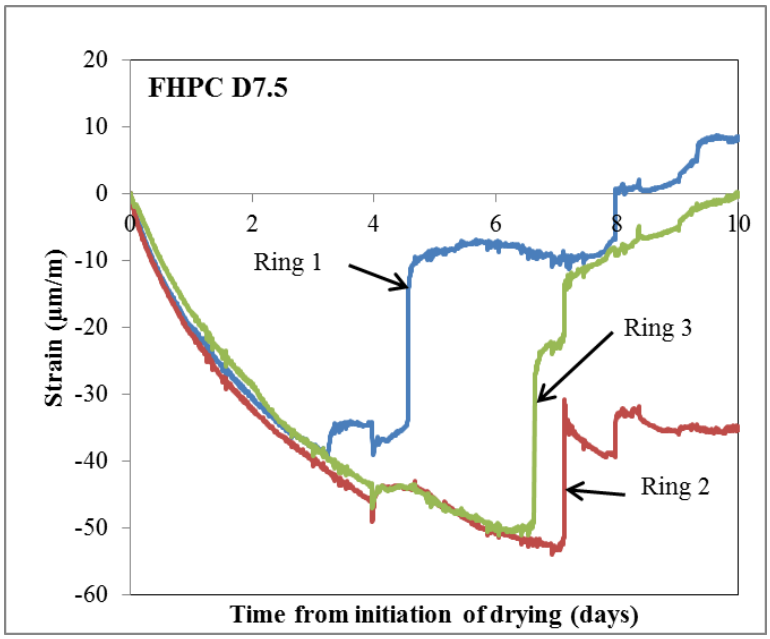

Figure 4.8: Restrained shrinkage strain data for 7.5lb/yd^3 fiber dosage (FHPC D7.5)

The fluctuation observed in FHPC D7.5 was not as pronounced as the fluctuation in FHPC D5 and FHPC D10 (see Figure 4.9 below).

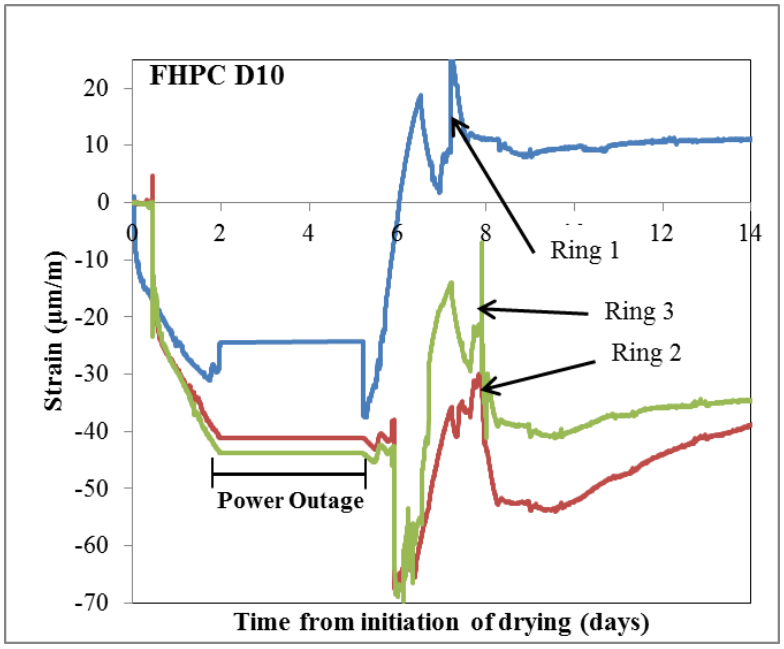

Figure 4.9: Restrained shrinkage strain data for 10lb/^{yd3} fiber dosage (FHPC D10)

Also, in FHPC D10 some data were lost due to power failure. Based on visual inspection, no cracking was observed during the power outage (3 days); therefore, the test was continued. Upon cracking FHPC D10 showed more restraint compared to HPC1. The data shows some reduction in stress during the 6-7.5 day time period indicating that there was some internal cracking that was restrained by the fibers. At the time of cracking the sharp decrease in strain was not as pronounced as it was in the HPC1 mixture. In CHPC (see Figure 4.10 below), the strain data for Ring 1 and Ring 3 showed no clear indication of cracking. By visual inspection the rings cracked at 9 days. In addition, the stress rate was much lower (see Table 4.3) than all other mixtures. This strain behavior also was noticed in previous work in the mixture labelled "LS", which contained a limestone coarse aggregate (Fu and Ideker 2013). The only similarity between the CHPC and LS mixtures is the coarse aggregate angularity.

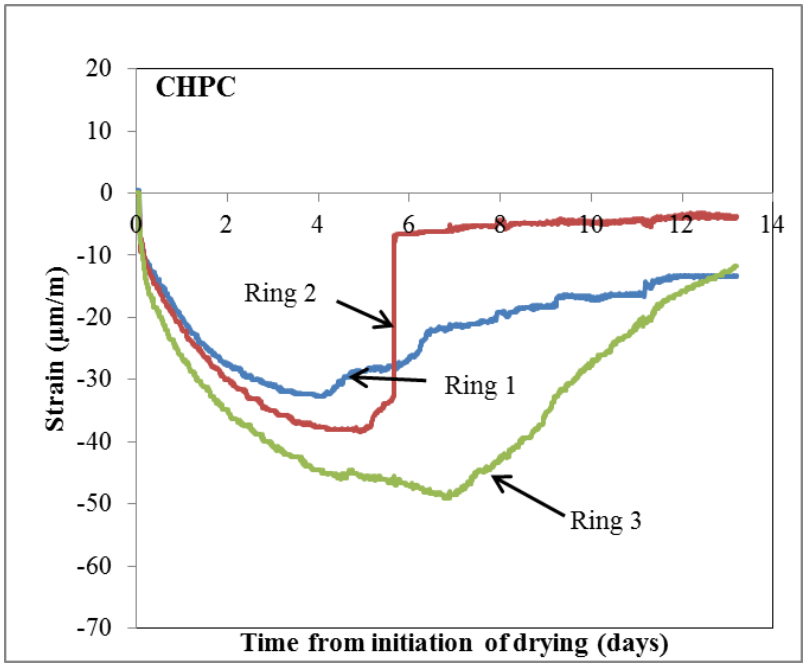

Figure 4.10: Restrained shrinkage strain data for CHPC

Overall, the inclusion of synthetic blended fibers showed improved performance in cracking resistance while being subjected to ASTM 1581. The additional restraint provided by the synthetic fiber blend prolonged the time-to-cracking of the concrete when compared to HPC1. There may be a link between coarse aggregate angularity and cracking risk of concrete. Shown below in Figure 4.11 is the restrained shrinkage data for the limestone mixture.

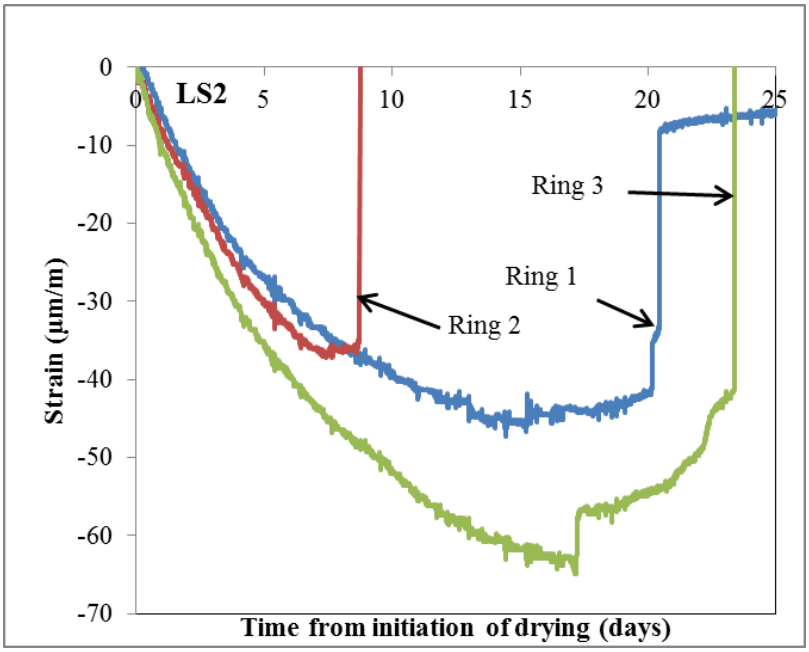

Figure 4.11: Restrained shrinkage data for LS2

LS2 showed the lowest cracking risk, which was shown in both the time-to-cracking (17.5 days average) and the stress rate (23 psi/day average). Ring 2 cracked prematurely at 8.7 days of drying; regardless, the overall potential for cracking remained in the ML category.

4.3.3 Crack Monitoring

After initial exposure to drying all ring specimens were monitored daily for signs of cracking. After the rings had completely cracked (vertical crack from top to bottom), the cracks widths were measured. The time-to-cracking shown in the strain data was consistent with visual inspection. Shown below in Figures **Error! Not a valid bookmark self-reference.**-Figure 4.15 are the crack widths of the fiber mixtures and the HPC control mixture.

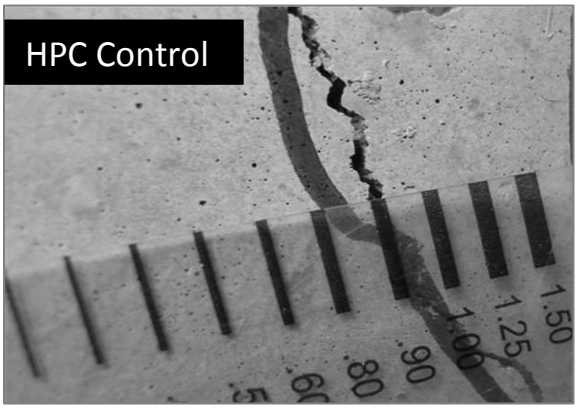

Figure 4.12: Crack width- 0.035in

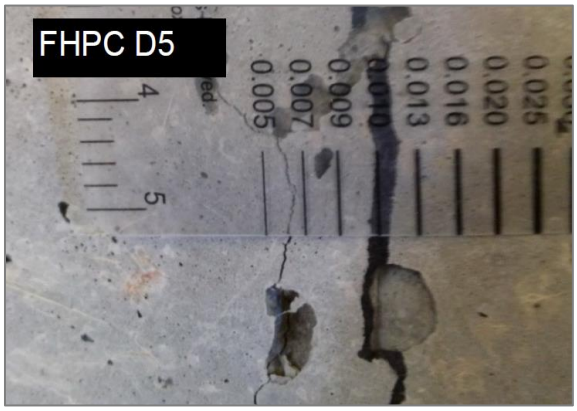

Figure 4.13: Crack width- 0.005in-0.007in

Figure 4.15: Crack width- 0.008in

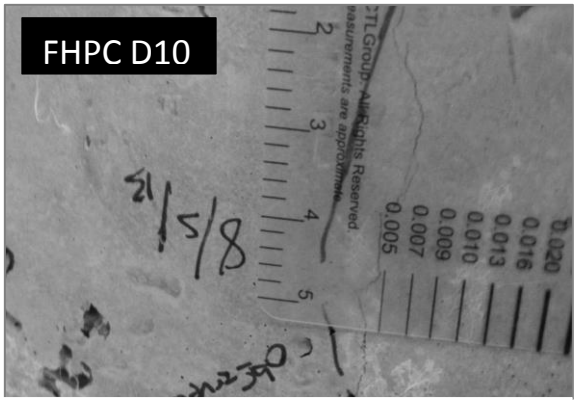

Figure 4.14: Crack width- 0.005in

The crack widths were notably reduced when compared to the HPC control mixture. On average mixtures with fibers showed a crack width of 0.006 in when compared to the cracks observed in the control mixture which were in the range of 0.035in. This suggests that the use of blended synthetic fibers controls cracking and minimizes the chances of future durability concerns. Shown below in Table 4.4 are the largest crack widths measured for each mixture.

Table 4.4: Crack widths for each specimen (in)

Mixture	Ring 1	Ring 2	Ring 3	Average
HPC Control	0.035	0.020	0.031	0.029
FHPC D5	0.005	0.007	0.007	0.007
FHPC D7.5	0.008	0.005	0.005	0.007
FHPC D10	0.005	0.005	0.005	0.005

The reduction in crack width is likely due to the restraint provided by the blended synthetic fibers, which do not allow the cracks to propagate once the tensile stress in the concrete from drying overwhelms the tensile capacity. The average crack widths of the fiber mixtures were similar, which suggests that there was adequate fiber distribution to minimize the crack widths at all dosages.

4.4 FREEZE/THAW ASTM C666

Freeze thaw samples were moist cured for 28 days before being introduced to freezing and thawing conditions and tested according to ASTM C666-03. The relative dynamic modulus of elasticity (RDME) was recorded every 36 cycles, and the test was terminated at 300 cycles. Only FHPC D7.5 and FHPCD10 were tested for freeze/thaw resistance due to their higher time-to-cracking in the restrained ring test. Both mixtures were air entrained with at least 6.0% air. To pass ASTM C666 the relative dynamic modulus must be above 60% and the specimen must show not show severe signs of degradation over the 300 cycles. RDME results are shown below in Figure 4.16.

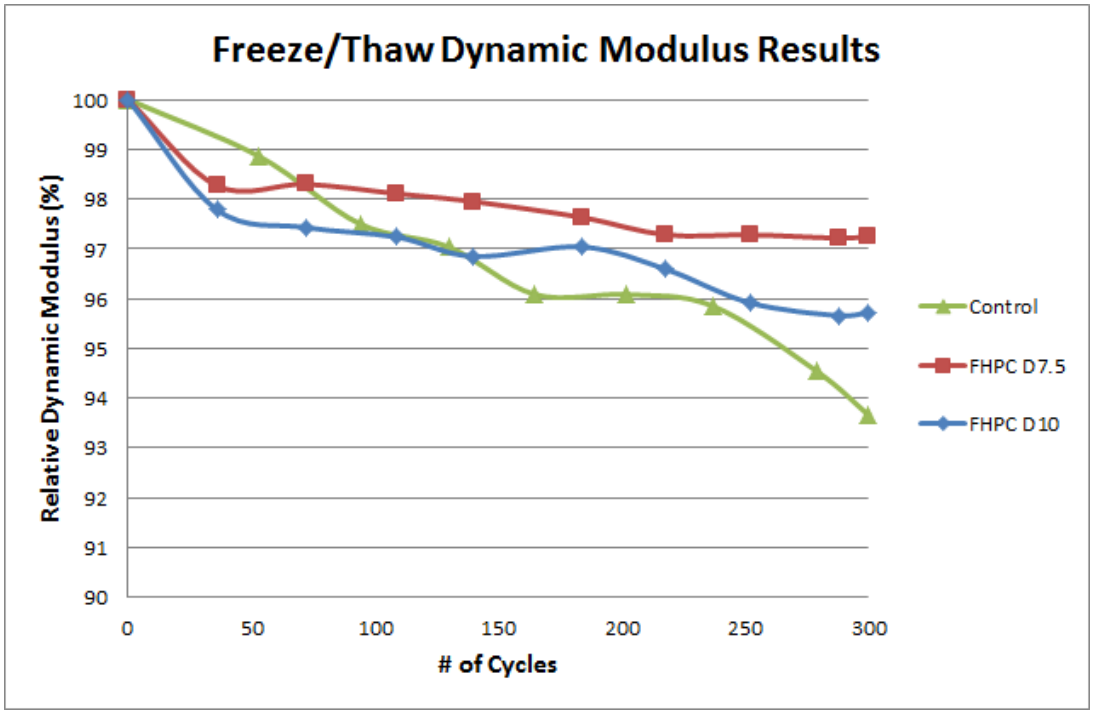

Figure 4.16: Relative Dynamic Modulus of Elasticity Results

The mixtures with fibers had a higher RDME, which suggests that the fibers may increase freeze/thaw performance. In addition to the RDME measurements, the mass was recorded over 300 cycles. Mass change and RDME results are shown in Table 4.5.

Table 4.5: Mass Loss and RDME after 300 Cycles

Mixture ID	Mass change (%)	RDME
Control	-0.80	90%
FHPC D7.5	-0.15	97%
FHPC D10	-0.19	96%

The control lost roughly 5 times more mass when compared to FHPC D7.5 and about 4 times more mass when compared to FHPC D10. However, scaling was observed on all specimens. It was observed that that FHPC D10 had a higher level of scaling than FHPC D7.5. In FHPC D10 more macro-synthetic fibers were exposed at the surface of the specimens. Once these fibers became exposed the paste around the fiber began to scale. Since FHPC D10 had a higher number of macro-synthetic fibers exposed more deterioration was observed. This effect may also be due to the fiber distribution in each specimen. Figure 4.17 shows the FHPC D7.5 specimens after 300 cycles. The specimen on the top of the picture showed little to no deterioration. However, the specimen on the bottom of the picture showed more macro-synthetic fibers exposed to the surface and some clumping on the left side of the specimen. The clumping of the fibers increased the severity of deterioration due to freezing and thawing. These specimens were cast from the same mixture.

Figure 4.17: FHPC D7.5 specimens after 300 cycles

The clumping effect was also noticed in FHPC D10 where a significant amount of paste and small aggregates were scaled. Figure 4.18 shows a FHPC D10 specimen after 300 cycles. The area with the highest severity of deterioration is at the right of the specimen where clumping of the fibers was observed.

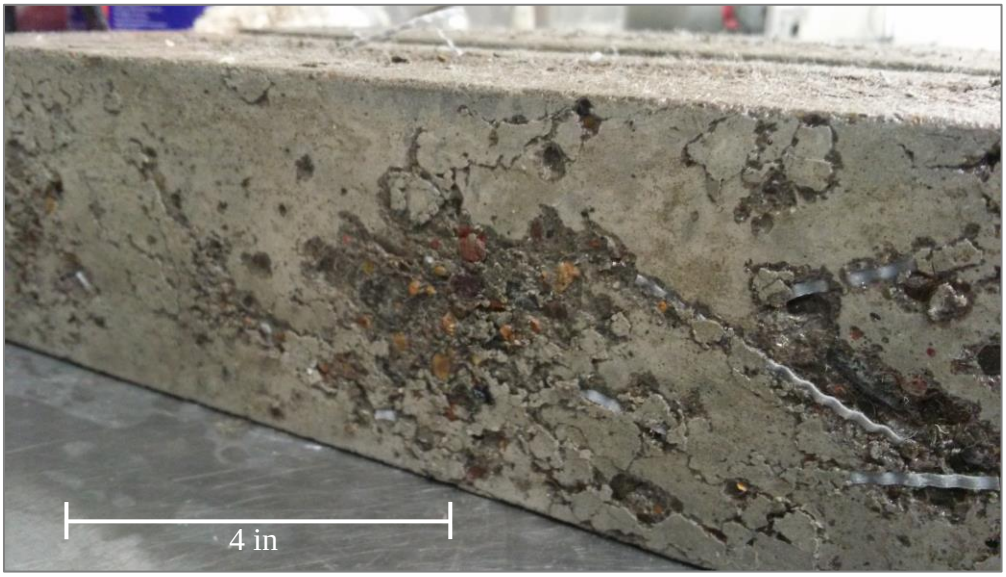

Figure 4.18: FHPC D10 specimen after 300 cycles

Although the fibers may lead to increased scaling during freezing and thawing there was no significant cracking observed, and the RDME was maintained at a higher percentage than the control. The damage shown in figures Figure 4.17 and Figure 4.18 is only on the surfaces of the specimens. Scaling is the result of local peeling or flacking on the surface of concrete. These localized areas can extend to patches and merge into larger areas thereafter. According to Fabri et al., moderate to severe scaling expose the coarse aggregate from the concrete surface and may involve losses up to 0.012- 0.40 in (3-10 mm) from the concrete surface, which reduces the clear cover of the steel reinforcement (Fabri et al. 2008). When coupled with deicing salts (also well known to cause scaling), the damage can be more detrimental.

The 7.5lb/yd^3 fiber dosage rate showed the best freeze/thaw protection in both visual degradation and RDME. Similar RDME results were observed by Richardson et al., where the use of micro-synthetic polypropylene fibers provided superior freeze/thaw protection than plain concrete (Richardson et al. 2012). However, it should be noted that Richardson et. al. studied a mixture with low frost resistance (w/cm=0.80). Generally concrete mixtures with a w/cm ratio less than

0.40 do not experience significant durability concerns under freezing/thawing conditions (Jacobsen et al. 1996). The theory behind these findings is that the inclusion of polypropylene reduces water absorption and increases the air void system and thus increases freeze thaw resistance (Richardson et al. 2012).

4.5 RCPT ASTM C1202

Samples cast for rapid chloride permeability testing were wet cured for 56 days prior to testing. In order to meet the "very low" chloride ion penetrability, according to ASTM C1202, the total charge passed must be below 1000 coulombs. Shown below in Table 4.6 is the total charge passed over the 6-hour duration of the RCPT.

Table 4.6: Total charge passed (RCPT)

Mixture ID	Total Charge Passed (Coulombs)
Control	860
FHPC D7.5	560
FHPC D10	693

Although all samples were within the "very low" category according to ASTM C1202, both fiber dosages reduced the total charge passed. In recent studies, Nayaran found that there was a marginal improvement in total charge passed when using polypropylene fibers (Narayan 2013). To further investigate the effect of fibers on ion penetrability, it is recommended to use a control mixture with higher permeability. A mixture with a higher w/cm ratio and no added SCM's may be appropriate for such testing and comparison.

5.0 CONCLUSIONS AND RECOMENDATIONS

5.1 CONCLUSIONS

In this project the use of blended synthetic fibers for reducing the risk of cracking in high performance concrete was investigated. The impact of shrinkage resulting from modifications to the paste portion of the high performance concrete was also investigated. Standard durability tests, ASTM C666 and ASTM C1202 were also done to determine the impact that the inclusion of fibers had on the freeze-thaw performance and chloride ion penetrability of these mixtures. It was found that:

- For specimens wet cured for 14 or 28 days prior to initiation of drying, the incorporation of fibers at three different dosage rates (5 lb/yd^3, 7.5 lb/yd^3 and 10 lb/yd^3) had a minimal impact on the 90-day drying shrinkage of high performance concrete specimens compared to the control.

- For specimens wet cured for only 3 days prior to initiation of drying, the incorporation of fibers at three different dosage rates (5 lb/yd^3, 7.5 lb/yd^3 and 10 lb/yd^3) showed a slight increase in the 90-day drying shrinkage of high performance concrete specimens compared to the control.

- The incorporation of fibers into high performance concrete (HPC) increased the time-to-cracking in restrained ring testing over the HPC control and also markedly changed the post-crack behavior of the concrete indicating the fiber's ability to limit the propagation of cracks once they start forming.

- In restrained ring testing the HPC control mixtures showed average crack widths of 0.035 in. In all mixtures containing fibers, the crack widths were significantly reduced to 0.005-0.008 in.

- The replacement of cement with 30% slag rather than 30% fly ash (as in the standard HPC control mixture) reduced the cracking risk in restrained ring testing by extending the time to cracking by days (could also mention stress rate).

- The incorporation of fibers into HPC was shown to improve the freeze-thaw resistance of the mixtures according to ASTM C666 Procedure A resulting in a higher relative dynamic modulus at the end of 300 cycles compared to the HPC control. There was a slight increase in scaling of the mixtures incorporating fibers, but this appeared to be superficial and did not negatively affect the integrity of the specimens.

- The incorporation of fibers into HPC did not impact the ASTM C 1202 (rapid chloride penetration test) results compared to the control. All mixtures still fell within the "very low" category for chloride ion penetrability.

- Reducing the cement content of the mixtures lowered the compressive strength as much as 25% below the 4000 psi minimum threshold and did not reduce free shrinkage.

- Aggregate angularity may have a positive effect on the cracking risk of HPC. The strain data suggested that the 2 of the rings had not cracked. In addition, the stress rate was significantly lower than the control.

- The use of limestone coarse aggregate most significantly reduced both the drying shrinkage and cracking risk.

5.2 RECOMMENDATIONS

Based on the results of this research project the incorporation of fibers into high performance concrete mixtures should reduce the potential for both early and later-age cracking for ODOT bridge decks. The results support that the incorporation of fibers should also help to control crack widths even if cracking does occur in the HPC. Importantly the use of fibers did not impact either freeze-thaw performance or chloride ion penetrability of the mixtures investigated in this study. In fact the incorporation of fibers may further improve the freeze-thaw resistance of HPC. In terms of fiber dosage rates, all those investigated improved concrete properties in terms of cracking resistance. At the higher fiber dosage rate of 10 lb/yd^3 there were marked decreases in concrete workability. These were overcome with increasing dosages of superplasticizer. However, it is not expected that this high of a dosage rate of fibers will provide such significant improvement in performance that the higher dosage rate is justified. Therefore,

a dosage rate of 5 lb/yd^3 or 7.5 lb/yd^3 is recommended. These dosage rates may be further modified based on the results of current and/or future HPC decks that incorporate fibers.

5.3 FUTURE RESEARCH

The most important recommendation from this research project is to verify the laboratory findings with field experience of HPC incorporating blended fibers. Long-term periodic investigations of the bridge decks will confirm that the use of fibers is 1) reducing or even eliminating cracking in HPC 2) maintaining crack widths that are smaller in width and length compared to HPC without fibers and 3) promoting long-term durability. An investigation on the effect of GGBS to reduce the cracking risk of HPC is suggested. Further research into the impact of manufactured (e.g. crushed) aggregates compared to rounded river gravels should be undertaken. Previous research showed that a crushed limestone aggregate also had superior cracking resistance compared to the HPC control with rounded river gravel. This was further confirmed with cracking risk and drying shrinkage results from LS2. The impact of surface texture and mineralogy on cracking resistance bears further research as a possible method to reduce cracking in high performance concrete. To determine the effect of fiber dosage on the crack widths on the rings specimens an aggressive testing regime is suggested. The rings should only be cured for 1 day and immediately exposed to drying. This will cause higher drying shrinkage stresses and cause the rings to crack sooner. The crack widths in each ring can be monitored thereafter. It is predicted that under higher stresses the crack widths be more pronounced, and the effect of the fiber dosage will be more prominent.

6.0 REFERENCES

AASHTO T334-08. "Standard Method of Test for Estimating the Cracking Tendency of Concrete." (2008).

ACI Committee 233, "Slag Cement in Concrete and Mortar," *ACI Manual of Concrete Practice, American Concrete Institute,* Farmington Hills, MI, (2004).

American Concrete Institute (ACI). "Plastic Cracking." *Concrete.org*. n.d. Web. (2014).

Adam, A. A. "Strength and Durability Properties of Alkali Activated Slag and Fly Ash-Based Geopolymer Concrete." *RMIT University*, Melbourne, Australia (2009).

Aitcin, P.C. "Autogenous Shrinkage Measurement." *Proc., Autoshrink '98: International Workshop on Autogenous Shrinkage of Concrete,* Hiroshima, Japan. (1998): 245-256.

Al-Amoudi, O.S.B., Maslehuddin M., Shameem, M., and Ibrahim, M. "Shrinkage of Plain and Silica Fume Cement Concrete Under Hot Weather." *Cement and Concrete Composites,* 29.9 (2007): 690-699.

Al-Manaseer, A. and S. Ristanovic, "Predicting Drying Shrinkage of Concrete." *Concrete International*, 26.8 (2004): 79-83.

Aly, T., Sanjayan, J.G. and Collins, F. "Effect of Polypropylene Fibers on Shrinkage and Cracking of Concretes." *Journal of Materials and Structures,* 41.10 (2008):1741–1753.

Atis, C.D. "High-Volume Fly Ash Concrete with High Strength and Low Drying Shrinkage." *Journal of Materials in Civil Engineering,* (2003): p. 153-156.

Andrade C., Sarría J. and Alonso C. “Relative Humidity in the Interior of Concrete Exposed to Natural and Artificial Weathering.” *Cement and Concrete Research*, 29 (1999): 1249-1259.

ASTM C157-06: Standard Test Method for Length Change of Hardened Hydraulic-Cement Mortar and Concrete, *ASTM International*, (2006).

ASTM C618-09: Standard Specification for Coal Fly Ash and Raw or Calcined Natural Pozzolan for Use in Concrete, *ASTM International*, (2009).

ASTM C666-03*:* Standard Test Method for Resistance of Concrete to Rapid Freezing and Thawing. *ASTM International* (2003).

ASTM C1202-12: Standard Test Method for Electrical Indication of Concrete's Ability to Resist Chloride Ion Penetration. *ASTM International* (2012).

ASTM C1581-09a. "Standard Test Method for Determining Age at Cracking and Induced Tensile Stress Characteristics of Mortar and Concrete under Restrained Shrinkage." ASTM International (2009).

ASTM C1589-13. “Standard Test Method for Evaluating Plastic Shrinkage Cracking of Restrained Fiber Reinforced Concrete (Using a Steel Form Insert).” *ASTM International* (2013).

Babaei. K., and Purvis. R. "Report on Surveys of Existing Bridges." Wilbur Smith Associates Rep. on PennDOT Proj. No. 89-01, Falls Church, Va. (1994).

Banthia, N., and Gupta, R. “Influence of Polypropylene Fibre Geometry on Plastic Shrinkage Cracking in Concrete.” *Cement and Concrete Research*, 36.7 (2006): 1263–1267.

Bayasi, Z., Zeng, J., "Properties of Polypropylene Fiber-reinforced Concrete," *ACI Materials Journal,* 90.6 (1993): 605-610.

Beaudoin, J. J., and Liu, Z. (2000). "The Permeability of Cement Systems to Chloride Ingress and Related Test Methods." *Cement, Concrete, and Aggregates,* 22.1 (2000): 16-23.

Bentur A, Igarashi S., and Kovler K. "Prevention of Autogenous Shrinkage in High Strength Concrete by Internal Curing Using Wet Lightweight Aggregates." *Cement and Concrete Research,* 31.11 (2001):1587–91.

Bentz, D. P. "Influence of Curing Conditions on Water Loss and Hydration in Cement Pastes with and without Fly Ash Substitution." *National Institute of Science and Technology,* NISTIR 6886 (2002).

Bouzoubaâ, N., Bilodeau, A., Sivasundaram, V., Fournier, B., and Golden, D. M. "Development of Ternary Blends for High-performance Concrete." *ACI Materials Journal*, 101.1 (2004): 19-29.

Brandt, A.M. "Fibre reinforced cement-based (FRC) composites after over 40 years of development in building and civil engineering." *Composite Structures* 86 (2008): 3-9.

Brooks, J.J., Megat Johari, M.A., and Mazloom, M., "Effect of admixtures on the setting times of high-strength concrete," *Cement and Concrete Composites* 22 (2000): 293-301.

Brooks, E.W., "Polypropylene Fiber-Reinforced Microsilica Concrete Bridge Deck Overlay At Link River Bridge." *Oregon Department of Transportation* (2000).

Brown, M.D., Smith, C.A., Sellers, J.G., Folliard, K.J., and Breen, J.E., "Use of Alternative Materials to Reduce Shrinkage Cracking in Bridge Decks," *ACI Materials Journal,* 104.6 (2006): 629-637.

Cha Y., Kim K. and Kim D. “Evaluation on the Fracture Toughness and Strength of Fiber Reinforced Brittle Matrix Composites.” *KSME International Journal*, 12.3 (1997): 370-379.

Chen, P. and Chung, D.D.L. “Low-drying-shrinkage Concrete Containing Carbon Fiber.” *Composites: Part B 27B* (1996): 269-274

Cusson, D. and T. Hoogeveen, “Internal Curing of High-Performance Concrete with Pre-soaked Fine Lightweight Aggregate for Prevention of Autogenous Shrinkage Cracking.” *Cement and Concrete Research*, 38 (2008):757-765.

Darwin D., J. Browning, W. Lindquist, H. McLeod, J. Yuan, M. Toledo, and D. Reynolds, "Low-Cracking, High-Performance Concrete Bridge Decks," *Transportation Research Record: Journal of the Transportation Research Board*, 2202 (2010): 61-69, 2010.

Darwin et al. “Low-Cracking, High-Performance Concrete Bridge Decks: Case Studies over First 6 Years.” *Transportation Research Record: Journal of the Transportation Research Board*, 2202.1 (2010): 61-69.

Deebodt, T., Ideker J.H., and Fu T. "Internal Curing of High-performance Concrete for Bridge Decks." *Oregon Department of Transportation (ODOT)*, SPR 711. (2013).

Delatte, N. “Reducing Cracking of High Performance Concrete Bridge Decks.” *TRB 2007 Annual Meeting* (2007).

Dossey, T. and McCullough, B.F., “Controlling Early-Age Cracking in Continuously Reinforced Concrete Pavement: Observations from 12 Years of Monitoring Experimental Test Sections in Houston, Texas” *Transportation Research Record*, 1684 (1999): 35-43.

Fabbri, A., Coussy, O., Fen-Chong, T., and Monteiro, P. (2008). ”Are Deicing Salts Necessary to Promote Scaling in Concrete?” *Journal of Engineering Mechanics*, 134.7 (2008): 589-598.

Feldman, R., Prudencio, L. R., and Chan, G. "Rapid Chloride Permeability Test on Blended Cement and Other Concretes: Correlations Between Charge, Initial Current and Conductivity." *Construction and Building Materials,* 13 (1999): 149-154.

Folliard, K., Simpson, B., "Low-Volume Polymeric Fiber-Reinforced Concrete Fiber reinforced Concrete: Present and Future." *Canadian Society for Civil Engineering* (1998): 133-147.

Folliard, K., Sutfin, D., Turner, R. and Whitney, D.P., "Fiber in Continuously Reinforced Cocnrete Pavements," *Texas Department of Transportation* Project Report FHWA/TX-07/0-4392-2 (2006).

Fu, T. "Autogenous Deformation and Chemical Shrinkage of High Performance Cementitious Systems." Master's Thesis, *Oregon State University* (2011).

Fu, T., T. Deboodt, and J.H. Ideker, "A Simple Procedure on Determining Long-Terms Chemical Shrinkage for Cementitious Systems Using Improved Chemical Shrinkage Test." *Submitted to ASCE Journal of Materials*, (2011).

Fu, T. and Ideker, J.H., "Development of Testing Protocols and Shrinkage Limits for ODOT High Performance Concrete." Oregon Department of Transportation, SPR 728 (2013).

Gopalaratnam V.S. et al. "Fracture Toughness of Fiber Reinforced Concrete." *ACI Materials Journal* 88.4 (1991): 339-353.

Goto, Y. and Fujiwara, T. "Volumetric Change of Aggregate by Absorption and Drying." *Proceeding of JSCE* 247 (1976) 97-108.

Hansen W. "Drying Shrinkage Mechanisms in Portland Cement Paste." *Journal of American Ceramic Society* 70.5 (1987): 323-328.

Holt, E.E. “Early-Age Autogenous Shrinkage of Concrete.” Technical Research Centre of Finland, *VTT Publications*, 446 (2001).

Huo X. and Wong L.U., "Early-Age Shrinkage of HPC Decks under Different Curing Methods," Philadelphia, Pennsylvania, USA, (2000): 168.

Hsie, M. Tu, C. and Song P.S. “Mechanical Properties of Polypropylene Hybrid Fiber-reinforced concrete.” *Material Science and Engineering* A 494 (2008): 153-157.

Jacobsen, S., and Matala, S. “Frost Durability of High Strength Concrete: Effect of Internal Cracking on Ice Formation.” *Cement and Concrete Research,* 26.6 (1996): 919-931.

Jensen, O.M. and P.F. Hansen. “Autogenous Deformation and RH-Change in Perspective.” *Cement and Concrete Research*, 31.12 (2001):1859-1865.

Jensen, O.M., and Hansen, P.F., “Water-Entrained Cement-Based Materials: II. Experimental Observations,” *Cement and Concrete Research*, 32.6 (2002): 973-978.

Jensen O.M. “Use of Superabsorbent Polymers in Concrete.” *Concrete International* (2013): 48-52.

Jianyong, L. and Yan, Y. “A Study on Creep and Drying Shrinkage of High Performance Concrete.” *Cement and Concrete Research*, 31 (2001): 1203-1206.

Juenger et al. “Effects of Supplementary Cementing Materials on the Setting Time and Early Strength of Concrete.” *Texas Department of Transportation (TXDOT)* (2008).

Kosmatka S.H. and Wilson M.L. “Design and Control of Concrete Mixtures: The guide to applications, methods and materials.” Washington, DC: *Portland Cement Association (PCA)* (2011). Print.

Kovler, K., Sikuler, J. and Bentur, A. "Free and Restrained Shrinkage of Fiber Reinforced Concrete with Low Polypropylene Fiber Content at Early Age." *Fourth RILEM International:* Symposium on Fiber Reinforced Cement and Concrete, International Union of Laboratories and Experts in Construction Materials, Systems and Structures (1992): 91–101.

Lane, D.S. "Thermal Properties of Aggregates," Significance of Tests and Properties of Concrete and Concrete-Making Materials, P. Klieger and J.F. Lamond, Eds, Report No. ASTM STP 169C. *American Society for Testing and Materials*, West Conshohocken, PA, (1994): 438–445.

Lane, S.N., "HPC Lessons Learned and Future Directions." IABMAS 2010: *The Fifth International Conference on Bridge Maintenance, Safety and Management*, International Association on Bridge Maintenance and Safety, Philadelphia, Pennsylvania, July 11-15 (2010).

Lindquist, W. D., D. Darwin, J. Browning, and G. G. Miller. "Effect of Cracking on Chloride Content in Concrete Bridge Decks." *ACI Materials Journal*, 103.6 (2006): 467–473.

Luna, P. "Lecture 3: Plastic Shrinkage and Cracking." EMPA (2011)

Lura, P. "Autogenous Deformation and Internal Curing of Concrete." Delft: DUP Science. XV, (2003):180.

Mehta, P.K. and P.J.M. Monteiro. "Concrete: Microstructure, Properties, and Materials." 3rd ed., New York: McGraw-Hill (2006).

Mu, R., Tian W., and Gou, Y. "Effect of Aggregate on Drying Shrinkage of Concrete." *Advanced Materials Research* 168-170 (2010): 701-708.

Myers, D., Kang, T.H.K. and Ramseyer, C. "Early-age Properties of Polymer Fiber-reinforced concrete." *International Journal of Concrete Structures and Materials* 2.1, (2008): 9–14.

Naaman A.E. l "Influence of Different Fibers on Plastic Shrinkage Cracking of Concrete" *ACI Materials Journal* (2005): 49-58.

Najafi M.H., et al. "Laboratory Study on the Effect of Polypropylene Fiber on Durability, And Physical and Mechanical Characteristic of Concrete for Application in Sleepers." *Construction & Building Materials*, 44 (2013): 411-418.

Nassif, H., Suksawang, N. and Mohammed, M. "Effect of Curing Methods on Early-age and Drying Shrinkage of High-performance Concrete." *Transportation Research Record: Journal of the Transportation Research Board,* 1834 (2003): 48-58.

Nayaran, KRS. " Polypropylene and Polyester Fiber Reinforced Concretes A Performance Study." *Concrete Research,* (2013): 188-195.

A. M. Neville: Properties of concrete (4th Edition), (Longman Scientific & Technical, UK 1995)

NRMCA. "CIP 42- Thermal Cracking of Concrete." *National Ready Mixed Concrete Association* (2009).

ODOT, "Oregon Standard and Specifications for Construction." *Oregon Department of Transportation (ODOT)* (2008): 814.

Ozyildirim, C. "High-Performance Fiber-Reinforced Concrete in Bridge Deck." *Virginia Department of Transportation* (2005).

Palecki, S., and Setzer, M. J. "Freeze-Thaw Durability of High-Performance Concrete Mechanism of Water Uptake and Internal Damage." Proceedings of the 2nd International

Symposium on Advances in Concrete through Science and Engineering, 11-13 (September 2006), Quebec City, Canada.

Tarr, Scott M., and Farny, James A. "Concrete Floors on Ground." EB075, Fourth Edition, *Portland Cement Association*, Skokie, Illinois, (2008): 256 pages.

Portland Cement Association (PCA). "Corrosion of Embedded Metals." *Cement.org* (2014). <http://www.cement.org/for-concrete-books-learning/concrete-technology/durability/corrosion-of-embedded-materials>

Radlinska, A., et al. "Shrinkage Mitigation Strategies in Cementitious Systems: A Closer Look at Differences in Sealed and Unsealed Behavior." *Transportation Research Record: Journal of the Transportation Research Board*, (2008): 59-67.

Radlinski M. and Olek J. "High-Performance Concrete Bridge Decks: A Fast Track Implementation Study Volume 2: Materials." *Joint Transportation Research Program* 2 (2010).

Ramey, G., Wolff, A., and Wright, R. "Structural Design Actions to Mitigate Bridge Deck Cracking." *Practice Periodical on Structural Design and Construction*, 2.3 (1997) 118–124.

Richardson, A.E., K.A. Coventry, and S. Wilkinson. "Freeze/Thaw Durability of Concrete with Synthetic Fibre Additions." *Cold Regions Science & Technology*, (2012): 49-56.

Rouhi J., et al. "The Effects Of Polypropylene Fibers On The Properties Of Reinforced Concrete Structures." *Construction & Building Materials*, 27.1 (2012): 73-77.

Rodriguez, D.E., Fu, T. and Ideker J.H. "Effect of Wet Curing Durations On Mechanical Properties and Pore Structure of High Performance Concrete," *Oregon State University*, (2014).

Roque R., Kim, N., Kim, B., and Lopp, G. "Durability of Fiber-Reinforced Concrete in Florida Environments." *Florida Department of Transportation*, (2009).

Saje, Drago, et al. "Shrinkage of Polypropylene Fiber-Reinforced High-Performance Concrete." *Journal of Materials in Civil Engineering*, 23.7 (2011): 941-952.

Sant, G., P. Lura, and J. Weiss, Measurements of Volume Change in Cementitious Materials at Early Ages: Review of Testing Protocols and Interpretation of Results. *Transportation Research Record: Journal of the Transportation Research Board*, (2006): 21-29.

Scanlon, J.M., and McDonald, J.E. 1994. "Thermal Properties," Significance of Tests and Properties of Concrete and Concrete-Making Materials, P. Klieger and J.F. Lamond, Eds., Report No. ASTM STP 169C. *American Society for Testing and Materials*, West Conshohocken, PA, (1994): 229–239.

See H. T., Attiogbe E. K., and Miltenberger M. A., "Potential for Restrained Shrinkage Cracking of Concrete and Mortar," *Cement, Concrete and Aggregates* 26 (2004): 123-130.

Slatnick, S. and K.J. Folliard, unpublished data. 2008, The University of Texas at Austin.

Subramaniam, Kolluru V., et al. "Influence of Ultrafine Fly Ash on the Early Age Response and the Shrinkage Cracking Potential of Concrete." *Journal of Materials in Civil Engineering*, 17.1 (2005): 45-53.

Swamy, R. (1994). "The Technology of Steel Fibre-reinforced Concrete for Practical Applications." *Proceedings-Institution of Civil Engineers*, 56(1), 143–159.

Tazawa, E., and Miyazawa, S., "Influence of Cement and Admixture on Autogenous Shrinkage of Cement Paste," *Cement and Concrete Research*, 25.2 (1995): 281-292.

Walker et al. “Petrographic Methods of Examining Hardened Concrete: A Petrographic Manual.” *Virginia Transportation Research Council*, (2006).

Wang et al. “Plastic Shrinkage Cracking in Concrete Materials Influence of Fly Ash and Fibers.” *ACI Materials Journal*, (2001): 458-464.

Weiss et al. “Shrinkage Cracking of Restrained Concrete Slabs.” *Journal of Material Mechanics*, 124.7 (1998): 765-774.

Wittmann, F. H., “On the Action of Capillary Pressure,” *Cement and Concrete Research*, 6.1 (1976). 49-56.

Zemajtis, J.Z. “Role of Concrete Curing.” *Portland Cement Association* (2014): <http://www.cement.org/for-concrete-books-learning/concrete-technology/concrete-construction/curing-in-construction>

Zhang, Jun, Yu Dong Han, and Yuan Gao. "Effects of Water-Binder Ratio and Coarse Aggregate Content on Interior Humidity, Autogenous Shrinkage, and Drying Shrinkage of Concrete." Journal of Materials in Civil Engineering 26.1 (2014): 184-189.

Zhang P., Qingfu L. and Zhang H. “Combined Effect of Polypropylene Fiber and Silica Fume on Mechanical Properties of Concrete Composite Containing Fly Ash.” *Journal of Reinforced Plastics and Composites* 30.16 (2011): 1349–1358.

Zhang, M.H., Tam, C.T. and Leow, M.P. “Effect of Water-to-cementitious Materials Ratio and Silica Fume on the Autogenous Shrinkage of Concrete.” *Cement and Concrete Research*, 33 (2003): 1687-1694.

APPENDIX A – TESTING RESULTS SUMMARY

Mix ID:	HPC1	Cast date:	4/4/2012	Curing time (days):	14
Mix description:	ODOT HPC control mix				

Fresh properties

Batch size(cu ft):	4.0	w/cm:	0.37	Temperature (°C):	23.0
Slump (in):	5	Air content (%):	5.0	Unit weight (pcf):	146.5

Hardened properties

28 day standard cure			28 day matched cure		
fc (psi)	ft (psi)	E (psi)	fc (psi)	ft (psi)	E (ksi)
5126	588	4679	5787	638	4449

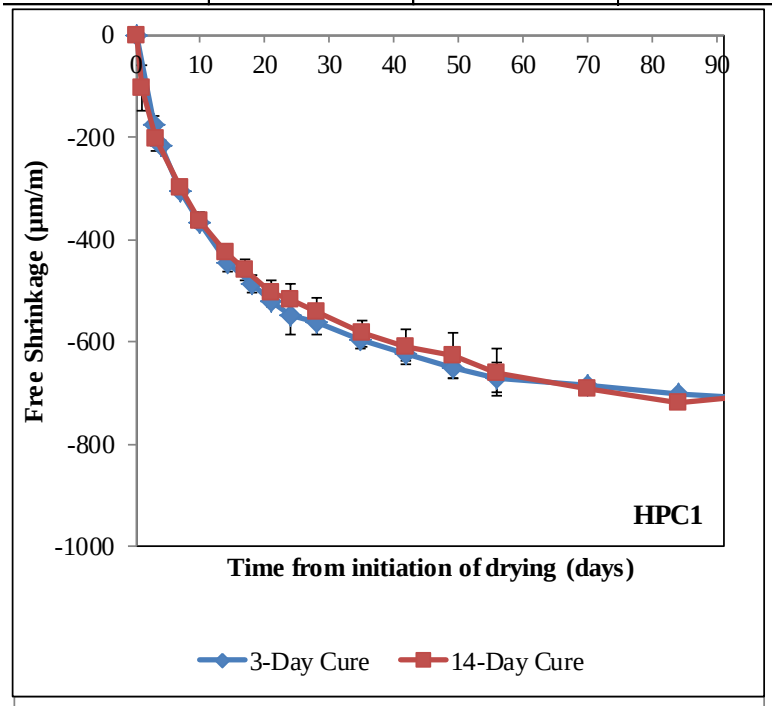

Drying Shrinkage (µm/m)

Approx. Time (Days)	3day Cure	14day Cure
0	0	0
4	-177	-103
7	-307	-203
10	-367	-300
14	-447	-363
21	-487	-503
28	-520	-540
42	-650	-610
56	-670	-660
70	-683	-690
100	-713	-703

**Time is for reference, kept consistant at ±2 days from approximate time

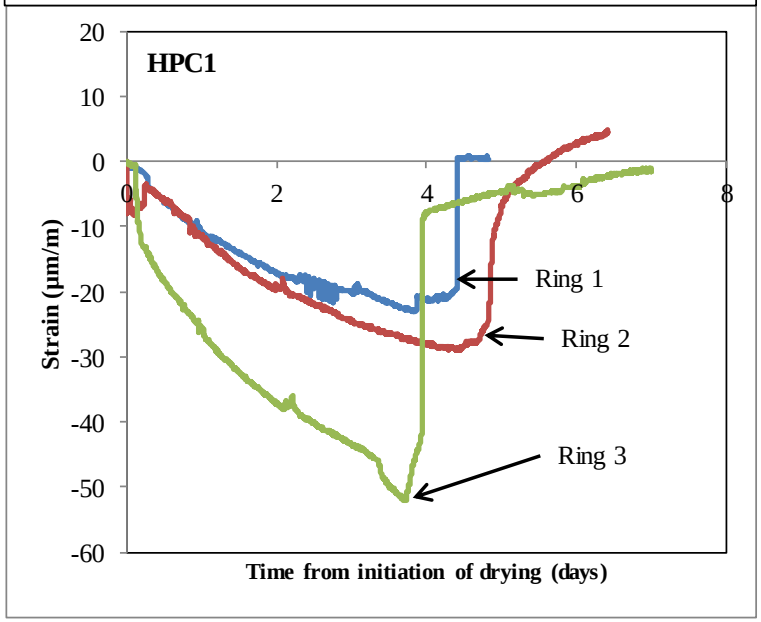

	ToC (days)	Stress Rate (psi/day)	Crack Risk Rating
Ring A	4.4	50	
Ring B	4.6	41	
Ring C	3.6	70	**H**
Average	**4.2**	**54**	

Mix ID:	HPC2	Cast date:	7/10/2013	Curing time (days):	14
Mix description:	ODOT HPC Control: 30% Slag and 4% Silica Fume replacement				

Fresh properties

Batch size(cu ft):	3.5	w/cm:	0.37	Temperature (°C):	20
Slump (in):	3	Air content (%):	6.0	Unit weight (pcf):	143

Hardened properties

28 day standard cure			28 day matched cure		
fc (psi)	ft (psi)	E (ksi)	fc (psi)	ft (psi)	E (ksi)
4615	485.00	4187.0	-	-	-

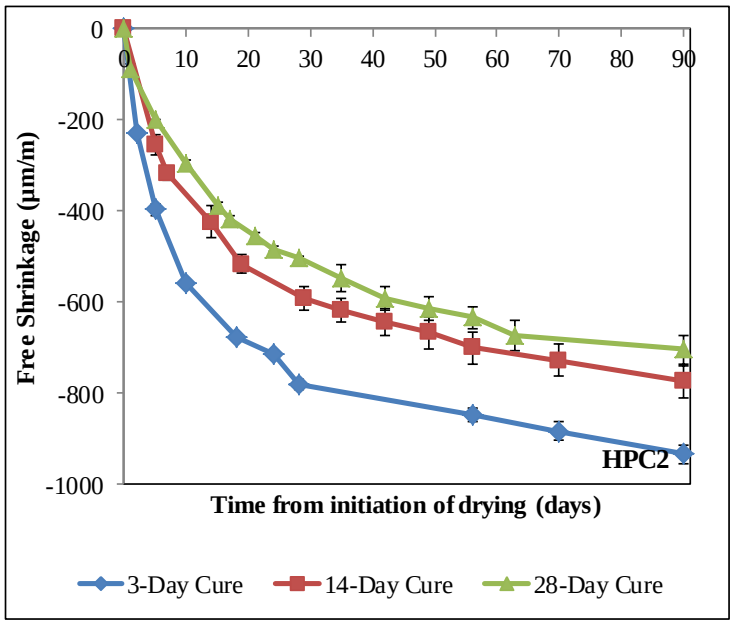

Drying Shrinkage (µm/m)

Approx. Time (Days)	3day Cure	14day Cure	28day Cure
0	0	0	0
4	-397	-253	-87
7	-	-317	-200
10	-557		-293
14	-	-423	-387
21	-	-517	-453
28	-780	-590	-503
42	-	-643	-590
56	-847	-700	-633
70	-883	-727	-
90	-933	-773	-703

**Time is for reference, kept consistant at ±2 days from approximate time

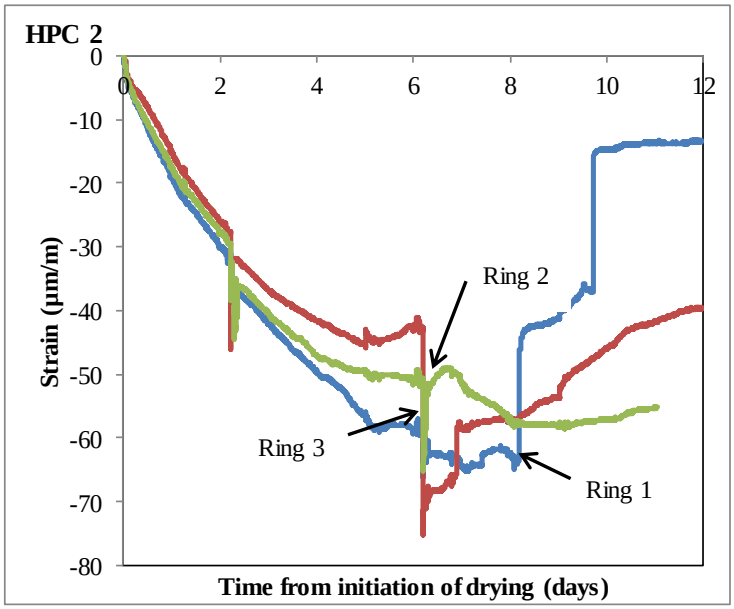

	ToC (days)	Stress Rate (psi/day)	Crack Risk Rating
Ring 1	8.2	43	MH
Ring 2	6.2	48	
Ring 3	6.2	40	
Average	**6.9**	**44**	

Mix ID:	FHPC D5	Cast date:	5/22/2013	Curing time (days):	14
Mix description:	Synthetic Blended Fiber Mix: Dosage Rate 5lb/yd^3				

Fresh properties

Batch size(cu ft):	3.5	w/cm:	0.37	Temperature (°C):	22
Slump (in):	2.5	Air content (%):	6.2	Unit weight (pcf):	143

Hardened properties

28 day standard cure			28 day matched cure		
fc (psi)	ft (psi)	E (ksi)	fc (psi)	ft (psi)	E (ksi)
3930.0	462.00	3480.0	-	-	-

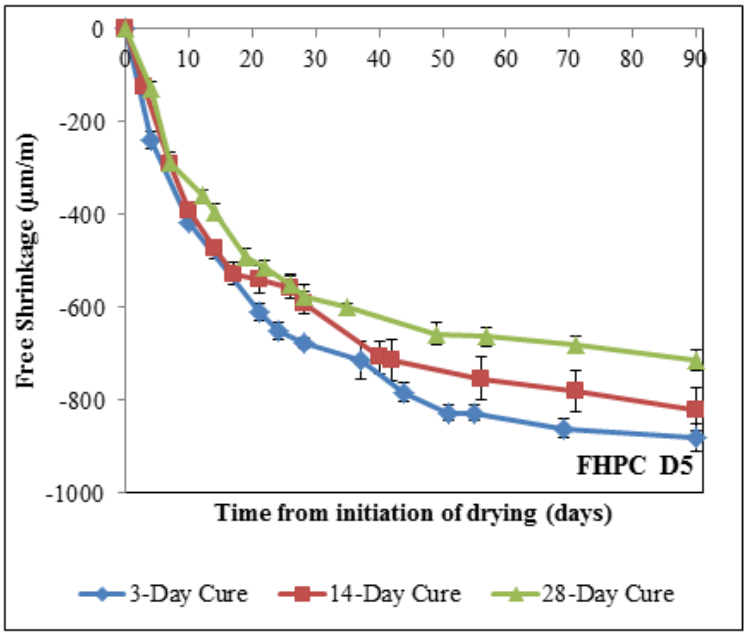

Drying Shrinkage (µm/m)

Approx. Time (Days)	3day Cure	14day Cure	28day Cure
0	0	0	0
4	-240	-123	-130
7	-417	-290	-287
10	-610	-390	-357
14	-650	-473	-393
21	-610	-540	-513
28	-650	-590	-577
42	-677	-713	-
56	-827	-753	-663
70	-860	-780	-680
90	-880	-820	-713

**Time is for reference, kept consistant at ±2 days from approximate time

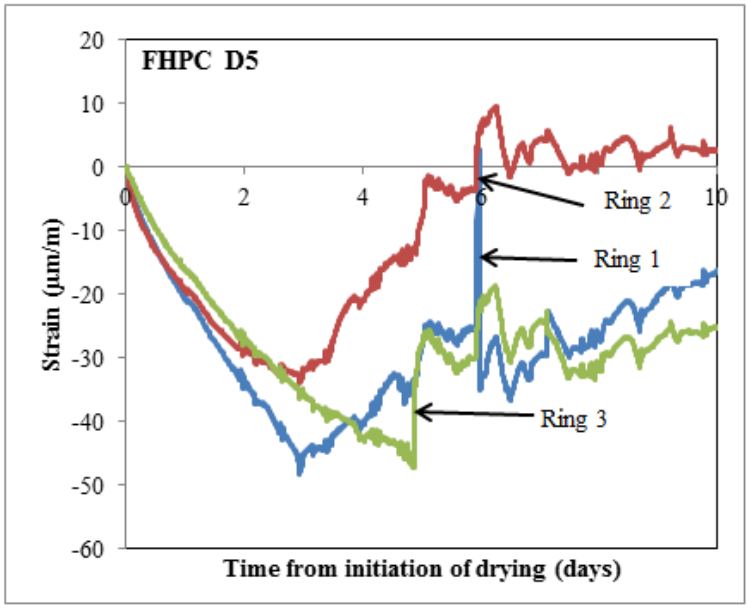

	ToC (days)	Stress Rate (psi/day)	Crack Risk Rating
Ring 1	5.9	64	H
Ring 2	5.9	45	
Ring 3	4.9	56	
Average	**5.6**	**55**	

Mix ID:	FHPC D7.5	Cast date:	8/28/2012	Curing time (days):	14
Mix description:	Synthetic Blended Fiber Mix: Dosage Rate 7.5lb/yd^3				

Fresh properties

Batch size(cu ft):	3.5	w/cm:	0.37	Temperature (°C):	24
Slump (in):	5.5	Air content (%):	7.0	Unit weight (pcf):	140

Hardened properties

28 day standard cure			28 day matched cure		
fc (psi)	ft (psi)	E (ksi)	fc (psi)	ft (psi)	E (ksi)
4050.0	436.00	3910.0	5010.0	536.00	4110.0

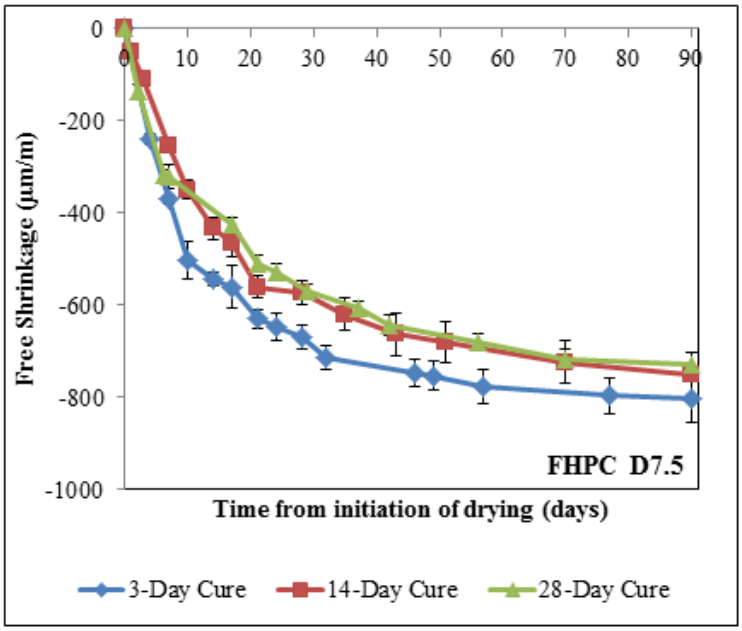

Drying Shrinkage (µm/m)

Approx. Time (Days)	3day Cure	14day Cure	28day Cure
0	0	0	0
4	-240	-50	-137
7	-370	-110	-317
10	-503	-253	-320
14	-543	-350	-393
21	-630	-433	-510
28	-670	-573	-573
42	-747	-663	-663
56	-777	-680	-680
70	-797	-723	-717
90	-803	-750	-727

**Time is for reference, kept consistant at ±2 days from approximate time

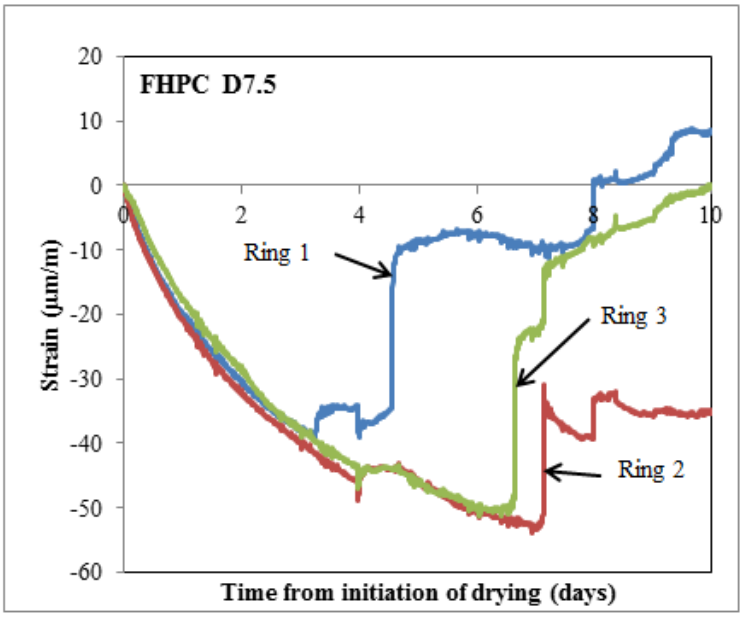

	ToC (days)	Stress Rate (psi/day)	Crack Risk Rating
Ring 1	4.6	53	
Ring 2	7.1	51	
Ring 3	6.6	53	**H**
Average	**6.1**	**52**	

Mix ID:	FHPC D10	Cast date:	7/10/2013	Curing time (days):	14
Mix description:	Synthetic Blended Fiber Mix: Dosage Rate 10lb/yd^3				

Fresh properties

Batch size(cu ft):	3.5	w/cm:	0.37	Temperature (°C):	20
Slump (in):	3	Air content (%):	6.0	Unit weight (pcf):	143

Hardened properties

28 day standard cure			28 day matched cure		
fc (psi)	ft (psi)	E (ksi)	fc (psi)	ft (psi)	E (ksi)
4090.0	520.00	3910.0	5180.0	511.00	4230.0

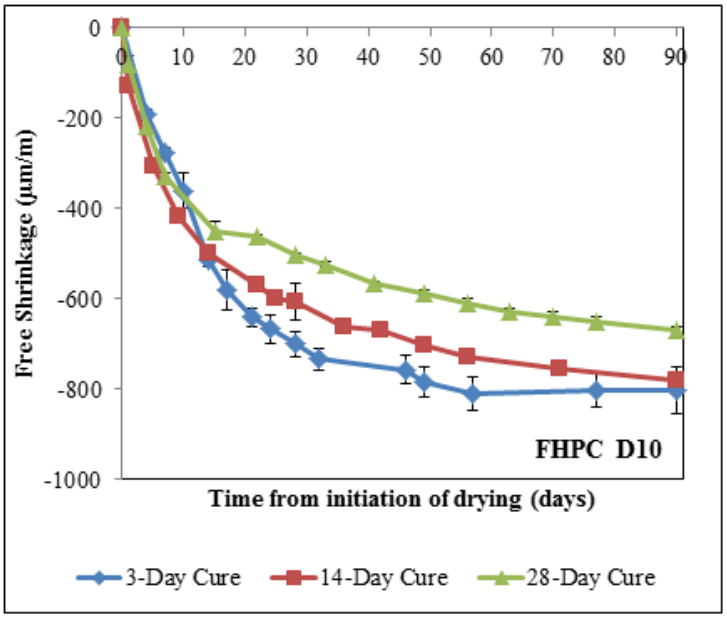

Drying Shrinkage (µm/m)

Approx. Time (Days)	3day Cure	14day Cure	28day Cure
0	0	0	0
4	-190	-130	-217
7	-277	-307	-330
10	-360	-417	-
14	-513	-500	-450
21	-640	-570	-463
28	-700	-607	-503
42	-757	-670	-567
56	-810	-727	-610
70	-803	-753	-640
90	-803	-780	-670

**Time is for reference, kept consistant at ±2 days from approximate time

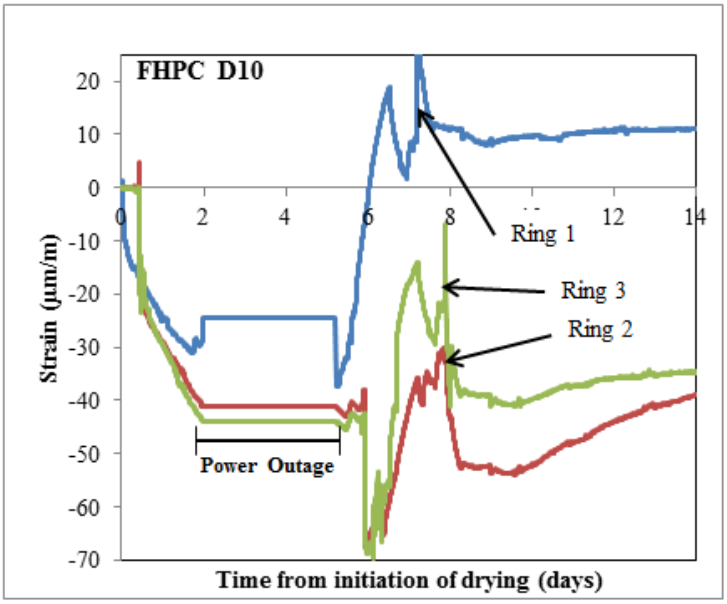

	ToC (days)	Stress Rate (psi/day)	Crack Risk Rating
Ring 1	7.2	49	
Ring 2	8.0	54	
Ring 3	7.9	56	**MH**
Average	**7.7**	**53**	

Mix ID:	CHPC	Cast date:	12/19/2013	Curing time (days):	14
Mix description:	ODOT HPC w/ Crushed Coarse 3/4" MSA				

Fresh properties

Batch size(cu ft):	3.5	w/cm:	0.37	Temperature (°C):	22
Slump (in):	3.3	Air content (%):	7.5	Unit weight (pcf):	139

Hardened properties

28 day standard cure			28 day matched cure		
fc (psi)	ft (psi)	E (ksi)	fc (psi)	ft (psi)	E (ksi)
3599	412	4103	3920	345	3793

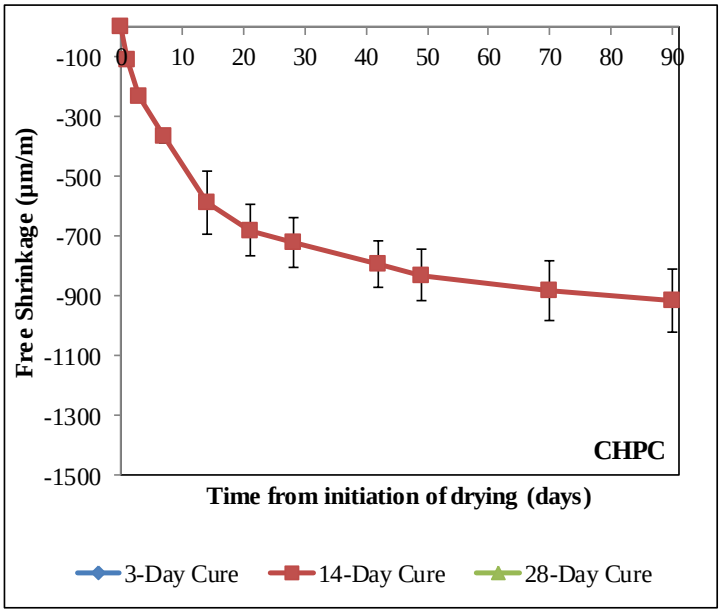

Drying Shrinkage (µm/m)

Approx. Time (Days)	14day Cure
0	0
4	-110
7	-230
10	-365
14	-
21	-680
28	-720
42	-795
56	-
70	-880
90	-915

**Time is for reference, kept consistant at ±2 days from approximate time

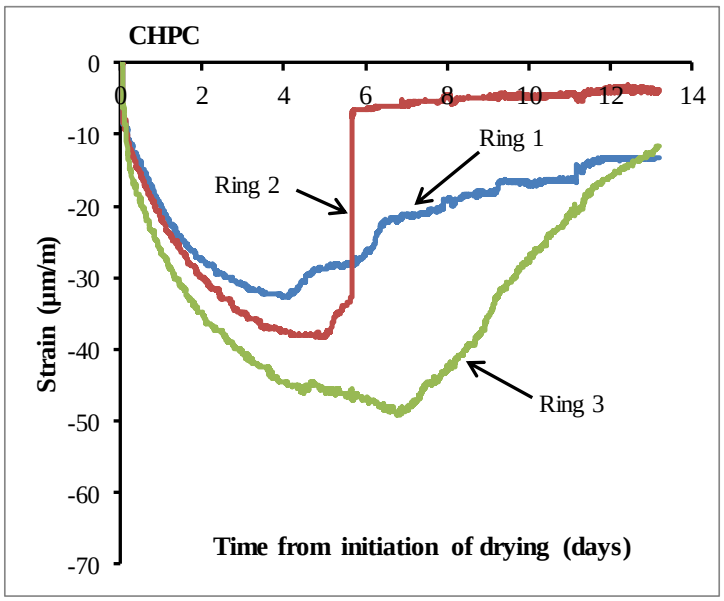

	ToC (days)	Stress Rate (psi/day)	Crack Risk Rating
Ring 1	9.0	37	**High**
Ring 2	5.7	32	
Ring 3	9.0	38	
Average	**7.9**	**36**	

Mix ID:	LS2	Cast date:	2/13/2014	Curing time (days):	14
Mix description:	HPC mixture using crushed limestone as a coarse aggregate				

Fresh properties

Batch size(cu ft):	3.5	w/cm:	0.37	Temperature (°C):	19
Slump (in):	2.5	Air content (%):	5.2	Unit weight (pcf):	145

Hardened properties

28 day standard cure			28 day matched cure		
fc (psi)	ft (psi)	E (ksi)	fc (psi)	ft (psi)	E (ksi)
5710	529	4411	6069	610	4745

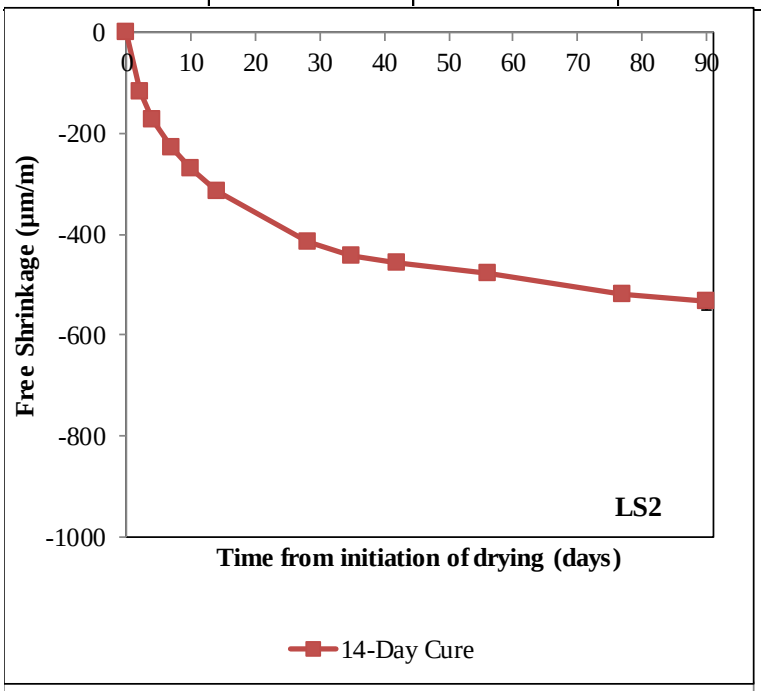

Drying Shrinkage (µm/m)

Approx. Time (Days)	14day Cure
0	0
4	-173
7	-227
10	-270
14	-313
21	-
28	-413
42	-457
56	-477
70	-
90	-533

**Time is for reference, kept consistant at ±2 days from approximate time

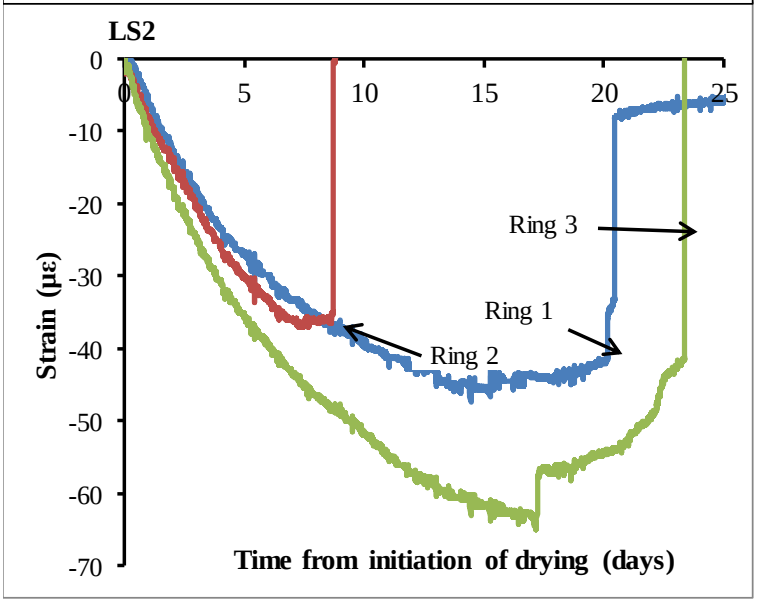

	ToC (days)	Stress Rate (psi/day)	Crack Risk Rating
Ring 1	20.5	21	
Ring 2	8.7	31	
Ring 3	23.4	18	**ML**
Average	**17.5**	**23**	

Mix ID:	LCM2	Cast date:	10/5/2012	Curing time (days):	14
Mix description:	Low Cement Content (550lb/yd^3) HPC Mix				

Fresh properties

Batch size(cu ft):	3.5	w/cm:	0.37	Temperature (°C):	24
Slump (in):	3	Air content (%):	8.0	Unit weight (pcf):	135

Hardened properties

28 day standard cure			28 day matched cure		
fc (psi)	ft (psi)	E (ksi)	fc (psi)	ft (psi)	E (ksi)
2979	392	3590	3090	392	3470

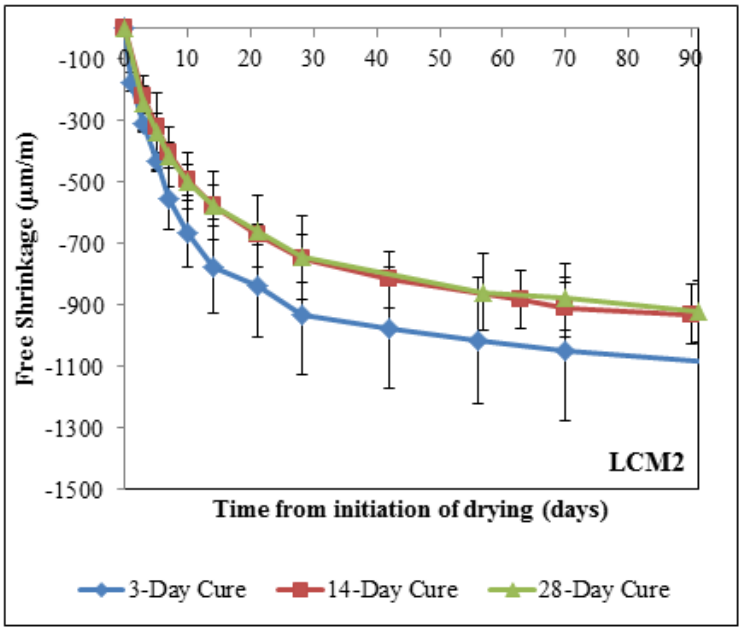

Drying Shrinkage (µm/m)

Approx. Time (Days)	3day Cure	14day Cure	28day Cure
0	0	0	0
4	-240	-220	-240
7	-333	-320	-337
10	-417	-403	-417
14	-503	-493	-497
21	-610	-573	-577
28	-650	-670	-660
42	-677	-750	-743
56	-713	-	-857
70	-783	-907	-873
90	-	-930	-920

**Time is for reference, kept consistant at ±2 days from approximate time

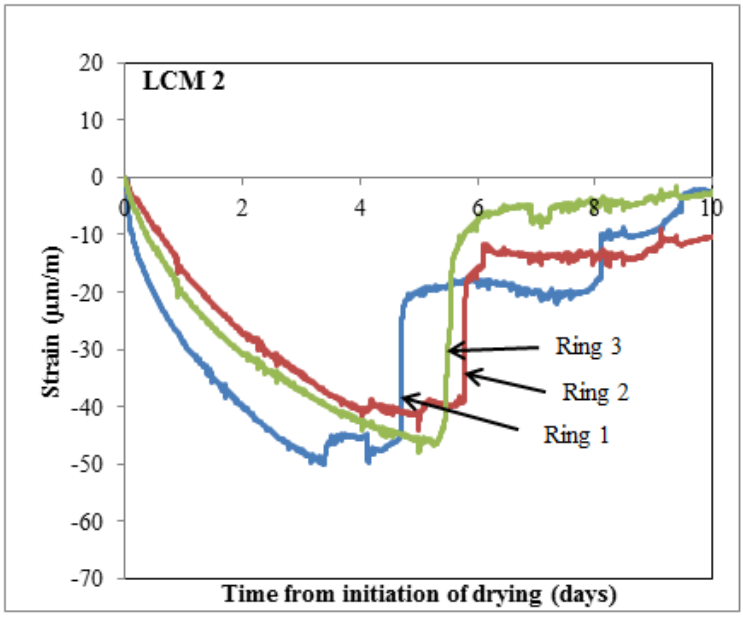

	ToC (days)	Stress Rate (psi/day)	Crack Risk Rating
Ring 1	4.7	87	
Ring 2	5.5	78	
Ring 3	5.8	64	**H**
Average	**5.3**	**76**	

Mix ID:	OPC1	Cast date:	7/18/2012	Curing time (days):	14
Mix description:	OPC w/ no SCM's				

Fresh properties

Batch size(cu ft):	4.0	w/cm:	0.37	Temperature (°C):	23.8
Slump (in):	8	Air content (%):	3.0	Unit weight (pcf):	151.1

Hardened properties

28 day standard cure			28 day matched cure		
fc (MPa)	ft (MPa)	E (GPa)	fc (psi)	ft (psi)	E (ksi)
6480	533	5260	6620	622	5400

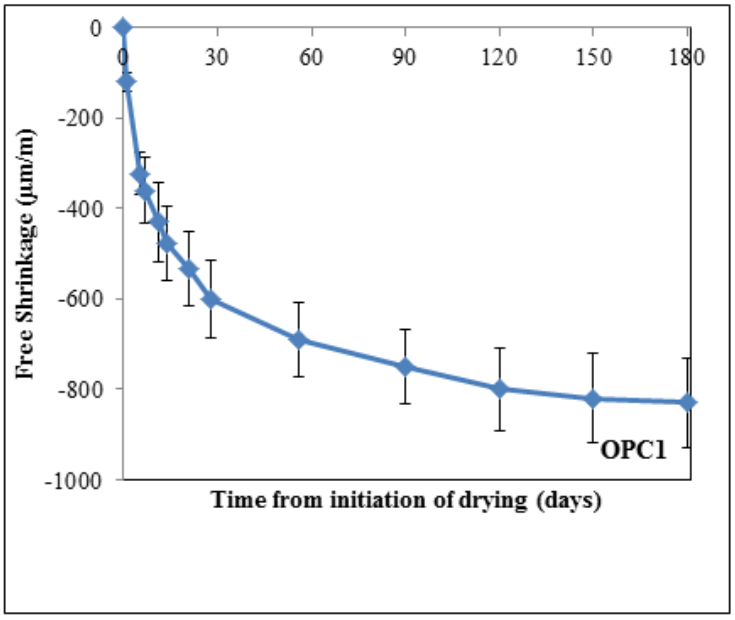

Approx. Time (Days)	14 day Shrinkage (µm/m)
0	0
1	-120
5	-323
7	-360
11	-430
14	-477
21	-533
28	-600
56	-690
90	-750

**Time is for reference, kept consistant at ±2 days from approximate time

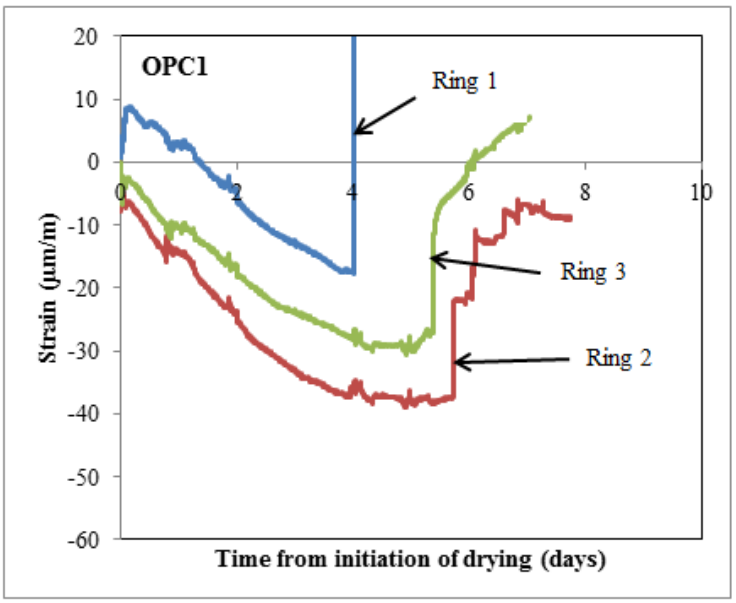

	ToC (days)	Stress Rate (psi/day)	Crack Risk Rating
Ring 1	2.7	40	MH
Ring 2	5.7	56	
Ring 3	5.4	46	
Average	**4.6**	**47**	

Mix ID:	FHPC D7.5	Cast date:	7/18/2012	Curing time (days):	14		
Mix description:	Synthetic Blended Fiber Freeze/Thaw Mix: Dosage Rate 7.5lb/yd^3						
Fresh properties							
Batch size(cu ft):	2.5	w/cm:	0.37	Temperature (°C):	24.0		
Slump (in):	2.5	Air content (%):	6.0	Unit weight (pcf):	140.0		
Dynamic Modulus (DM)							
# of Cycles	**DMA**	**DMB**	**DMC**	**DMA (%)**	**DMB (%)**	**DMC (%)**	**Avg (%)**
0	2065	2075	2071	100.0	100.0	100.0	100.0
36	2049	2058	2050	98.5	98.4	98.0	98.3
72	2049	2055	2054	98.5	98.1	98.4	98.3
109	2050	2054	2048	98.6	98.0	97.8	98.1
140	2048	2052	2047	98.4	97.8	97.7	98.0
184	2042	2052	2043	97.8	97.8	97.3	97.6
218	2038	2046	2042	97.4	97.2	97.2	97.3
252	2038	2046	2042	97.4	97.2	97.2	97.3
288	2038	2046	2040	97.4	97.2	97.0	97.2
300	2039	2046	2040	97.5	97.2	97.0	97.3

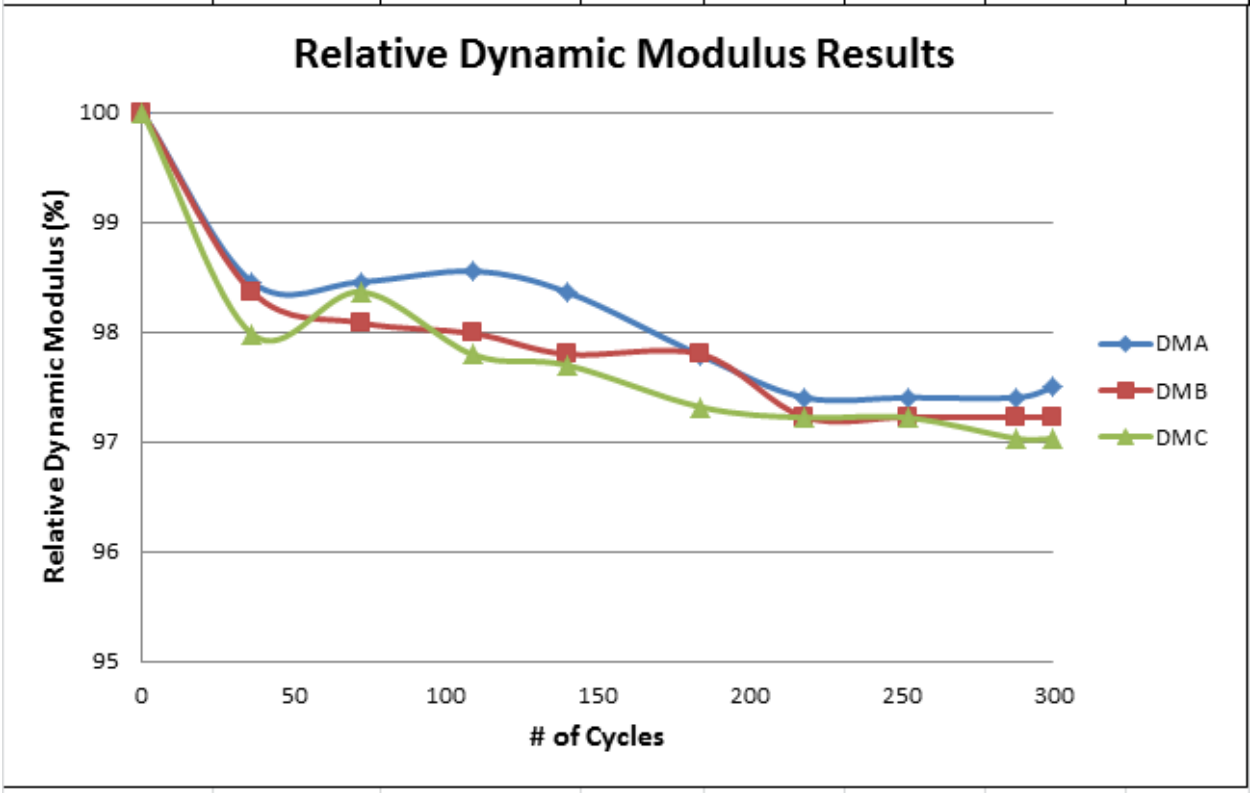

Mix ID:	FHPC D10	Cast date:	7/18/2012	Curing time (days):	14		
Mix description:	Synthetic Blended Fiber Freeze/Thaw Mix: Dosage Rate 10lb/yd^3						
Fresh properties							
Batch size(cu ft):	2.5	w/cm:	0.37	Temperature (°C):	26.0		
Slump (in):	2.5	Air content (%):	6.0	Unit weight (pcf):	140.0		
Dynamic Modulus (DM)							
# of Cycles	**DM-A**	**DM-B**	**DM-C**	**DM-A (%)**	**DM-B (%)**	**DM-C (%)**	**Avg (%)**
0	2032	2028	2048	100.0	100.0	100.0	100.0
36	2015	1997	2028	98.3	97.0	98.1	97.8
72	2010	1996	2023	97.8	96.9	97.6	97.4
109	2008	1995	2020	97.7	96.8	97.3	97.2
140	2006	1990	2015	97.5	96.3	96.8	96.8
184	2004	1990	2023	97.3	96.3	97.6	97.0
218	1994	1989	2020	96.3	96.2	97.3	96.6
252	1991	1975	2016	96.0	94.8	96.9	95.9
288	1989	1970	2015	95.8	94.4	96.8	95.7
300	1988	1970	2018	95.7	94.4	97.1	95.7

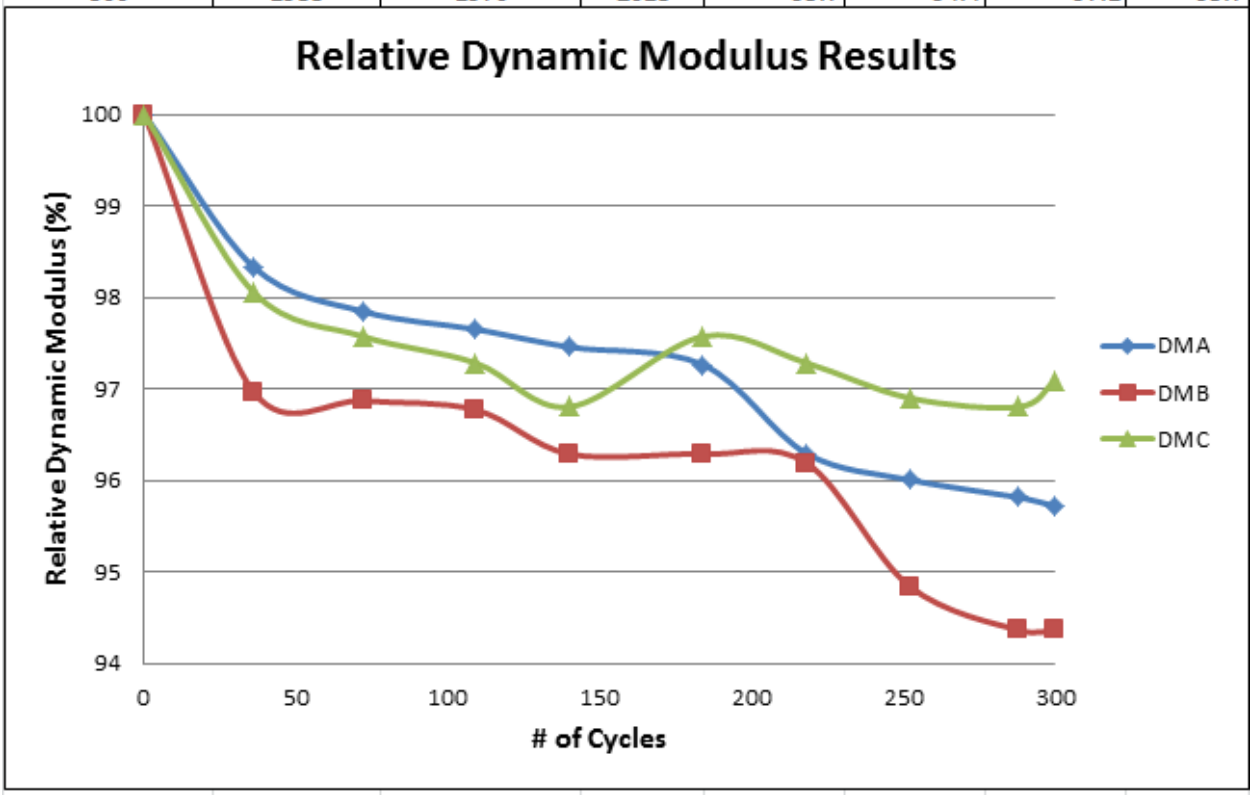

Mix ID:	FHPC D7.5	Cast date:	8/28/2012	Curing time (days):	56
Mix description:	Synthetic Blended Fiber Mix: Dosage Rate 7.5lb/yd^3				
Fresh properties					
Batch size(cu ft):	3.5	w/cm:	0.37	Temperature (°C):	24.0
Slump (in):	5.5	Air content (%):	7.0	Unit weight (pcf):	140.0

Manual Recordings

Time (Hours)	Cell 1	Cell2	Cell 3
0.0	23.7	22.1	25.9
0.5	22.1	22.6	24.9
1.0	22.7	23.3	26.4
1.5	23.9	23.7	27.0
2.0	24.7	24.0	27.6
2.5	25.4	24.4	25.5
3.0	25.8	24.9	28.1
3.5	26.4	25.1	29.3
4.0	26.6	25.2	29.5
4.5	27.3	25.2	30.1
5.0	27.8	25.7	30.4
5.5	27.8	26.3	31.1
6.0	29.3	27.1	31.6

Total Charge Passed (Coulombs)

Cell 1	545
Cell 2	519
Cell 3	617
Average	**560.34717**

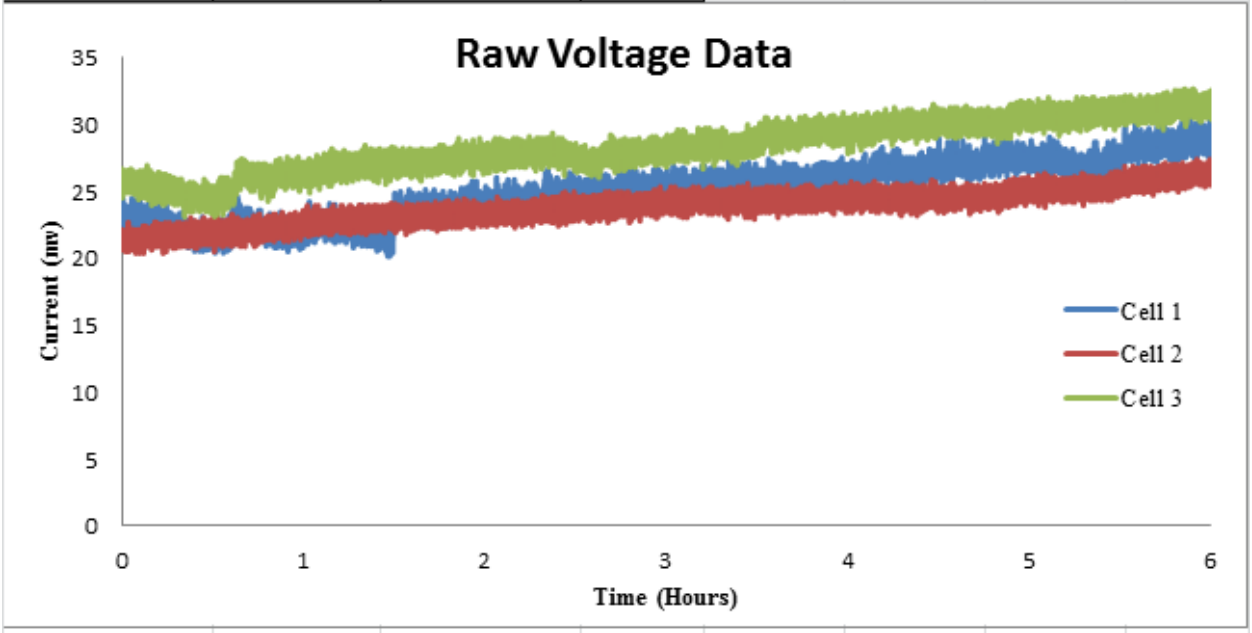

Mix ID:	FHPC D10	Cast date:	7/10/2013	Curing time (days):	56
Mix description:	Synthetic Blended Fiber Mix: Dosage Rate 10lb/yd^3				
Fresh properties					
Batch size(cu ft):	3.5	w/cm:	0.37	Temperature (°C):	20.0
Slump (in):	3	Air content (%):	6.0	Unit weight (pcf):	143.0

Manual Recordings

Time (Hours)	Cell 1	Cell2	Cell 3
0.0	29.1	26.0	26.2
0.5	27.1	27.5	26.2
1.0	29.8	28.4	28.2
1.5	31.8	29.9	28.9
2.0	32.2	31.1	30.0
2.5	32.6	31.7	30.3
3.0	33.5	32.2	30.6
3.5	34.2	33.4	31.2
4.0	35.4	33.9	31.6
4.5	35.8	34.5	31.9
5.0	37.2	35.3	31.6
5.5	38.4	35.8	32.4
6.0	39.2	36.2	33.7

Total Charge Passed (Coulombs)

Cell 1	714.65
Cell 2	681.35
Cell 3	684
Average	**693**

**Cell 3 calculated from manual entries